TITLE

Climatic drivers of (changes in) bat migration phenology at Bracken Cave (USA)

RUNNING TITLE

Climatic drivers of bat migration phenology

AUTHORS

Birgen Haest[1, *], Phillip M. Stepanian[2], Charlotte E. Wainwright[2], Felix Liechti[1], Silke Bauer[1]

AFFILIATIONS

[1] Swiss Ornithological Institute, Seerose 1, Sempach, CH-6204, Switzerland

[2] Department of Civil and Environmental Engineering and Earth Sciences, University of Notre Dame, Notre Dame, Indiana, 46556, USA

*Corresponding author: birgen.haest@protonmail.com; +49 176 749 782 82; ORCID: 0000-0002-8739-6460

AUTHOR CONTRIBUTIONS

B.H. conceptualized the study. P.S. and C.W. contributed the phenology dataset. B.H. designed and conducted the analyses. B.H. wrote the paper, with contributions of P.S., C.W., F.L. and S.B.

KEYWORDS

Brazilian free-tailed bat; Tadarida brasiliensis; fall; radar; wind; rainfall; environmental plasticity; climate change

ARTICLE TYPE

Primary Research Article

ABSTRACT

Climate change is drastically changing the timing of biological events across the globe. Changes in the phenology of seasonal migrations between the breeding and wintering grounds have been observed across biological taxa, including birds, mammals, and insects. For birds, strong links have been shown between changes in migration phenology and changes in weather conditions at the wintering, stopover, and breeding areas. For other animal taxa, the current understanding of, and evidence for, climate (change) influences on migration still remains rather limited, mainly due to the lack of long-term phenology datasets. Bracken Cave in Texas (USA) holds one of the largest bat colonies of the world. Using weather radar data, a unique 23-year (1995-2017) long time series was recently produced of the spring and autumn migration phenology of Brazilian free-tailed bats (*Tadarida brasiliensis*) at Bracken Cave. Here, we analyse these migration phenology time series in combination with gridded temperature, precipitation, and wind data across Mexico and southern USA, to identify the climatic drivers of (changes in) bat migration phenology. Perhaps surprisingly, our extensive spatiotemporal search did not find temperature to influence either spring or autumn migration. Instead, spring migration phenology seems to be predominantly driven by wind conditions at likely wintering or spring stopover areas during the migration period. Autumn migration phenology on the other hand, seems to be dominated by precipitation to the east and north-east of Bracken Cave. Long-term changes towards more frequent migration-favourable wind conditions have, furthermore, allowed spring migration to occur 16 days earlier. Our results illustrate how some of the remaining knowledge gaps on the influence of climate (change) on bat migration and abundance can be addressed using weather radar analyses.

INTRODUCTION

Every year, many billions of animals migrate across the globe in search of conditions that increase survival and reproductive success. In doing so, they contribute to the ecosystem functioning and provide invaluable ecosystem services, such as pest control and pollination, at the many locations along their migratory route (Bauer et al., 2019; Bauer & Hoye, 2014; Bowlin et al., 2010). Many populations of migratory animals have been steeply declining (Vickery et al., 2014; Wilcove & Wikelski, 2008), compromising their role in the ecosystems along their way. Knowledge on the timing of migration is a crucial factor in determining the relative impacts of migratory animals on those ecosystems, but also for implementing efficient conservation actions (Bauer & Hoye, 2014; Dechmann et al., 2017; Wilcove & Wikelski, 2008). Over the past decades, many species have changed their migratory timing in response to climate change (Thackeray et al., 2016). The direction and magnitude of these changes, however, vary across geographic locations and taxa (Charmantier & Gienapp, 2014; Chmura et al., 2019; Hurlbert & Liang, 2012).

To understand why species and populations differ in their phenological response to climate change, we first need to identify the environmental drivers of migration timing (Haest et al., 2018b, 2019; Shaw, 2016). Such an endeavour would not only advance our fundamental understanding of animal migration, but, more importantly, allow us to predict the consequences of ongoing and future climate change (Bowlin et al., 2010; Pettit & O'Keefe, 2017), identify the species most at risk (Bauer et al., 2011; Hurlbert & Liang, 2012; Wilcove & Wikelski, 2008), and support their conservation. While drivers of migration have been extensively studied in some taxa, e.g., birds, other taxa, e.g., bats and insects, are remarkably understudied (Bauer et al., 2011; Liechti & McGuire, 2017; Moussy et al., 2013; Popa-Lisseanu & Voigt, 2009; Wilcove & Wikelski, 2008).

The majority of bat species are considered sedentary (Hutterer et al., 2005). For many temperate bat species, this includes a winter hibernation period close to the summer habitat, even at higher latitudes (Fleming, 2019). With increasing latitude, however, an increasing number of species travel considerable distances (i.e. some hundreds up to perhaps three thousand kilometers) between winter and summer habitats. Particularly for bat species living in highly seasonal (temperate) environments, migration is an essential part of their ecology (Fleming & Eby, 2003; Hutterer et al., 2005). Because of their cryptic nocturnal activity patterns and often secretive roosting, bat behaviour (including migration) has remained notoriously difficult to study (Fleming, 2019; Krauel & McCracken, 2013; Liechti & McGuire, 2017; Smith & McWilliams, 2016; Weller et al., 2016). In Europe and North America, some knowledge on migratory and other movement patterns has been gathered over the past century using ringing (or banding) (Ellison, 2008; Hutterer et al., 2005; Petersons, 2004). Further insights into rough spatiotemporal movement patterns have also been gained from museum specimens (Cryan, 2003), stable isotope analyses (Britzke et al., 2009; Lehnert et al., 2018), acoustics (Rydell et al., 2014; Smith & McWilliams, 2016), and genetic analyses (Russell et al., 2005; Russell & McCracken, 2006). Gaining detailed insights into the migratory behaviour of individuals or populations has, however, proven difficult due to the lack of appropriate monitoring tools or technology to either: (a) mark and track individual bats (Holland & Wikelski, 2009; Krauel & McCracken, 2013; Roby et al., 2019); or (b) study the spatiotemporal dynamics of entire populations. Many bat species are rather small (and light-weight), limiting possibilities for long-term tracking devices (Moussy *et al.*, 2013; but see Weller *et al.*, 2016). Monitoring (seasonal) bat abundance at a single location such as large roosting colonies (e.g. maternity caves) is also far from straightforward (McCracken, 2003). In fact, studies taking advantage of technological (and algorithmic) developments, e.g. thermal imaging, have indicated that quantitative estimates in historical abundance census records are probably highly questionable (Hristov et al., 2010). Over the past decade, a handful of radio-tagging studies have produced the first insights into relationships between weather and bat migration phenology that go beyond the anecdotal (Dechmann et al., 2017; Jonasson & Guglielmo, 2019; McGuire et al., 2012; Roby et al., 2019). Reliable long-term datasets on bat migration phenology are, however, extremely rare (Stepanian & Wainwright, 2018; but see Pettit & O'Keefe, 2017 for a notable

exception). As such, potential effects of climate change on bat migration phenology have hitherto remained largely speculative.

Using weather radar data, a unique 23-year (1995-2017) continuous time series was recently produced of nightly population estimates of Brazilian free-tailed bats at Bracken Cave in Texas (USA) (Stepanian & Wainwright, 2018). Brazilian free-tailed bats are one of the most abundant (Davis et al., 1962) and probably best-studied bat species (Russell & McCracken, 2006). Long-term, often severe, declines in their abundance have repeatedly been reported (McCracken et al., 1994), although the magnitude of declines may have been overestimated due to inaccurate historical census data (Hristov et al., 2010). While much research has been dedicated to Brazilian free-tailed bats, many questions remain, especially pertaining to their variation in abundance and timing of life-history activities (Stepanian & Wainwright, 2018). Every summer, millions of female Brazilian free-tailed bats gather in large maternity colonies across the USA, with Bracken Cave being one of the biggest. Very little is known, however, on the exact locations and the ecology of Brazilian free-tailed bats during winter or migration periods, with the proportion of the North American population accounted for in suspected winter roosts estimated at less than 1% (López-González & Best, 2006) or perhaps up to 5% (Wiederholt et al., 2013).

Here, we use yearly spring and autumn migration phenology at Bracken Cave over the period 1995-2017, derived from the nightly abundance estimated by weather radar (Stepanian & Wainwright, 2018), in combination with gridded temperature, precipitation and wind data to first identify which weather at which location and over which time window is most likely influencing inter-annual phenology of Brazilian free-tailed bats. Subsequently, we show to what extent these drivers may have caused the observed long-term temporal trends in migration phenology.

MATERIALS AND METHODS

Spring and autumn migration phenology at Bracken Cave

Weather surveillance radars regularly detect large numbers of Brazilian free-tailed bats as they emerge from their roosts at dusk and take flight into the airspace (Frick et al., 2012; Stepanian & Wainwright, 2018). A previous study used radar observations of the dusk exodus flights of the bat colony inhabiting Bracken Cave (Texas, USA) to produce nightly colony population estimates over a continuous period spanning 20 March 1995 through 30 November 2017 (Stepanian & Wainwright, 2018). These high temporal resolution population estimates revealed cyclic seasonal changes in the Bracken Cave colony size that are indicative of migration phenology, and were used to extract quantitative annual phenophases corresponding with spring and autumn migration timing (Stepanian & Wainwright, 2018). The resulting dataset (Stepanian et al., 2020) provides annual dates on which 50% of the mean summer population is first detected at the cave (i.e., a quantitative metric for the onset of spring migratory arrivals to the cave), as well as the final dates on which 50% of the mean

summer population is detected (i.e., a quantitative metric for autumn dispersal out of the cave). These spring and autumn migration timings were obtained for 23 consecutive years (1995-2017; Figure 1). Spring migration showed a clear advancement over the study period (-0.64 days/year, standard error = 0.29, p-value t-test = 0.04), while autumn migration timing remained rather stable (-0.24 days/year, standard error = 0.49, p-value t-test = 0.63).

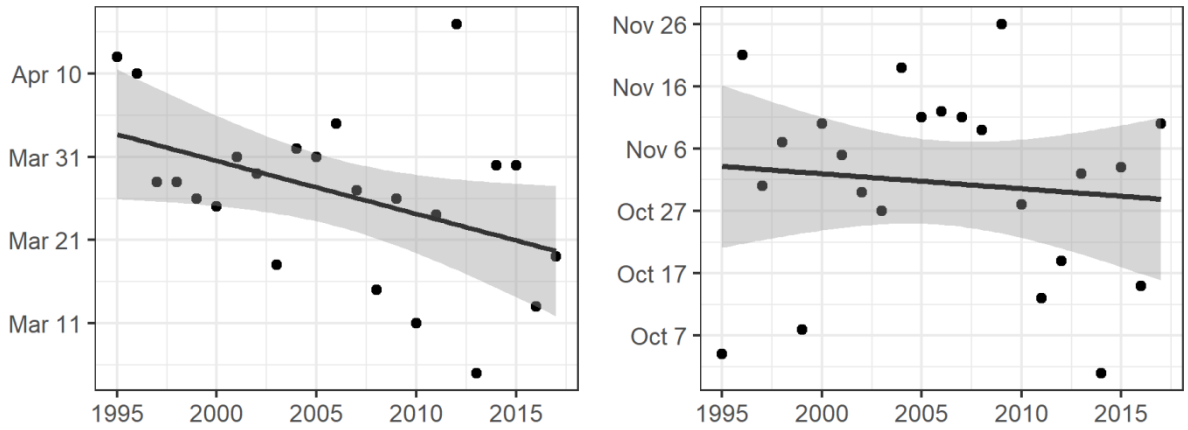

(a) Spring migration (b) Autumn migration

Figure 1 Spring (a) and autumn (b) migration timing of the bats at Bracken Cave over the period 1995-2017 as determined by Stepanian & Wainwright (2018). Lines represent estimated linear temporal trends (and grey areas the 95% confidence intervals). Spring migration (a) temporal slope coefficient = -0.64, standard error = 0.29, p-value (t-test) = 0.04; Autumn migration (b) temporal slope coefficient = -0.24, standard error = 0.49, p-value (t-test) = 0.63.

Weather data

We used the R package *RNCEP* (Kemp, van Loon, et al., 2012) to gather National Center for Environmental Prediction (NCEP) Reanalysis I data (Kalnay et al., 1996; Kanamitsu et al., 2002) on temperature, precipitation, and wind in an area from about 119° to 83° W, and 11° to 38° N (see maps in Appendix S1), which includes the entire countries of Honduras, El Salvador, Guatemala, Belize, and Mexico, and twenty south-western states of the USA partly or entirely. Ocean grid cells were masked from the analysis. While bats have been observed to migrate offshore (Hüppop & Hill, 2016), this is unlikely for bats passing through Bracken Cave (Wiederholt et al., 2013). The spatial resolution of a grid cell was 1.905° (latitude) x 1.875° (longitude) for temperature/precipitation and 2.5° x 2.5° for wind. At the northern edge of the analysed area, these resolutions correspond to 212 (latitude) x 164 (longitude) km, and 278 (latitude) x 217 (longitude) km, respectively. At the southern range of the studied area, the areas covered by the grid cells are somewhat larger, i.e. 212 (latitude) x 204 (longitude) km for temperature/precipitation and 278 (latitude) x 272 (longitude) km for wind. We derived eight variables from the NCEP data: mean daily air temperature at 2 meters above ground

level, daily accumulated precipitation at surface, daily mean wind direction at the 925, 850, and 700-hPa pressure levels, and daily mean wind assistance at the same three pressure levels (Appendix S1). The 925, 850, and 700-hPa atmospheric pressure levels roughly correspond to altitudes of 750, 1500, and 3000 m above-sea-level (asl), depending on geographic location and environmental conditions. In the time window analysis, the wind directions were used to calculate the number of days that wind at that location was in the direction towards, or coming from, Bracken Cave (at each of the atmospheric pressure levels), hence resulting in eleven variables in total being analysed. We did this by counting every day with a mean wind direction between -45° and 45° of the angle between Bracken Cave and the centre of the focal grid cell. Depending on the location of the grid cell relative to Bracken Cave, these winds were then interpreted as tail- or headwinds. In terms wind direction effects, we thus analysed two different potential hypotheses separately, i.e. days with headwinds delay migration and tailwinds advance migration. Additionally, we also analysed wind assistance to check for a joint effect of wind direction and wind speed. We calculated the wind assistance at each of the three atmospheric pressure levels with the *RNCEP* package (Kemp, van Loon, et al., 2012) using the „M.Groundspeed" equation (Kemp, Shamoun-Baranes, et al., 2012). While various approaches exist to calculate wind assistance, we deemed the „M.Groundspeed" approach most appropriate because Brazilian free-tailed bats have been observed (albeit during foraging flights) to maintain a relatively constant groundspeed irrespective of wind conditions (McCracken et al., 2016).

Determining the most likely combinations of "weather variable – location – time window" that influence migration phenology

To determine the combinations of "weather variable – location – time window" that most likely influence bat spring and autumn migration phenology, we used a method that has recently been shown effective on similar time series of bird migration phenology (Haest et al., 2018b, 2019, 2020b). The method consists of two consecutive analyses: (1) a broad search for all combinations of "weather variable – location – time window" that show a relationship with the migration phenology that is unlikely to be due to chance only (but might still be a false positive due to spatiotemporal correlation within and between the weather variables); and (2) a set of refined analyses to narrow down the candidates from the first step to the most likely influences.

More specifically, in the first step, a time-window analysis is performed for each weather variable on each grid cell to search for a (continuous) time window of any length that correlates better with the migration phenology data than is expected by chance. The time window search is performed using the *climwin* R package (Bailey & van de Pol, 2016; van de Pol et al., 2016). To determine the best-performing time window, the method compares AICc model values for each time window to a base reference model. We used a base reference model consisting of a linear temporal trend (i.e. a model with year as the independent variable) to avoid spurious correlations due to shared temporal trends (Haest et al., 2018a; Noriega & Ventosa-Santaulària, 2007). To estimate the probability of obtaining a

similarly performing `best` time window due to chance alone, the time window search is repeated on randomizations of the weather data. Ideally, at least a hundred randomizations are run to approximate the ΔAICc distribution of best-performing time windows obtainable by chance alone, which, however, quickly becomes highly resource-intensive. Therefore, we used the alternative probability statistic P_c of the *climwin* package, which uses as little as five randomizations to estimate the probability of obtaining a similarly performing best time window due to chance alone (Bailey & van de Pol, 2016; van de Pol et al., 2016). The P_c statistic ranges from 0 to 1, with values closer to 0 indicating a higher probability that the relationship is not due to chance. For a sample size of 23 (as the number of years in our study) and a cut-off value of $P_c < 0.5$, Bailey & van de Pol (2016) estimated the rate of false positives and negatives to be about 0.14 and 0.10, respectively. These rates, however, apply to simulated relationships ranging from 0.2 to 0.8 in strength (R^2). The stronger the simulated relationship with the response variable, the lower these rates become. To lower the probabilities of false positives in our analysis, we set the P_c threshold to 0.3 (instead of 0.5) (see Bailey & van de Pol, 2016). For ease of reference, all settings and decision rules of the time windows analyses are summarized in Table S1 and S2. From the output of the time window analyses, we created ΔAICc, R^2, and regression slope maps for each weather variable, representing the values of the best model for each grid cell, excluding the grid cells for which $P_c > 0.3$ (Figure S1 to S22). In many cases, neighbouring cells in these maps had similar time windows and ΔAICc for the best-performing model due to spatiotemporal autocorrelation in the weather variables. As a result, there are spatial gradients present in these maps. We considered the cells with regional ΔAICc maxima as the most representative of the potential relation between the weather variable for that (larger, correlated) area and the migration phenology at Bracken Cave. This first step of the analysis resulted in 43 and 56 potential "weather variable – location – time window" influences for spring and autumn migration, respectively (Figure S1 to S22).

In the second part of the analysis, we extracted those candidate signals from the potential influences that are most likely to have the strongest influence on the migration phenology. To do so, we first use a sequence of different variable filtering approaches to remove the (relatively) least likely candidates, followed by an ensemble of (relative) "variable importance" methods to determine the most likely final "weather variable – location – time window" influences. Throughout this analysis, we no longer include the temporal trend, i.e. the „year" variable, as spurious correlations due to shared trends were already excluded in the first part of the analysis. Instead, we now assess to what extent the relationship between the identified potential effects of weather and the observed migration phenology still holds when not accounting for temporal trends. In a first filtering, we compared AICc values for models with the identified effects of weather as the only independent variable to an intercept-only model. We removed two potential influences for spring migration (and none for autumn migration), because the AICc difference with the intercept-only model was less than two units. Subsequently, we checked for collinearity between the remaining candidate weather effects. For spring and autumn migration, we

removed 21 and 28 candidates, respectively, because they had a Pearson correlation > 0.7 (Dormann et al., 2013) with another candidate that had a larger ΔAICc with an intercept-only model. Next, we used the *boruta* method to further remove 6 and 14 candidate influences for spring and autumn migration, respectively, that had a variable importance that is likely to be obtained by chance (Kursa & Rudnicki, 2010). Finally, we used an ensemble of "variable importance" methods (Burnham & Anderson, 2002; Grömping, 2006, 2015; Kursa & Rudnicki, 2010) to identify the most likely "weather variable – location – time window" influences on bat spring and autumn migration phenology (Figure 2; Table S3 and S4).

Climatic contributions to trends in phenology

A weather variable that affects inter-annual variability in migration timing can only result in a temporal trend in migration phenology if it also shows a temporal trend. The overall contribution of a weather variable to the observed temporal trend in migration phenology can be calculated using the chain rule (Haest et al., 2019, 2020b; McLean et al., 2018):

$$\begin{matrix} climate\ contributions\ to \\ trend\ in\ migration\ phenology \end{matrix} = \sum_{i=1}^{n} \left(\frac{\partial MPD}{\partial Climate_i} \times \frac{dClimate_i}{dTime} \right),$$

with n being the total number of influencing weather variables for a given species; $\partial MPD/\partial Climate_i$ the regression coefficients of a multiple linear regression between (spring or autumn) migration passage date and all of the identified final weather variables; and $dClimate_i/dTime$ the regression coefficient of a simple linear regression between the respective weather variable and time, i.e. years. Standard errors were calculated following error propagation rules for multiplication (Taylor, 1997). Note that this approach ignores by definition any other (e.g. non-climatic) factors that might possibly affect changes in migration phenology over time.

RESULTS

Identified „weather variable – location – time window" influences

We found that during spring migration tailwinds in central North Mexico and West Texas to the west of Bracken Cave (Figure 2) explain about 84% of the observed variance in spring migration phenology (Table 1). The tailwinds were negatively related to spring migration phenology (Table 2). Thus, more days with tailwinds in central North Mexico and West Texas result in earlier spring passage or arrival at Bracken Cave. For each (additional) day of tailwind during spring migration, bats passed on average about 2 to 2.2 days earlier at Bracken Cave. The central North Mexico tailwind occurred at the 850-hPa pressure level (i.e. roughly 1500 m asl), while the western Texas tailwind was at the 925-hPa level (i.e. roughly 750 m asl).

For autumn migration, summer and autumn precipitation to the east-northeast of Bracken Cave (Figure 2) explained about 83% of the observed variance. The two precipitation signals had contrasting effects (Figure 4 and Table 2), i.e. precipitation in Northeast Texas / Southeast Oklahoma / Arkansas / West Louisiana results in later average autumn migration, while precipitation in eastern Texas and Louisiana results in earlier autumn migration. Additionally, we found strong statistical support for an influence of headwind at the 700-hPa level (i.e. approximately 3000 m asl) in north-western Mexico (Sonora / Baja California / Chihuahua) on autumn migration phenology.

Table 1 Explained variance (adjusted R^2) and predictive performance (predictive R^2) for spring and autumn migration phenology using a linear model with the final identified weather signals (see Figure 1), but not the temporal trend. Adjusted R^2 is defined as in Miles (2005). Predictive R^2 was calculated as leave-one-year-out.

Season	Weather variables	Adjusted R^2	Predictive R^2
Spring	Both wind variables	0.84	0.81
Autumn	Both precipitation + the wind variable	0.88	0.86
Autumn	Both precipitation variables	0.83	0.79

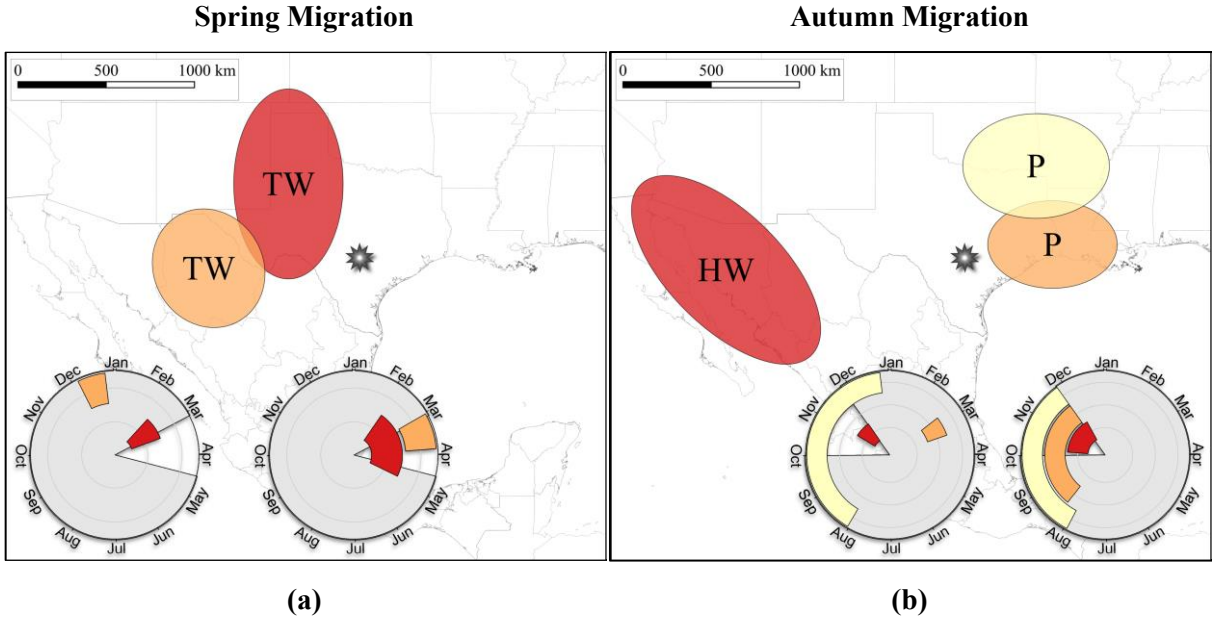

Figure 2 Location and timing of the identified most important weather variables that are likely to influence (a) spring and (b) autumn migration timing at Bracken Cave. The timelines in each plot represent the period of the single best time window (left) and of the medians for the time window opening and closing of the 95% confidence interval of all time windows (right). P: precipitation; HW: headwind; TW: tailwind. The location of Bracken Cave is marked with a star. The white background triangles in the time window subfigures represent the migration period at Bracken Cave, i.e. the period between the earliest and latest estimated average migration time at Bracken Cave over the entire study period (see Stepanian and Wainwright, 2018).

Although our analyses included a large area of potential effects of weather - from Nicaragua in the south, Nevada in the northwest, and Kentucky to the northeast (Appendix S1) - four of the five identified influences lie within distances up to 1100 km around Bracken Cave, i.e. well within the

currently known (maximum) migration distance of Brazilian free-tailed bats (Cockrum, 1969; Glass, 1982). The times during which the weather variables influence migration span the period from about two months prior to the earliest and up to the latest estimated mean migration time, in both spring and autumn. Due to the inherent temporal autocorrelation of weather variables, the exact timing of the time windows remains somewhat uncertain (Figure 2).

Predictive R^2 (calculated using leave-one-year-out) were not much lower (0.03 for spring and 0.04 for autumn) than adjusted R^2 (Miles, 2005), indicating that the final identified effects of weather are robust, i.e. the models do not suffer from overfitting. We did not find any support for influences of either temperature or wind assistance on spring or autumn migration.

Table 2 Effect sizes and standard errors (SE) for the identified most influential weather variables, estimated using the full linear model consisting of the migration phenology as the dependent response variable and all of the identified weather variables (but not the temporal trend) as the independent variables.

Season	Weather variable	Location	Effect Size	SE
Spring	tailwind 925-hPa	North Coahuila de Zaragoza / East New Mexico / West Texas	-2.20	0.45
	tailwind 850-hPa	Central North Mexico (Chihuahua)	-2.06	0.36
Autumn	precipitation	Northeast Texas / Southeast Oklahoma / Arkansas / West Louisiana	0.06	0.01
	precipitation	East Texas / Louisiana	-0.41	0.07
	headwind 700-hPa	Sonora / Baja California / Chihuahua	-2.46	0.75

Contributions of climatic influences to temporal trends in migration phenology

The wind conditions in north Mexico and western Texas did not only have a strong effect on inter-annual variability in spring migration phenology, they also showed temporal trends over the 1995-2017 study period (Figure 3, Table S5). More days with tailwinds at both locations have led to a systematically earlier mean spring migration at Bracken Cave, with advancements of approximately 5 and 12 days over the period 1995-2017 (Figure 3 and Table S5).

A decrease in the (positively associated) summer and autumn precipitation in Northeast Texas, Southeast Oklahoma, Arkansas, and West Louisiana seems to have pushed towards a slight advancement in autumn migration timing at Bracken Cave, while lower spring precipitation in East Texas and Louisiana seems to have resulted in a slight delay (Figure 4, Table S5). Please note, however, that autumn migration timing at Bracken Cave did not show a significant temporal trend over the study period (Stepanian & Wainwright, 2018; Figure 1).

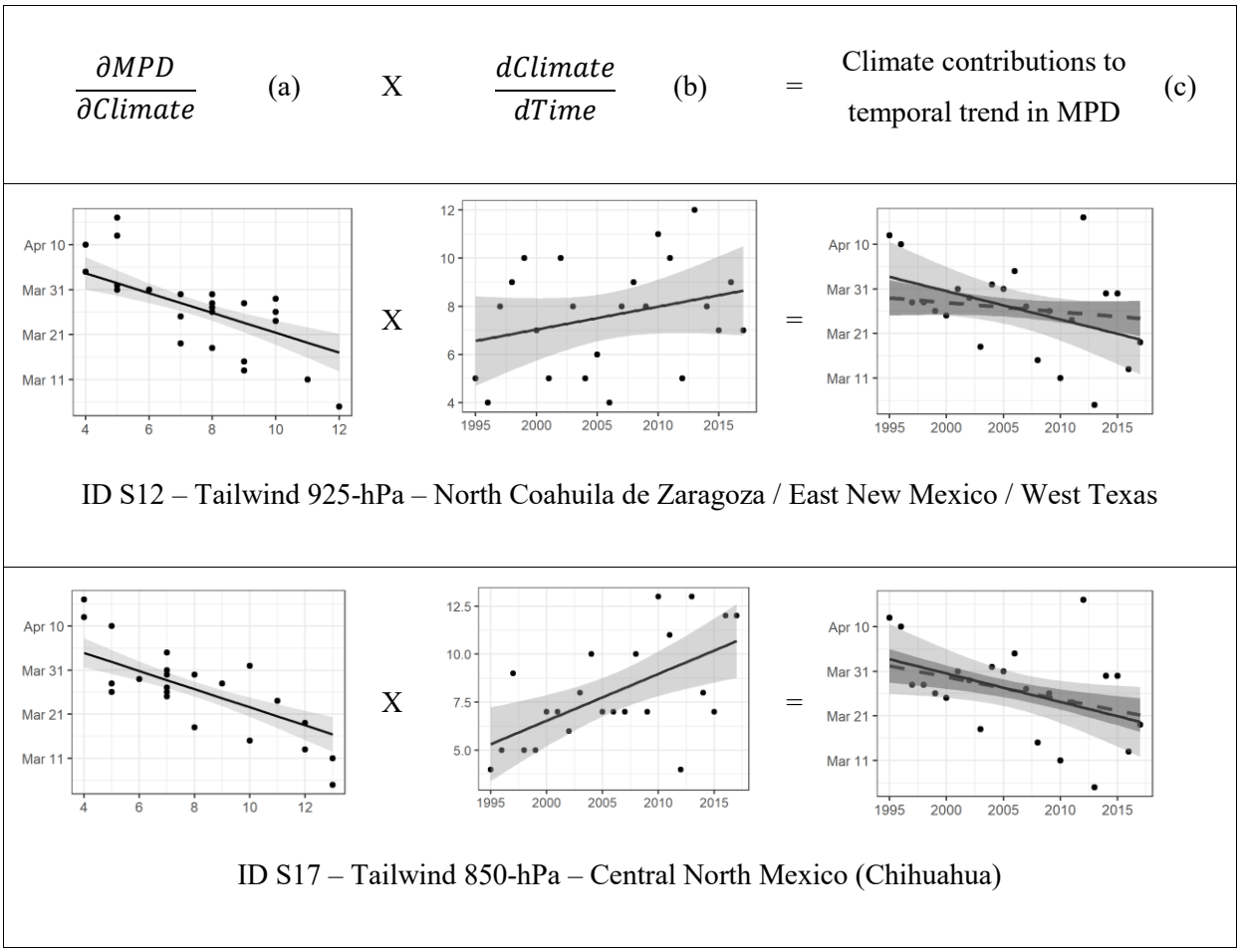

Figure 3 Overview of (a) the effect of the identified weather signals on spring migration phenology of Brazilian free-tailed bats at Bracken Cave; (b) the temporal trends in these weather variables; and (c) the resulting contribution to the overall temporal trends in spring migration phenology. In (c), the dashed lines represent the calculated trend contributions using the chain rule (see Table S5), and the full lines the overall observed trends in spring migration phenology (see Figure 1). Dark grey ribbons in (c) are the 95% confidence interval for the estimated trend contribution, and light grey for the overall temporal trend.

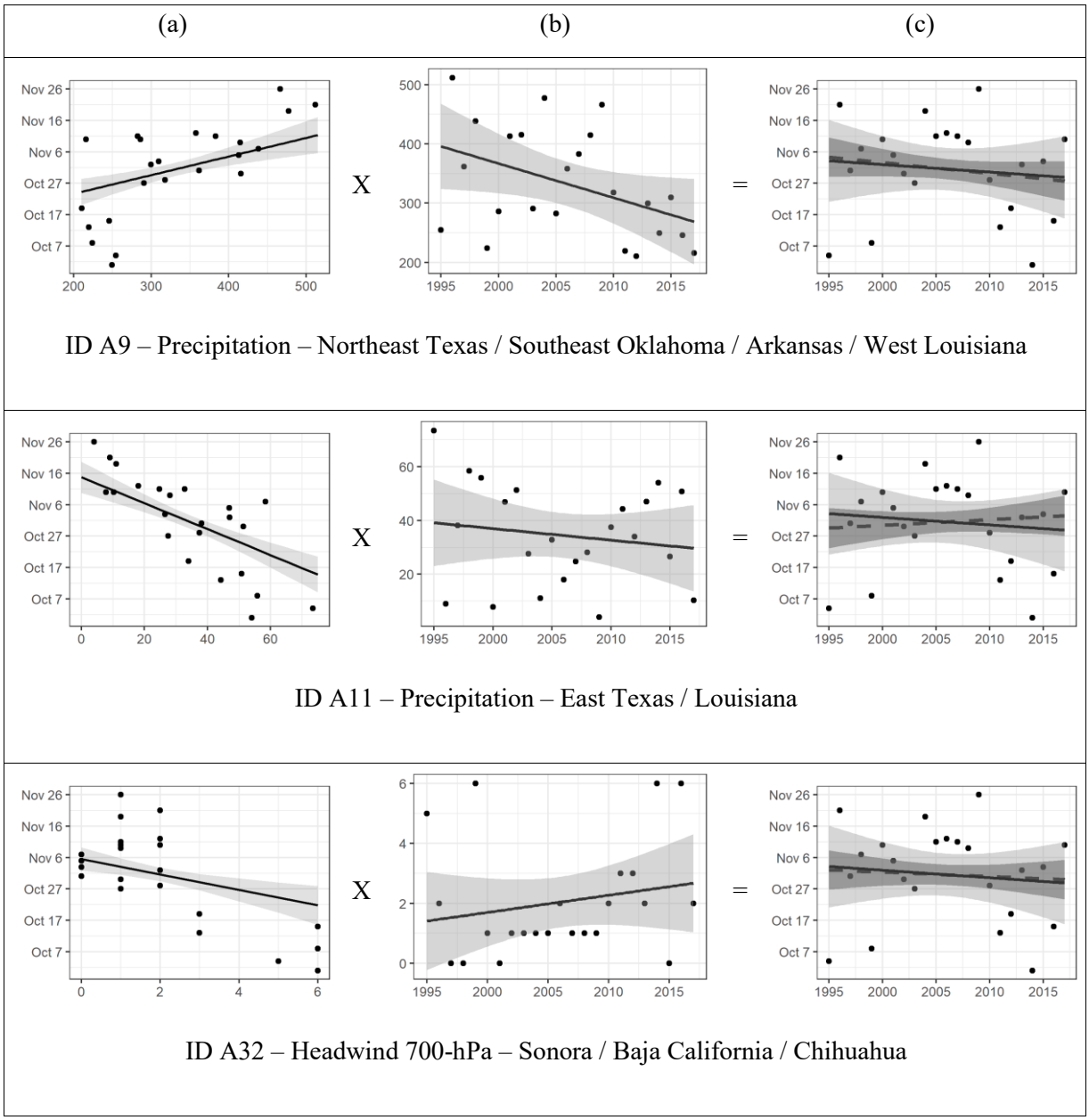

Figure 4 Overview of (a) the effect of the identified weather signals on autumn migration phenology of Brazilian free-tailed bats at Bracken Cave; (b) the temporal trends in these weather variables; and (c) the resulting contribution to the overall temporal trends in autumn migration phenology. In (c), the dashed lines represent the calculated trend contributions using the chain rule (see Table S5), and the full lines the overall observed trends in autumn migration phenology (see Figure 1). Dark grey ribbons in (c) are the 95% confidence interval for the estimated trend contribution, and light grey for the overall temporal trend.

DISCUSSION

Migration and population structure of Brazilian free-tailed bats at Bracken Cave

Our results suggest that in spring Brazilian free-tailed bats that use Bracken Cave as a spring stopover or maternity location move eastward. These bats seem to originate from central North Mexico (Figure 2) and western Texas, and these areas could be wintering grounds, spring stopover, mating locations,

or a mixture of all of these (see also Wiederholt et al., 2013). Brazilian free-tailed bats mate in spring. Where bats exactly congregate to mate has, however, remained largely elusive (Keeley & Keeley, 2004; Svoboda et al., 1985). It has been suggested that they gather in transitional roosts in Mexico shortly before or during northward migration (McCracken et al., 1994; Russell & McCracken, 2006; Wilkins, 1989), although copulation has also been observed during March and April in central Texas (Keeley & Keeley, 2004). The combined location and timing of our spring wind influences, i.e. December to April, suggests that these might be the locations (and times) where mating (mainly) occurs. Individuals from many different maternity roosts (ranging from west to east USA) perhaps mingle at these locations during spring migration, which may also explain the observed lack of genetic structuring in the North American populations (McCracken et al., 1994; Russell & McCracken, 2006).

Surprisingly, we did not find weather at Bracken Cave itself to influence autumn migration phenology. Instead, migration phenology at Bracken Cave was dominated by precipitation to the east and northeast of Bracken Cave (Figure 2). These areas might represent maternity colonies of bats that stopover in Bracken Cave, post-parturition feeding grounds of adult females and juveniles (of perhaps also bats from the Bracken Cave maternity colony), or a mixture of these (see also McCracken et al., 2018). Alternatively, the weather at these locations could also affect migratory decisions at Bracken Cave indirectly, e.g. through insect migrations originating from these areas (Krauel et al., 2015, 2018). Adult female Brazilian free-tailed bats (likely) leave their maternity colonies (such as Bracken Cave) after they weaned their young (Davis et al., 1962; Hristov et al., 2010; Krauel & McCracken, 2013), and often even move northwards (Glass, 1982; Russell & McCracken, 2006). Autumn movements in the direction of and to, as well as spring stopover at Bracken Cave by bats from (maternity) colonies in Oklahoma have also been observed before from banding recoveries (Glass, 1959, 1982).

The contrasting directions of the precipitation effects on autumn migration phenology may seem contradictory (Figure 2 and Table 2). However, if, for example, precipitation affects migration phenology through insect abundance, differences in insect abundance at the two locations may affect bat survival and result in different abundances (Frick et al., 2010) or reproductive rates (Adams, 2010) at each location. If the populations at each location tend to migrate through Bracken Cave at different times, these differences in abundances between the two populations may, hence, change the overall observed autumn migration phenology at Bracken Cave in different directions. Alternatively, precipitation in spring and autumn may have contrasting effects, i.e. higher precipitation in autumn leads to later autumn migration, whereas higher spring precipitation leads to earlier autumn migration.

The influence of headwind in northwest Mexico (Figure 2) seems to challenge the current knowledge on migration patterns of Brazilian free-tailed bats (but see ring recovery maps in Villa & Cockrum, 1962; and Wiederholt et al., 2013). Although we have tailored our approach towards avoiding false positives, we can not exclude them entirely (Bailey & van de Pol, 2016). Nevertheless, such long-distance West-East movements have, albeit perhaps more rarely, been observed in banding studies, including an individual that was banded in Nevada and recovered in Kansas (Baker, 1978; Cockrum,

1969; Fleming & Eby, 2003; Svoboda et al., 1985). Additionally, the ecology of Brazilian free-tailed bats during winter is hardly known, including exact locations and time periods. While their summer ecology is generally better known, much of the knowledge originates from females and first-year juveniles while the ecology of males is much less known.

Bats that use Bracken Cave in spring and autumn do not necessarily originate from the same populations, i.e. some populations may use it as a spring transient roost, and others in autumn. While winter site fidelity has been suggested in other (hibernating) migratory bat species (Lehnert et al., 2018), migratory routes and stopover routes need not be identical in spring and autumn. In general, our results suggest more of an East-West, instead of North-South, migratory movement of Brazilian free-tailed bats passing at Bracken Cave (Figure 2). Interestingly, a similar observation was recently made, also contradicting expectation, for Indiana bats (*Myotis sodalis*) (Roby et al., 2019).

Drivers of bat migration phenology

The importance of climate and atmospheric conditions for bat migration ecology has long been recognized (Liechti & McGuire, 2017). Until recently, however, the proposed influences of weather on bat migration were almost exclusively based on anecdotal observations of weather conditions during (migratory) flight activity (e.g. Baker, 1978; Davis et al., 1962; Petersons, 2004). Temperature, precipitation, pressure, wind conditions, and lunar illumination have all been suggested as likely migratory drivers (Dechmann et al., 2017; Pettit & O'Keefe, 2017; Roby et al., 2019; Smith & McWilliams, 2016). While perhaps all of these weather conditions may, to a certain degree, have a direct impact on (migratory) flight activity, the exact cues, drivers, and underlying mechanisms of seasonal bat migration have not been identified due to a lack of long-term (i.e. multi-annual) data and detailed knowledge on spatiotemporal migratory patterns (Pettit & O'Keefe, 2017).

We found wind conditions, i.e. the frequency of days with tailwinds during spring migration, to explain most of the inter-annual variability in spring migration phenology of bats at Bracken Cave (Figure 2 and Table 1). Wind in favourable directions also influenced spring migration departure probability of European common noctule bats (*Nyctalus noctula*) (Dechmann et al., 2017). Effects of winds are probably direct, i.e. by influencing departure decisions or migratory flight progress. Brazilian free-tailed bats appear to adjust their airspeed to maintain similar ground speeds regardless of wind support, and ground speeds also do not seem influenced by the direction of prevailing winds (McCracken et al., 2016). Additionally, we did not find any support for an influence of wind assistance on migratory timing. This suggests that advanced or delayed spring migrations with tailwinds and headwinds, respectively, do not result from increased or decreased distances covered but, instead, from decisions to continue migration or stay at a (transient) roost. Combined with the findings of Dechmann et al. (2017) and Pettit & O'Keefe (2017), this indicates that bats rely primarily on day (or night) length as the cue for initiating spring migration, but that the decision to effectively depart or continue the spring migratory journey is strongly determined by wind conditions. Even

though (insectivorous) bats generally live energetically demanding lives, both migration and reproduction (i.e. late pregnancy and lactation) periods are even more energetically demanding (Sommers et al., 2019). Choosing favourable wind conditions for migration is a simple effective mechanism to save energy during movement and arrive in good body condition at the maternity grounds.

While knowledge on flight altitudes of bats during migration specifically is sparse, the highest densities of Brazilian free-tailed bats during foraging flights have been shown to occur at around 400 to 600 m above-ground-level (agl) (McCracken et al., 2008). For spring migration, we found a tailwind influence at the 850- and 925-hPa pressure level, i.e. approximately 1500 and 750 m asl. The higher ground elevations (Figure S23) at the approximate location (Figure 2) of the 850-hPa tailwind effect compared to those at the 925-hPa tailwind location, indicate that the difference in pressure levels or elevations asl between these effects probably does not reflect differences in migration altitudes, but instead mainly differences in ground elevations. Hence, while Brazilian free-tailed bats have been observed at altitudes exceeding 3000 m agl (Williams et al., 1973), our results point towards flight altitudes during (spring) migration similar to those during foraging flights (McCracken et al., 2008). The autumn wind influence at the 700-hPa or approximately 3000 m asl altitude, however, perhaps indicates higher flight altitudes during autumn migration.

We found precipitation to be the main driver of autumn migration phenology of bats at Bracken Cave (Figure 2 and Table 1). While precipitation has often been suggested to affect bat migration, it has yet to be determined how this exactly works and how important the effect of precipitation is relative to other variables. One possibility is a direct negative influence of precipitation on (migratory) flight activity (McGuire et al., 2012; Pettit & O'Keefe, 2017; Voigt et al., 2011). Another might be the indirect (positive) influence of precipitation on insect abundance (Hristov et al., 2010), and perhaps particularly the abundance of migratory insects (Krauel et al., 2018; Lee & McCracken, 2005). Furthermore, precipitation may also influence migratory timing through other indirect pathways, e.g. carry-over effects of the timing of reproduction (Grindal et al., 1992; Linton & Macdonald, 2018) or effects on reproductive rates (Linton & Macdonald, 2018). We found a positive association between autumn precipitation and migration phenology, i.e. passage or departure at Bracken Cave is later in years with more autumn precipitation (Figure 2, Table S5). This positive relationship conforms to expectations for a (negative) direct effect of precipitation on (migratory) flight activity, as well as an indirect effect through either increased insect abundance or delayed insect migration that may result in delayed bat migration. Unfortunately, very little is known about the drivers and mechanisms influencing migratory behaviour (e.g. timing) of insects in general (Satterfield et al., 2020), and even less so for autumn migration specifically (Krauel et al., 2015). Increased insect abundance is, however, often linked to higher precipitation levels (Krauel et al., 2018), and migration theory predicts the optimal time for bat migration to be determined by (changes in) insect abundance (Hedenström, 2009; Krauel & McCracken, 2013). The effect of insect abundance on Brazilian free-tailed bat migration has

previously been suggested to work through the effect wind has on migratory insects (Krauel et al., 2015). Our results suggest that it is mainly precipitation that affets overall insect abundance, including those of migratory populations. Finally, the timing of our precipitation effects in autumn suggests that it does not work through carry-over effects of delayed parturition or increased reproductive success (Figure 2). Wet springs, however, have also been associated with reduced insect abundance (Krauel et al., 2015; Lee & McCracken, 2005; Pair & Westbrook, 1995), which could also result in earlier autumn migration.

We found no influence of temperature. Brazilian free-tailed bats seem to be highly physiologically and morphologically adapted to living under relatively extreme (both warm and cold) temperature conditions but occur mostly in relatively warm geographic areas (Reichard et al., 2010). Moreover, a small overwintering population has been shown to inhabit Bracken Cave across the duration of the 23-year period, demonstrating the physiological ability for bats to even survive the winter at this site (Stepanian & Wainwright, 2018). This may explain why migration in Brazilian free-tailed bats is not driven by temperature but by precipitation and wind - contrary to species in regions with more extreme inter-seasonal temperature differences, e.g. at higher latitudes. Some studies of migratory bats (at higher latitudes) in northern Europe or North America, have indeed suggested that temperature plays an important role in migration timing (Jonasson & Guglielmo, 2019; Muthersbaugh et al., 2019; Pettit & O'Keefe, 2017; Roby et al., 2019; Rydell et al., 2014; Smith & McWilliams, 2016), although temperature was often investigated alone, neglecting possible precipitation and wind effects. However, it is possible that wind and precipitation become primary drivers of migratory timing in regions where a minimum temperature threshold for survivability is met throughout the migration period. Note that we analysed mean daily air temperatures in this study, and influences of other temperature-based metrics, e.g. daily minimum temperature, cannot be entirely excluded.

In birds, it has repeatedly been shown that the relative influence of different weather variables on migration phenology is strongly species-, but also context-dependent (Gordo, 2007; Haest et al., 2018b, 2019; Shaw, 2016), and a similarly diverse response to weather has been suggested for bats (Muthersbaugh et al., 2019). Therefore, future studies on other bat species and populations may find our results of wind being highly important for spring migration and precipitation for autumn migration timing to be specific for Brazilian free-tailed bats. However, we think that the migration of bats adheres to general principles that determine which weather variables will be relevant for migration timing: (1) optimization of (metabolic) migratory costs by choosing the atmospheric conditions (including wind, temperature, and precipitation) that favour efficient energy use; and (2) adjustment to (current or expected) changes in food availability, e.g. insect prey (Bauer et al., 2011; Fleming & Eby, 2003; Krauel & McCracken, 2013; Pettit & O'Keefe, 2017). Depending on the geographic, climatic, and individual context, the relative importance of these principles may vary, and thus also the relative importance of the weather (and other) variables that influence specific species/populations.

Climate change, bat migration, and conservation of bats

For climate change to cause changes in the timing of a biological event, weather does not only need to influence the biological event, i.e. cause inter-annual variability, but the relevant weather variable also needs to show a distinct temporal trend. Our results indicate that the spring migration phenology of Brazilian free-tailed bats at Bracken Cave advanced because wind conditions favourable for migration occurred more frequently (Figure 3). Interestingly, favourable wind conditions are expected to continue becoming more prevalent over the next century in this part of the USA (La Sorte et al., 2019), raising questions on whether and how this will continue to affect bat migration timing at Bracken Cave.

Brazilian free-tailed bats have been proposed as a key indicator species for climate-change impacts on global migratory bat species (Newson et al., 2009). Yet, even in this relative intensively-studied bat species, large uncertainties remain on (changes in) colony-specific population sizes, and hence even more so on overall species abundance (McCracken, 2003; Stepanian & Wainwright, 2018). Even less is known on how weather and climate change may cause inter-annual differences or long-term trends in bat population sizes. Effects of weather on processes directly affecting population sizes, such as reproductive success (Linton & Macdonald, 2018) and timing (Grindal et al., 1992), have been suggested in some bat species. Since long-term data across species and large scales are still largely lacking, the specific pathways through which weather affects abundances remain unidentified (Sherwin et al., 2013). Over the period 1995-2017, the mean summer population of Brazilian free-tailed bats at Bracken Cave did not show any significant temporal trend (Stepanian & Wainwright, 2018), suggesting that the trends in phenology have not (yet) had consequences on population levels of Brazilian free-tailed bats at Bracken Cave. Our results illustrate how long-term time series derived from weather radar data can provide unique insights into climate change impacts on Brazilian free-tailed and other, especially cave-dwelling, bat colonies. In this paper, we focused on identifying the effects of climate (change) on migration phenology, but a similar approach could be used to assess the potential relationship between changes in inter-annual population sizes and climate (change).

DATA AVAILABILITY STATEMENT

The phenology data necessary to replicate the results of this study have been deposited in the Zenodo repository, https://doi.org/10.5281/zenodo.3945907 (Stepanian et al., 2020). The code from (Haest et al., 2020a) can be used to replicate the analysis. NCEP Reanalysis data provided by the NOAA/OAR/ESRL PSL, Boulder, Colorado, USA, and downloaded from their Web site at https://psl.noaa.gov/.

ACKNOWLEDGEMENTS

This research was funded through the 2017-2018 Belmont Forum and BiodivERsA joint call for research proposals, under the BiodivScen ERA-Net COFUND programme, and with the funding organisations Swiss National Science Foundation (SNF 31BD30_184120), Belgian Federal Science Policy Office (BelSPO BR/185/A1/GloBAM-BE), Netherlands Organisation for Scientific Research (NWO E10008), Academy of Finland (aka 326315) and National Science Foundation (NSF 1927743). P. Stepanian was supported by NSF Division of Emerging Frontiers Grant 1840230. We would also like to thank the editor and an anonymous reviewer for their constructive comments.

REFERENCES

Adams, R. A. (2010). Bat Reproduction Declines When Conditions Mimic Climate Change Projections for Western North America. *Ecology*, *91*(8), 2437–2445. https://doi.org/10.1890/09-0091

Bailey, L. D., & van de Pol, M. (2016). climwin: An R Toolbox for Climate Window Analysis. *PLoS ONE*, *11*(12), e0167980. https://doi.org/10.1371/journal.pone.0167980

Baker, R. R. (1978). *The Evolutionary Ecology of Animal Migration*. Holmes & Meier Publishers.

Bauer, S., & Hoye, B. J. (2014). Migratory Animals Couple Biodiversity and Ecosystem Functioning Worldwide. *Science*, *344*(6179), 1242552–1242552. https://doi.org/10.1126/science.1242552

Bauer, S., Nolet, B. A., Giske, J., Chapman, J. W., Åkesson, S., Hedenström, A., & Fryxell, J. M. (2011). Cues and Decision Rules in Animal Migration. In E. J. Milner-Gulland, J. M. Fryxell, & A. R. E. Sinclair (Eds.), *Animal Migration: A synthesis* (pp. 68–87). Oxford University Press. https://doi.org/10.1093/acprof

Bauer, S., Shamoun-Baranes, J., Nilsson, C., Farnsworth, A., Kelly, J. F., Reynolds, D. R., Dokter, A. M., Krauel, J. F., Petterson, L. B., Horton, K. G., & Chapman, J. W. (2019). The grand challenges of migration ecology that radar aeroecology can help answer. *Ecography*, *42*(5), 861–875. https://doi.org/10.1111/ecog.04083

Bowlin, M. S., Bisson, I.-A., Shamoun-Baranes, J., Reichard, J. D., Sapir, N., Marra, P. P., Kunz, T. H., Wilcove, D. S., Hedenström, A., Guglielmo, C. G., Åkesson, S., Ramenofsky, M., & Wikelski, M. (2010). Grand challenges in migration biology. *Integrative and Comparative Biology*, *50*(3), 261–279. https://doi.org/10.1093/icb/icq013

Britzke, E. R., Loeb, S. C., Hobson, K. A., Romanek, C. S., & Vonhof, M. J. (2009). Using Hydrogen Isotopes to Assign Origins of Bats in the Eastern United States. *Journal of Mammalogy*, *90*(3), 743–751. https://doi.org/10.1644/08-MAMM-A-211R2.1

Burnham, K. P., & Anderson, D. R. (2002). *Model Selection and Multimodel Inference: A Practical Information-Theoretic Approach - 2nd edition*. Springer Science+Business Media LLC.

Charmantier, A., & Gienapp, P. (2014). Climate change and timing of avian breeding and migration: evolutionary versus plastic changes. *Evolutionary Applications*, *7*(1), 15–28. https://doi.org/10.1111/eva.12126

Chmura, H. E., Kharouba, H. M., Ashander, J., Ehlman, S. M., Rivest, E. B., & Yang, L. H. (2019). The mechanisms of phenology: the patterns and processes of phenological shifts. *Ecological Monographs*, *89*(1), e01337. https://doi.org/10.1002/ecm.1337

Cockrum, E. L. (1969). Migration in the guano bat, Tadarida brasiliensis. In J. K. J. Jones (Ed.), *Contributions in mammalogy* (pp. 303–336). Museum of Natural History, Miscellaneus Publication No. 51. Lawrence: Univ. Kansas Printing Service, 428 pp.

Cryan, P. M. (2003). Seasonal distribution of migratory tree bats (Lasiurus and Lasionycteris) in North America. *Journal of Mammalogy*, *84*(2), 579–593.

Davis, R. B., Herreid II, C. F., & Short, H. L. (1962). Mexican Free-Tailed Bats in Texas. *Ecological Monographs*, *32*(4), 311–346.

Dechmann, D. K. N., Wikelski, M., Ellis-Soto, D., Safi, K., & O'Mara, M. T. (2017). Determinants of

spring migration departure decision in a bat. *Biology Letters*, *13*(9), 20170395. https://doi.org/10.1098/rsbl.2017.0395

Dormann, C. F., Elith, J., Bacher, S., Buchmann, C. M., Carl, G., Carré, G., Marquéz, J. R. G., Gruber, B., Lafourcade, B., Leitão, P. J., Münkemüller, T., Mcclean, C., Osborne, P. E., Reineking, B., Schröder, B., Skidmore, A. K., Zurell, D., & Lautenbach, S. (2013). Collinearity: A review of methods to deal with it and a simulation study evaluating their performance. *Ecography*, *36*(1), 027–046. https://doi.org/10.1111/j.1600-0587.2012.07348.x

Ellison, L. E. (2008). Summary and Analysis of the U.S. Government Bat Banding Program: U.S. Geological Survey Open-File Report 2008-1363. *Program*, 117.

Fleming, T. H. (2019). Bat Migration. In *Encyclopedia of Animal Behavior* (Issues 2nd edition, Volume 3, pp. 605–610). Elsevier. https://doi.org/10.1016/B978-0-12-809633-8.20764-4

Fleming, T. H., & Eby, P. (2003). Ecology of Bat migration. In T. H. Kunz & M. B. Fenton (Eds.), *Bat Ecology* (pp. 156–208). The University of Chicago Press, Chicago, IL.

Frick, W. F., Reynolds, D. S., & Kunz, T. H. (2010). Influence of climate and reproductive timing on demography of little brown myotis Myotis lucifugus. *Journal of Animal Ecology*, *79*(1), 128–136. https://doi.org/10.1111/j.1365-2656.2009.01615.x

Frick, W. F., Stepanian, P. M., Kelly, J. F., Howard, K. W., Kuster, C. M., Kunz, T. H., & Chilson, P. B. (2012). Climate and weather impact timing of emergence of bats. *PLoS ONE*, *7*(8), 1–8. https://doi.org/10.1371/journal.pone.0042737

Glass, B. P. (1959). Additional Returns from Free-Tailed Bats Banded in Oklahoma. *Journal of Mammalogy*, *40*(4), 542–545.

Glass, B. P. (1982). Seasonal Movements of Mexican Freetail Bats Tadarida brasiliensis mexicana Banded in the Great Plains. *The Southwestern Naturalist*, *27*(2), 127–133.

Gordo, O. (2007). Why are bird migration dates shifting? A review of weather and climate effects on avian migratory phenology. *Climate Research*, *35*(1–2), 37–58. https://doi.org/10.3354/cr00713

Grindal, S. D., Collard, T. S., Brigham, R. M., & Barclay, R. M. R. (1992). The Influence of Precipitation on Reproduction by Myotis Bats in British Columbia. *The American Midland Naturalist*, *128*, 339–344.

Grömping, U. (2006). R package relaimpo: relative importance for linear regression. *Journal Of Statistical Software*, *17*(1), 139–147. https://doi.org/10.1016/j.foreco.2006.08.245

Grömping, U. (2015). Variable importance in regression models. *Wiley Interdisciplinary Reviews: Computational Statistics*, *7*(2), 137–152. https://doi.org/10.1002/wics.1346

Haest, B., Hüppop, O., & Bairlein, F. (2018a). Challenging a 15-year-old claim: The North Atlantic Oscillation index as a predictor of spring migration phenology of birds. *Global Change Biology*, *24*(4), 1523–1537. https://doi.org/10.1111/gcb.14023

Haest, B., Hüppop, O., & Bairlein, F. (2018b). The influence of weather on avian spring migration phenology: What, where and when? *Global Change Biology*, *24*(12), 5769–5788. https://doi.org/10.1111/gcb.14450

Haest, B., Hüppop, O., & Bairlein, F. (2020a). *Code and data for: "Weather at the winter and stopover areas determines spring migration onset, progress, and advancements in Afro-Palearctic migrant birds."* https://doi.org/10.5281/zenodo.3629178

Haest, B., Hüppop, O., & Bairlein, F. (2020b). Weather at the winter and stopover areas determines spring migration onset, progress, and advancements in Afro-Palearctic migrant birds. *Proceedings of the National Academy of Sciences*, *117*(29), 17056–17062. https://doi.org/10.1073/pnas.1920448117

Haest, B., Hüppop, O., Pol, M., & Bairlein, F. (2019). Autumn bird migration phenology: A potpourri of wind, precipitation and temperature effects. *Global Change Biology*, *25*(12), 4064–4080. https://doi.org/10.1111/gcb.14746

Hedenström, A. (2009). Optimal Migration Strategies in Bats. *Journal of Mammalogy*, *90*(6), 1298–1309. https://doi.org/10.1644/09-mamm-s-075r2.1

Holland, R. A., & Wikelski, M. (2009). Studying the Migratory Behavior of Individual Bats: Current Techniques and Future Directions. *Journal of Mammalogy*, *90*(6), 1324–1329. https://doi.org/10.1644/09-mamm-s-086r2.1

Hristov, N. I., Betke, M., Theriault, D. E. H., Bagchi, A., & Kunz, T. H. (2010). Seasonal variation in colony size of Brazilian free-tailed bats at Carlsbad Cavern based on thermal imaging. *Journal of Mammalogy*, *91*(1), 183–192. https://doi.org/10.1644/08-MAMM-A-391R.1

Hüppop, O., & Hill, R. (2016). Migration phenology and behaviour of bats at a research platform in the south-eastern North Sea. *Lutra*, *59*, 5–22. https://www.researchgate.net/publication/313239319

Hurlbert, A. H., & Liang, Z. (2012). Spatiotemporal variation in avian migration phenology: Citizen science reveals effects of climate change. *PLoS ONE*, *7*(2). https://doi.org/10.1371/journal.pone.0031662

Hutterer, R., Ivanova, T., Meyer-Cords, C., & Rodrigues, L. L. (2005). *Bat Migrations in Europe: A Review of Banding Data and Literature*. Federal Agency for Nature Conservation, Bonn, Germany.

Jonasson, K. A., & Guglielmo, C. G. (2019). Evidence for spring stopover refuelling in migrating silver-haired bats (Lasionycteris noctivagans). *Canadian Journal of Zoology*, *97*(11), 961–970. https://doi.org/10.1139/cjz-2019-0036

Kalnay, E., Kanamitsu, M., Kistler, R., Collins, W., Deaven, D., Gandin, L., Iredell, M., Saha, S., White, G., Woollen, J., Zhu, Y., Chelliah, M., Ebisuzaki, W., Higgins, W., Janowiak, J., Mo, K. C., Ropelewski, C., Wang, J., Leetmaa, A., … Joseph, D. (1996). The NCEP NCAR 40-Year Reanalysis Project. *Bulletin of the American Meteorological Society*, *77*(3), 437–472.

Kanamitsu, M., Ebisuzaki, W., Woollen, J., Yang, S.-K., Hnilo, J. J., Fiorino, M., & Potter, G. L. (2002). NCEP–DOE AMIP-II Reanalysis (R-2). *Bulletin of the American Meteorological Society*, *83*(11), 1631–1643. https://doi.org/10.1175/BAMS-83-11-1631(2002)083<1631:NAR>2.3.CO;2

Keeley, A. T. H., & Keeley, B. W. (2004). The Mating System of Tadarida brasiliensis (Chiroptera: Molossidae) in a Large Highway Bridge Colony. *Journal of Mammalogy*, *85*(1), 113–119. https://doi.org/10.1644/bme-004

Kemp, M. U., Shamoun-Baranes, J., van Loon, E., McLaren, J. D., Dokter, A. M., & Bouten, W. (2012). Quantifying flow-assistance and implications for movement research. *Journal of Theoretical Biology*, *308*(June), 56–67. https://doi.org/10.1016/j.jtbi.2012.05.026

Kemp, M. U., van Loon, E., Shamoun-Baranes, J., & Bouten, W. (2012). RNCEP: Global weather and climate data at your fingertips. *Methods in Ecology and Evolution*, *3*(1), 65–70. https://doi.org/10.1111/j.2041-210X.2011.00138.x

Krauel, J. J., Brown, V. A., Westbrook, J. K., & McCracken, G. F. (2018). Predator–prey interaction reveals local effects of high-altitude insect migration. *Oecologia*, *186*(1), 49–58. https://doi.org/10.1007/s00442-017-3995-0

Krauel, J. J., & McCracken, G. F. (2013). Recent Advances in Bat Migration Research. In *Bat Evolution, Ecology, and Conservation* (pp. 293–313). Springer New York. https://doi.org/10.1007/978-1-4614-7397-8_15

Krauel, J. J., Westbrook, J. K., & McCracken, G. F. (2015). Weather-driven dynamics in a dual-migrant system: Moths and bats. *Journal of Animal Ecology*, *84*(3), 604–614. https://doi.org/10.1111/1365-2656.12327

Kursa, M. B., & Rudnicki, W. R. (2010). Feature Selection with the Boruta Package. *Journal Of Statistical Software*, *36*(11), 1–13. http://www.jstatsoft.org/v36/i11/paper

La Sorte, F. A., Horton, K. G., Nilsson, C., & Dokter, A. M. (2019). Projected changes in wind assistance under climate change for nocturnally migrating bird populations. *Global Change Biology*, *25*(2), 589–601. https://doi.org/10.1111/gcb.14531

Lee, Y.-F., & McCracken, G. F. (2005). Dietary Variation of Brazilian Free-Tailed Bats Links To Migratory Populations of Pest Insects. *Journal of Mammalogy*, *86*(1), 67–76. https://doi.org/10.1644/1545-1542(2005)086<0067:dvobfb>2.0.co;2

Lehnert, L. S., Kramer-Schadt, S., Teige, T., Hoffmeister, U., Popa-Lisseanu, A. G., Bontadina, F., Ciechanowski, M., Dechmann, D. K. N., Kravchenko, K., Presetnik, P., Starrach, M., Straube, M., Zoephel, U., & Voigt, C. C. (2018). Variability and repeatability of noctule bat migration in Central Europe: evidence for partial and differential migration. *Proceedings of the Royal Society B: Biological Sciences*, *285*(1893), 20182174. https://doi.org/10.1098/rspb.2018.2174

Liechti, F., & McGuire, L. P. (2017). Facing the Wind: The Aeroecology of Vertebrate Migrants. In *Aeroecology* (pp. 179–198). Springer International Publishing. https://doi.org/10.1007/978-3-319-68576-2_8

Linton, D. M., & Macdonald, D. W. (2018). Spring weather conditions influence breeding phenology and reproductive success in sympatric bat populations. *Journal of Animal Ecology*, *87*(4), 1080–

1090. https://doi.org/10.1111/1365-2656.12832
López-González, C., & Best, T. L. (2006). Current Status of wintering sites of Mexican free-tailed bats Tadarida brasiliensis mexicana (Chiroptera: Molossidae) from Carlsbad Cavern, New Mexico. *Vertebrata Mexicana*, *18*, 13–22.
McCracken, G. F. (2003). Estimates of Population Sizes in Summer Colonies of of Brazilian Free-Tailed Bats (Tadarida brasiliensis). In T. J. O‟Shea & M. A. Bogan (Eds.), *Monitoring Trends in Bat Populations of the United States and Territories: Problems and Prospects: U.S. Geological Survey, Biological Resource Discipline, Information and Technology Report, USGS/BRD/ITR–2003-0003* (pp. 21–30).
McCracken, G. F., Bernard, R. F., Gamba-Rios, M., Wolfe, R., Krauel, J. J., Jones, D. N., Russell, A. L., & Brown, V. A. (2018). Rapid range expansion of the Brazilian free-tailed bat in the southeastern United States, 2008-2016. *Journal of Mammalogy*, *99*(2), 312–320. https://doi.org/10.1093/jmammal/gyx188
McCracken, G. F., Gillam, E. H., Westbrook, J. K., Lee, Y.-F., Jensen, M. L., & Balsley, B. B. (2008). Brazilian free-tailed bats (Tadarida brasiliensis: Molossidae, Chiroptera) at high altitude: Links to migratory insect populations. *Integrative and Comparative Biology*, *48*(1), 107–118. https://doi.org/10.1093/icb/icn033
McCracken, G. F., McCracken, M. K., & Vawter, A. T. (1994). Genetic Structure in Migratory Populations of the Bat Tadarida brasiliensis mexicana. *Journal of Mammalogy*, *75*(2), 500–514. https://doi.org/10.2307/1382574
McCracken, G. F., Safi, K., Kunz, T. H., Dechmann, D. K. N., Swartz, S. M., & Wikelski, M. (2016). Airplane tracking documents the fastest flight speeds recorded for bats. *Royal Society Open Science*, *3*(11). https://doi.org/10.1098/rsos.160398
McGuire, L. P., Guglielmo, C. G., Mackenzie, S. A., & Taylor, P. D. (2012). Migratory stopover in the long-distance migrant silver-haired bat, Lasionycteris noctivagans. *Journal of Animal Ecology*, *81*(2), 377–385. https://doi.org/10.1111/j.1365-2656.2011.01912.x
McLean, N., van der Jeugd, H. P., & Van De Pol, M. (2018). High intra-specific variation in avian body condition responses to climate limits generalisation across species. *PLoS ONE*, *13*(2), 1–25. https://doi.org/10.1371/journal.pone.0192401
Miles, J. (2005). R-squared, Adjusted R-squared. In B. S. Everitt & D. C. Howell (Eds.), *Encyclopedia of Statistics in Behavioral Science - Volume 4* (pp. 1655–1657). John Wiley & Sons, Ltd, Chichester.
Moussy, C., Hosken, D. J., Mathews, F., Smith, G. C., Aegerter, J. N., & Bearhop, S. (2013). Migration and dispersal patterns of bats and their influence on genetic structure. *Mammal Review*, *43*(3), 183–195. https://doi.org/10.1111/j.1365-2907.2012.00218.x
Muthersbaugh, M. S., Mark Ford, W., Powers, K. E., & Silvis, A. (2019). Activity patterns of bats during the fall and spring along ridgelines in the central Appalachians. *Journal of Fish and Wildlife Management*, *10*(1), 180–195. https://doi.org/10.3996/082018-JFWM-072
Newson, S. E., Mendes, S., Crick, H. Q. P., Dulvy, N., Houghton, J., Hays, G., Hutson, A., Macleod, C., Pierce, G., & Robinson, R. (2009). Indicators of the impact of climate change on migratory species. *Endangered Species Research*, *7*(May), 101–113. https://doi.org/10.3354/esr00162
Noriega, A. E., & Ventosa-Santaulària, D. (2007). Spurious regression and trending variables. *Oxford Bulletin of Economics and Statistics*, *69*(3), 439–444. https://doi.org/10.1111/j.1468-0084.2007.00481.x
Pair, S. D., & Westbrook, J. K. (1995). Agro-ecological and climatological factors potentially influencing armyworm populations and their movement in the Southeastern United States. *Southwestern Entomologist*, *18*, 101–118.
Petersons, G. (2004). Seasonal migrations of north-eastern populations of Nathusius‟ bat Pipistrellus nathusii (Chiroptera). *Myotis*, *41–2*(November), 29–56.
Pettit, J. L., & O‟Keefe, J. M. (2017). Day of year, temperature, wind, and precipitation predict timing of bat migration. *Journal of Mammalogy*, *98*(5), 1236–1248. https://doi.org/10.1093/jmammal/gyx054
Popa-Lisseanu, A. G., & Voigt, C. C. (2009). Bats on the Move. *Journal of Mammalogy*, *90*(6), 1283–1289. https://doi.org/10.1644/09-mamm-s-130r2.1
Reichard, J. D., Prajapati, S. I., Austad, S. N., Keller, C., & Kunz, T. H. (2010). Thermal windows on Brazilian free-tailed bats facilitate thermoregulation during prolonged flight. *Integrative and*

Comparative Biology, *50*(3), 358–370. https://doi.org/10.1093/icb/icq033
Roby, P. L., Gumbert, M. W., & Lacki, M. J. (2019). Nine years of Indiana bat (Myotis sodalis) spring migration behavior. *Journal of Mammalogy*, *100*(5), 1501–1511. https://doi.org/10.1093/jmammal/gyz104
Russell, A. F., & McCracken, G. F. (2006). Chapter 13: Population Genetic Structure of Very Large Populations: The Brazilian Free-Tailed Bat, Tadarida brasiliensis. In A. Zubaid, G. F. McCracken, & T. H. Kunz (Eds.), *Functional and Evolutionary Ecology of Bats* (pp. 227–247).
Russell, A. F., Medellín, R. A., & McCracken, G. F. (2005). Genetic variation and migration in the Mexican free-tailed bat (Tadarida brasiliensis mexicana). *Molecular Ecology*, *14*(7), 2207–2222. https://doi.org/10.1111/j.1365-294X.2005.02552.x
Rydell, J., Bach, L., Bach, P., Diaz, L. G., Furmankiewicz, J., Hagner-Wahlsten, N., Kyheröinen, E.-M., Lilley, T., Masing, M., Meyer, M. M., Ptersons, G., Šuba, J., Vasko, V., Vintulis, V., & Hedenström, A. (2014). Phenology of Migratory Bat Activity Across the Baltic Sea and the South-Eastern North Sea. *Acta Chiropterologica*, *16*(1), 139–147. https://doi.org/10.3161/150811014x683354
Satterfield, D. A., Sillett, T. S., Chapman, J. W., Altizer, S., & Marra, P. P. (2020). Seasonal insect migrations: massive, influential, and overlooked. *Frontiers in Ecology and the Environment*, fee.2217. https://doi.org/10.1002/fee.2217
Shaw, A. K. (2016). Drivers of animal migration and implications in changing environments. *Evolutionary Ecology*, *30*(6), 991–1007. https://doi.org/10.1007/s10682-016-9860-5
Sherwin, H. A., Montgomery, W. I., & Lundy, M. G. (2013). The impact and implications of climate change for bats. *Mammal Review*, *43*(3), 171–182. https://doi.org/10.1111/j.1365-2907.2012.00214.x
Smith, A. D., & McWilliams, S. R. (2016). Bat activity during autumn relates to atmospheric conditions: Implications for coastal wind energy development. *Journal of Mammalogy*, *97*(6), 1565–1577. https://doi.org/10.1093/jmammal/gyw116
Sommers, A. S., Rogers, E. J., & McGuire, L. P. (2019). Migration and reproduction are associated with similar degrees of phenotypic flexibility in an insectivorous bat. *Oecologia*, *190*(4), 747–755. https://doi.org/10.1007/s00442-019-04449-2
Stepanian, P. M., & Wainwright, C. E. (2018). Ongoing changes in migration phenology and winter residency at Bracken Bat Cave. *Global Change Biology*, *24*(7), 3266–3275. https://doi.org/10.1111/gcb.14051
Stepanian, P. M., Wainwright, C. E., Liechti, F., Bauer, S., & Haest, B. (2020). *Data for: "Climatic drivers of (changes in) bat migration phenology at Bracken Cave (USA)."* https://doi.org/10.5281/zenodo.3945907
Svoboda, P. L., Choate, J. R., & Chesser, R. K. (1985). Genetic Relationships among Southwestern Populations of the Brazilian Free-Tailed Bat. *Journal of Mammalogy*, *66*(3), 444–450. https://doi.org/10.2307/1380918
Taylor, J. R. (1997). *An introduction to error analysis, the study of uncertainties in physical measurements, Second Edition*. University Science Books.
Thackeray, S. J., Henrys, P. A., Hemming, D. L., Bell, J. R., Botham, M. S., Burthe, S., Helaouet, P., Johns, D. G., Jones, I. D., Leech, D. I., Mackay, E. B., Massimino, D., Atkinson, S., Bacon, P. J., Brereton, T. M., Carvalho, L., Clutton-Brock, T. H., Duck, C., Edwards, M., … Wanless, S. (2016). Phenological sensitivity to climate across taxa and trophic levels. *Nature*, *535*(7611), 241–245. https://doi.org/10.1038/nature18608
van de Pol, M., Bailey, L. D., McLean, N., Rijsdijk, L., Lawson, C. R., & Brouwer, L. (2016). Identifying the best climatic predictors in ecology and evolution. *Methods in Ecology and Evolution*, *7*(10), 1246–1257. https://doi.org/10.1111/2041-210X.12590
Vickery, J. A., Ewing, S. R., Smith, K. W., Pain, D. J., Bairlein, F., Škorpilová, J., & Gregory, R. D. (2014). The decline of Afro-Palaearctic migrants and an assessment of potential causes. *Ibis*, *156*(1), 1–22. https://doi.org/10.1111/ibi.12118
Villa, B. R., & Cockrum, E. L. (1962). Migration in the Guano Bat Tadarida brasiliensis mexicana (Saussure). *Journal of Mammalogy*, *43*(1), 43. https://doi.org/10.2307/1376879
Voigt, C. C., Schneeberger, K., Voigt-Heucke, S. L., & Lewanzik, D. (2011). Rain increases the energy cost of bat flight. *Biology Letters*, *7*(5), 793–795. https://doi.org/10.1098/rsbl.2011.0313
Weller, T. J., Castle, K. T., Liechti, F., Hein, C. D., Schirmacher, M. R., & Cryan, P. M. (2016). First

Direct Evidence of Long-distance Seasonal Movements and Hibernation in a Migratory Bat. *Scientific Reports*, *6*(1), 34585. https://doi.org/10.1038/srep34585

Wiederholt, R., López-Hoffman, L., Cline, J., Medellin, R. A., Cryan, P. M., Russell, A. F., McCracken, G. F., Diffendorfer, J., & Semmens, D. (2013). Moving across the border: Modeling migratory bat populations. *Ecosphere*, *4*(9). https://doi.org/10.1890/ES13-00023.1

Wilcove, D. S., & Wikelski, M. (2008). Going, going, gone: Is animal migration disappearing? *PLoS Biology*, *6*(7), 1361–1364. https://doi.org/10.1371/journal.pbio.0060188

Wilkins, K. T. (1989). Tadarida brasiliensis. *Mammalian Species*, *331*, 1. https://doi.org/10.2307/3504148

Williams, T. C., Ireland, L. C., & Williams, J. C. (1973). High altitude flights of the free-tailed bat, Tadarida brasiliensis, observed with Radar. *Journal of Mammalogy*, *54*(4), 807–821. https://doi.org/10.1644/870.1.Key

Supporting Information for:

Climatic drivers of (changes in) bat migration phenology at Bracken Cave (USA)

Authors

Birgen Haest[1, *], Phillip M. Stepanian[2], Charlotte E. Wainwright[2], Felix Liechti[1], Silke Bauer[1]

Affiliations

[1] Swiss Ornithological Institute, Seerose 1, Sempach, CH-6204, Switzerland

[2] Department of Civil and Environmental Engineering and Earth Sciences, University of Notre Dame, Notre Dame, Indiana, 46556, USA

*Corresponding author: birgen.haest@protonmail.com; +49 176 749 782 82; ORCID: 0000-0002-8739-6460

This PDF file includes:

Appendix S1
Supplementary Figure S1 to S22
Supplementary Tables S1 to S5
SI References

Appendix S1 Properties and pre-processing of the weather data that were acquired from the NCEP Reanalysis I database.

Weather variable	NCEP variable	Spatial Resolution (in degrees)	Number of analysed grid cells	Data pre-processing and comments
temperature	„air.2m", i.e. air temperature at 2 meters (above ground level)	1.905° x 1.875° (latitude x longitude) (T62 Gaussian grid)	179	We calculated daily mean temperatures from the four 6-hour temperature values.
Precipitation	„prate.sfc", i.e. precipitation rate at surface level	1.905° x 1.875° (latitude x longitude) (T62 Gaussian grid)	179	Precipitation rate data were converted to mm/day.
Wind direction	(East-West) „uwnd" and (North-South) „vwnd" at the 925, 850, and 700-hPa pressure levels	2.5° x 2.5°	111	The 925, 850, and 700-hPa pressure levels roughly corresponds to 750, 1500 and 3000 m altitude above-sea-level. For each pressure level, we calculated daily mean wind directions using the average of the four 6-hour wind values for each of the two wind components.
Wind assistance	(East-West) „uwnd" and (North-South) „vwnd" at the 925, 850, and 700-hPa pressure levels	2.5° x 2.5°	111	For each pressure level (i.e. 925, 850, and 700-hPa), we calculated daily mean wind assistance using the average of the four 6-hour wind values for each of the two wind components. Wind assistance was calculated with the RNCEP package (Kemp *et al.*, 2012a) using the „M.Groundspeed" equation (Kemp *et al.*, 2012b). To do so, we assumed a groundspeed of 5.7 m/s in still air conditions (based on results from McCracken *et al.*, 2016), and a preferred direction of movement from each grid cell centre towards Bracken Cave.

Grid cells analysed for each of the weather variables, illustrating the full spatial extent of the analysis and the spatial resolution (i.e. detail):

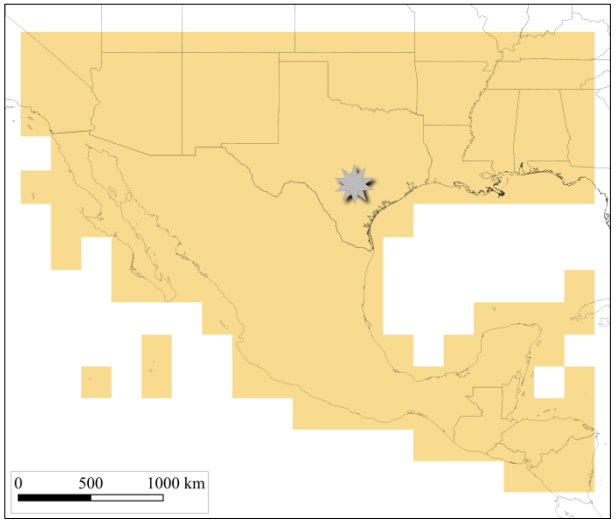

Temperature and precipitation

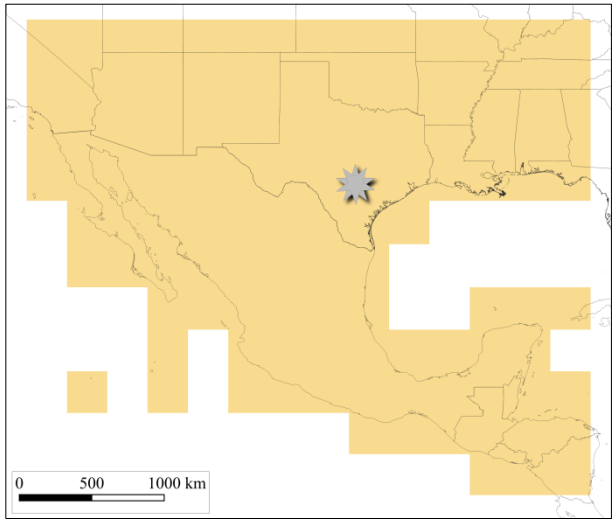

Wind

Figure S1 Per species ΔAICc, adjusted R^2, and regression coefficient maps of the identified best time windows for temperature influence on spring migration phenology. The ΔAICc values are the difference of the AICc value of the model with the selected best time window for each grid cell with the AICc value of the baseline model (arrival/passage = α + β*year). ΔAICc values are only shown for grid cells that had a probability Pc value < 0.3, i.e., grid cells for which the relation between the identified time window and arrival/passage dates had a ΔAICc that is less likely to obtain due to chance. The adjusted R^2 values are for the models that have as independent variables both the best identified time window for temperature and the „year" term to account for trends. The regression coefficient maps show the regression coefficient (days/°C) of the best identified time window for temperature when „year" terms to account for trends are also included in the model. Yellow dots with annotated numbers indicate the candidate grid cells selected as potentially influencing spring migration phenology at Bracken Cave. The ID values are used consistently throughout all supplementary figures and tables for ease of reference.

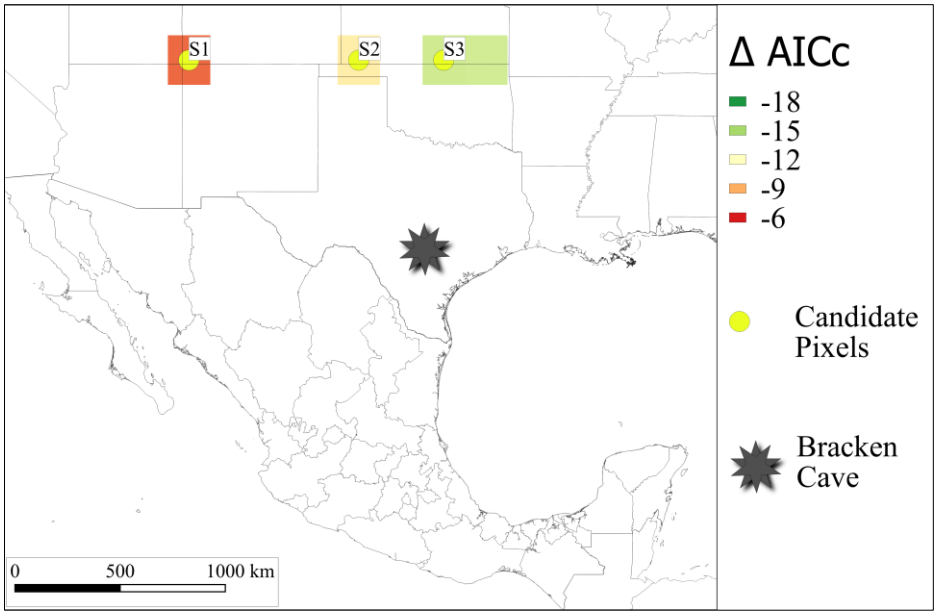
S1
S2
S3
Δ AICc
-18
-15
-12
-9
-6
Candidate Pixels
Bracken Cave
0
500
1000 km

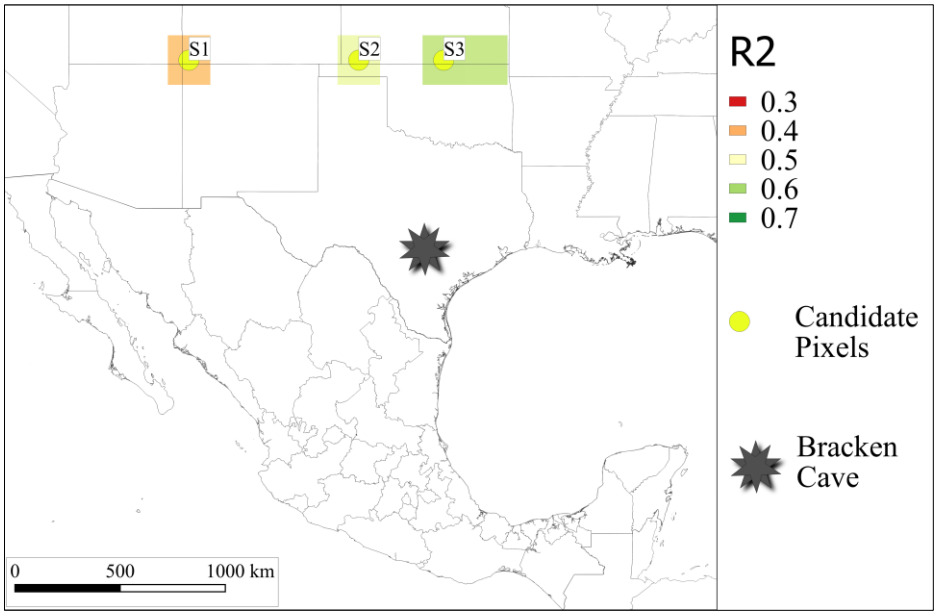
S1
S2
S3
R2
0.3
0.4
0.5
0.6
0.7
Candidate Pixels
Bracken Cave
0
500
1000 km

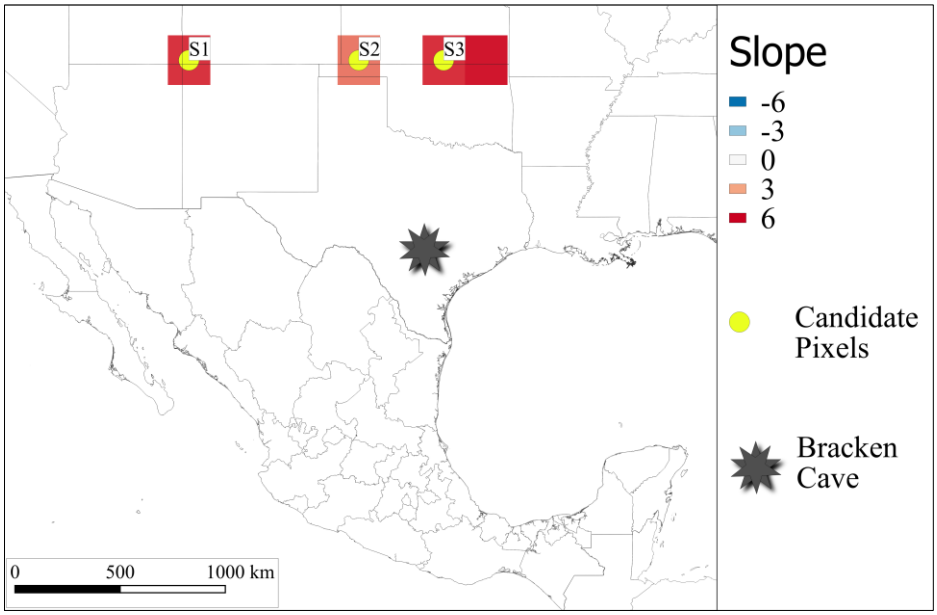
S1
S2
S3
Slope
-6
-3
0
3
6
Candidate Pixels
Bracken Cave
0
500
1000 km

Figure S2 Per species ΔAICc, adjusted R^2, and regression coefficient maps of the identified best time windows for precipitation influence on spring migration phenology. The ΔAICc values are the difference of the AICc value of the model with the selected best time window for each grid cell with the AICc value of the baseline model (arrival/passage = α + β*year). ΔAICc values are only shown for grid cells that had a probability Pc value < 0.3, i.e., grid cells for which the relation between the identified time window and arrival/passage dates had a ΔAICc that is less likely to obtain due to chance. The adjusted R^2 values are for the models that have as independent variables both the best identified time window for precipitation and the „year" term to account for trends. The regression coefficient maps show the regression coefficient (days/mm) of the best identified time window for precipitation when „year" terms to account for trends are also included in the model. Yellow dots with annotated numbers indicate the candidate grid cells selected as potentially influencing spring migration phenology at Bracken Cave. The ID values are used consistently throughout all supplementary figures and tables for ease of reference.

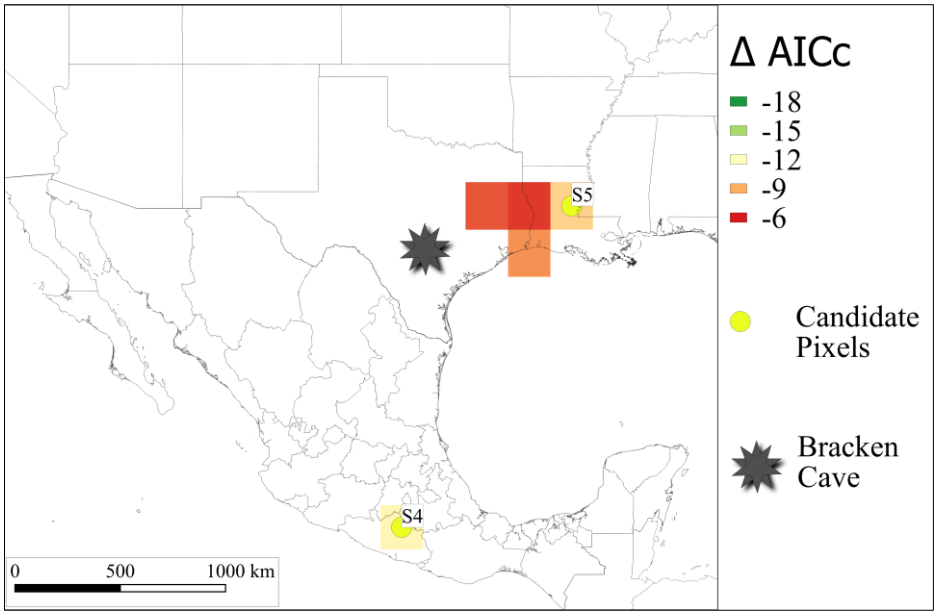
Δ AICc
-18
-15
-12
-9
-6
Candidate Pixels
Bracken Cave
S5
S4
0
500
1000 km

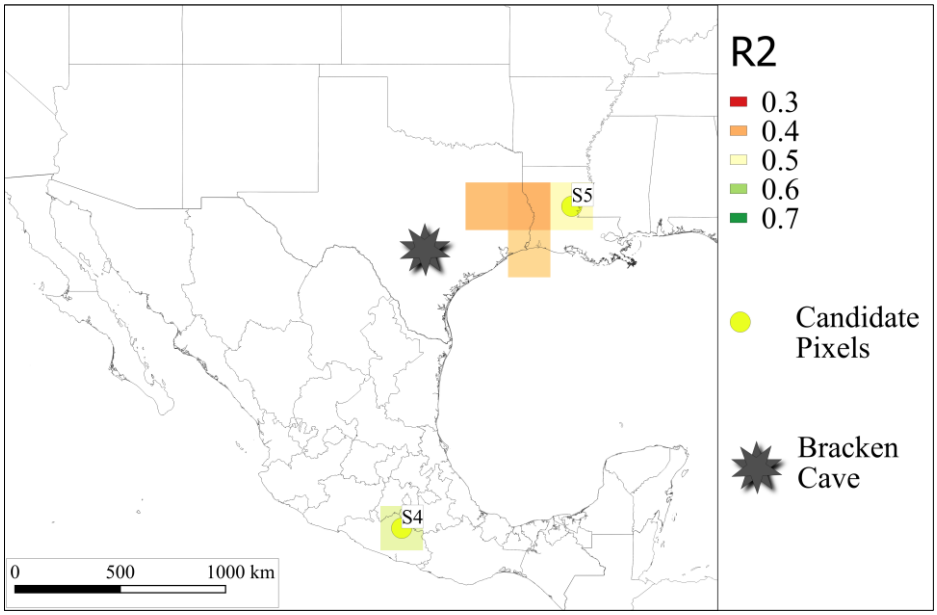
R2
0.3
0.4
0.5
0.6
0.7
Candidate Pixels
Bracken Cave
S5
S4
0
500
1000 km

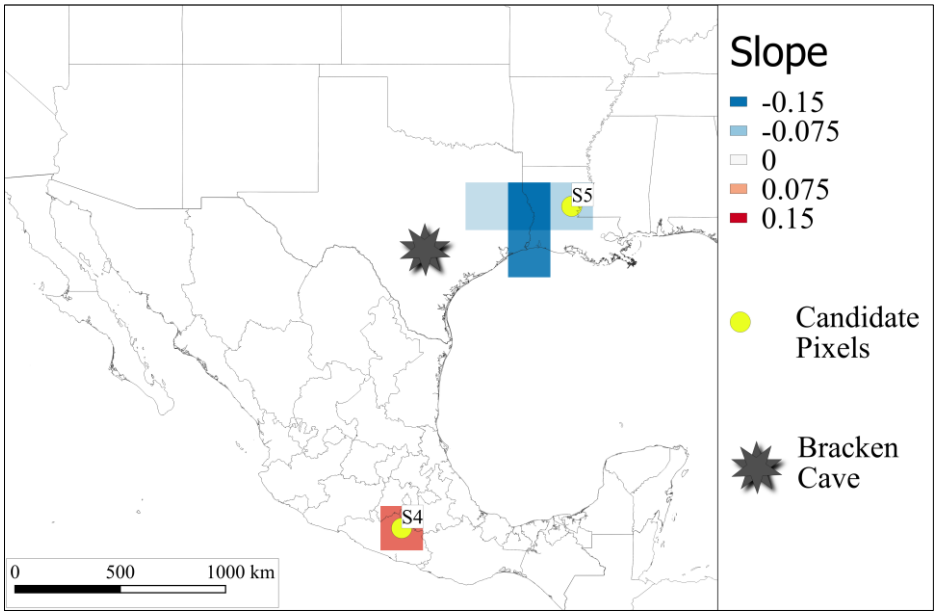
Slope
-0.15
-0.075
0
0.075
0.15
Candidate Pixels
Bracken Cave
S5
S4
0
500
1000 km

Figure S3 Per species ΔAICc, adjusted R^2, and regression coefficient maps of the identified best time windows for the influence on spring migration phenology of the number of days with winds at the 925-hPa pressure level coming from the direction of Bracken Cave. The ΔAICc values are the difference of the AICc value of the model with the selected best time window for each grid cell with the AICc value of the baseline model (arrival/passage = $\alpha + \beta$*year). ΔAICc values are only shown for grid cells that had a probability Pc value < 0.3, i.e., grid cells for which the relation between the identified time window and arrival/passage dates had a ΔAICc that is less likely to obtain due to chance. The adjusted R^2 values are for the models that have as independent variables both the best identified time window for number of days with wind coming from Bracken Cave and the „year" term to account for trends. The regression coefficient maps show the regression coefficient (days/day) of the best identified time window for the number of days with wind coming from Bracken Cave when „year" terms to account for trends are also included in the model. Yellow dots with annotated numbers indicate the candidate grid cells selected as potentially influencing spring migration phenology at Bracken Cave. The ID values are used consistently throughout all supplementary figures and tables for ease of reference.

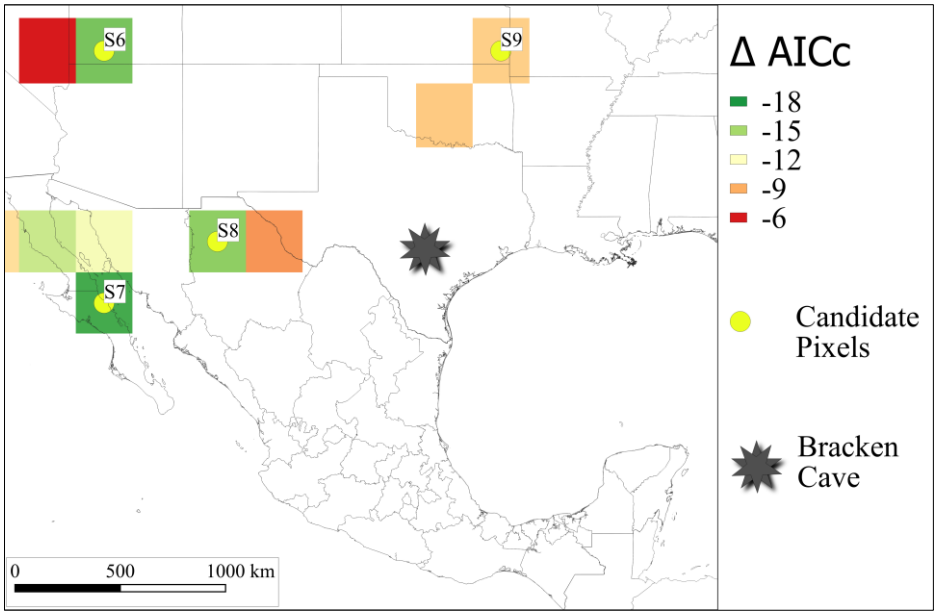
S6
S9
S8
S7
0
500
1000 km
Δ AICc
-18
-15
-12
-9
-6
Candidate Pixels
Bracken Cave

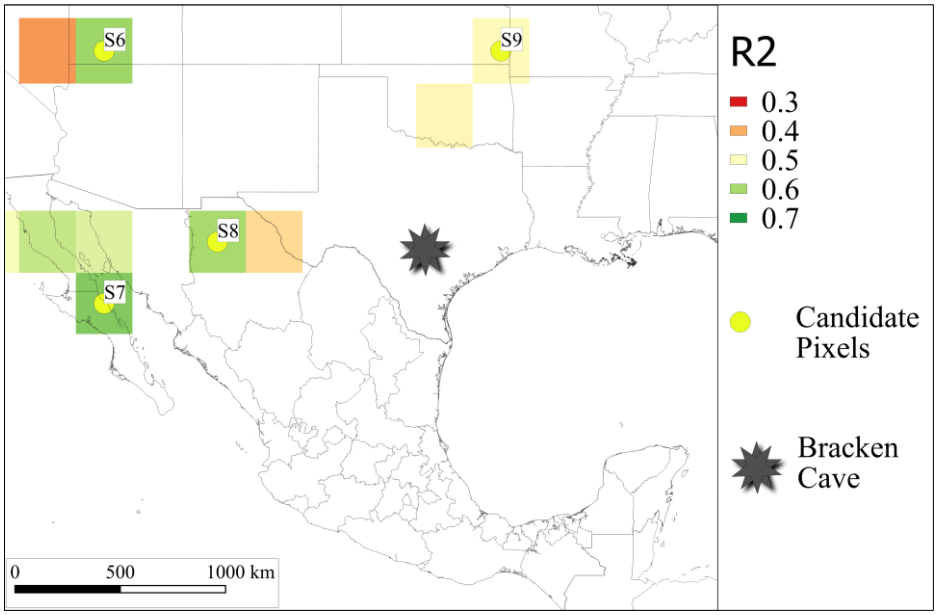
S6
S9
S8
S7
0
500
1000 km
R2
0.3
0.4
0.5
0.6
0.7
Candidate Pixels
Bracken Cave

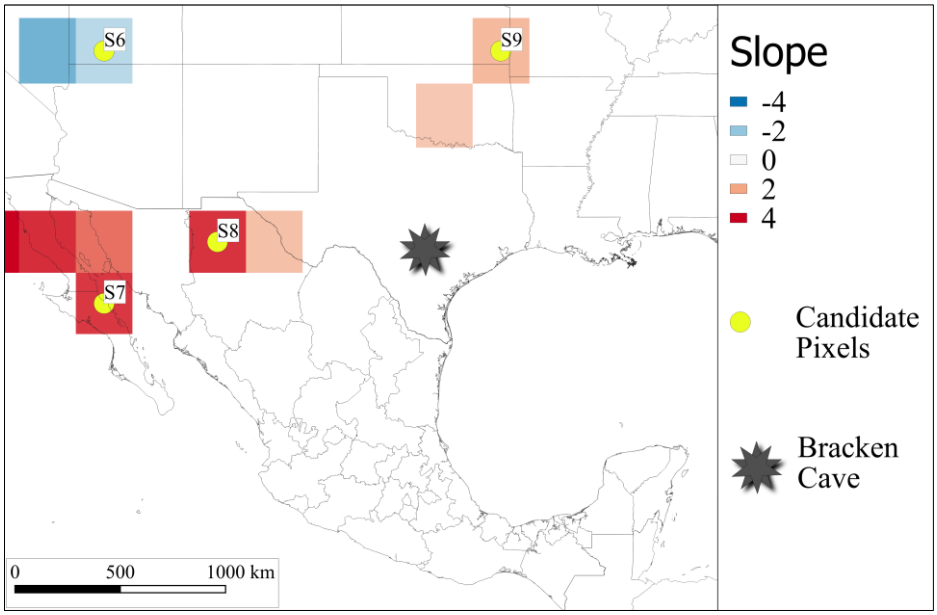
S6
S9
S8
S7
0
500
1000 km
Slope
-4
-2
0
2
4
Candidate Pixels
Bracken Cave

Figure S4 Per species ΔAICc, adjusted R^2, and regression coefficient maps of the identified best time windows for the influence on spring migration phenology of the number of days with winds at the 925-hPa pressure level going in the direction of Bracken Cave. The ΔAICc values are the difference of the AICc value of the model with the selected best time window for each grid cell with the AICc value of the baseline model (arrival/passage = $\alpha + \beta$*year). ΔAICc values are only shown for grid cells that had a probability Pc value < 0.3, i.e., grid cells for which the relation between the identified time window and arrival/passage dates had a ΔAICc that is less likely to obtain due to chance. The adjusted R^2 values are for the models that have as independent variables both the best identified time window for number of days with wind going in the direction of Bracken Cave and the „year" term to account for trends. The regression coefficient maps show the regression coefficient (days/day) of the best identified time window for the number of days with wind going in the direction of Bracken Cave when „year" terms to account for trends are also included in the model. Yellow dots with annotated numbers indicate the candidate grid cells selected as potentially influencing spring migration phenology at Bracken Cave. The ID values are used consistently throughout all supplementary figures and tables for ease of reference.

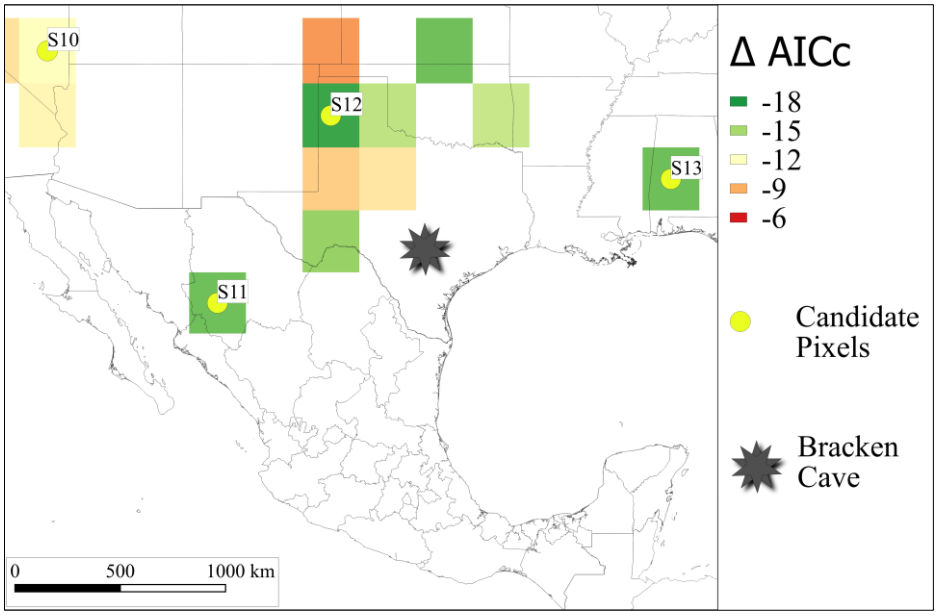
S10
S12
S13
S11
0
500
1000 km
Δ AICc
-18
-15
-12
-9
-6
Candidate Pixels
Bracken Cave

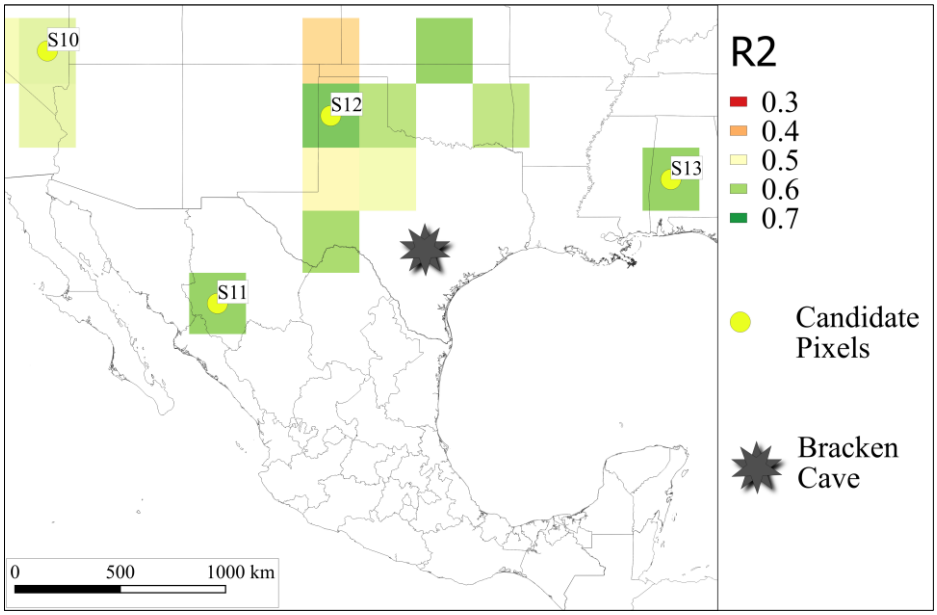
S10
S12
S13
S11
0
500
1000 km
R2
0.3
0.4
0.5
0.6
0.7
Candidate Pixels
Bracken Cave

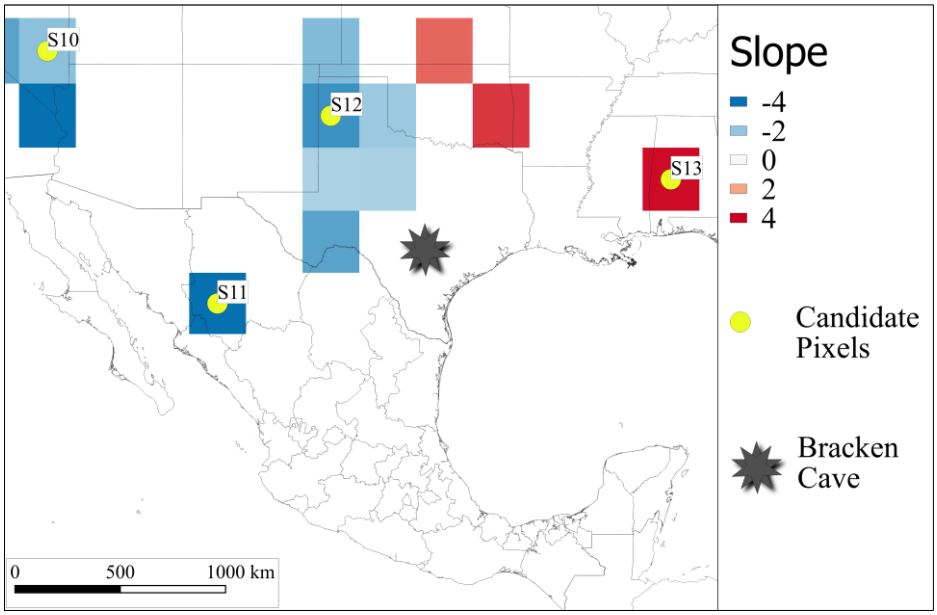
S10
S12
S13
S11
0
500
1000 km
Slope
-4
-2
0
2
4
Candidate Pixels
Bracken Cave

Figure S5 Per species ΔAICc, adjusted R^2, and regression coefficient maps of the identified best time windows for the influence on spring migration phenology of the number of days with winds at the 850-hPa pressure level coming from the direction of Bracken Cave. The ΔAICc values are the difference of the AICc value of the model with the selected best time window for each grid cell with the AICc value of the baseline model (arrival/passage = $\alpha + \beta$*year). ΔAICc values are only shown for grid cells that had a probability Pc value < 0.3, i.e., grid cells for which the relation between the identified time window and arrival/passage dates had a ΔAICc that is less likely to obtain due to chance. The adjusted R^2 values are for the models that have as independent variables both the best identified time window for number of days with wind coming from Bracken Cave and the „year" term to account for trends. The regression coefficient maps show the regression coefficient (days/day) of the best identified time window for the number of days with wind coming from Bracken Cave when „year" terms to account for trends are also included in the model. Yellow dots with annotated numbers indicate the candidate grid cells selected as potentially influencing spring migration phenology at Bracken Cave. The ID values are used consistently throughout all supplementary figures and tables for ease of reference.

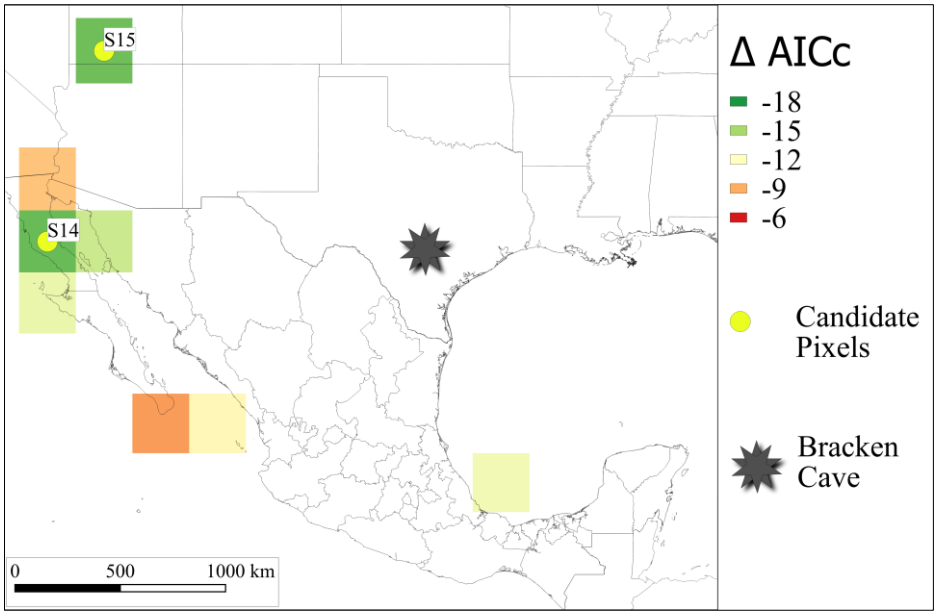
S15
S14
Δ AICc
-18
-15
-12
-9
-6
Candidate Pixels
Bracken Cave
0
500
1000 km

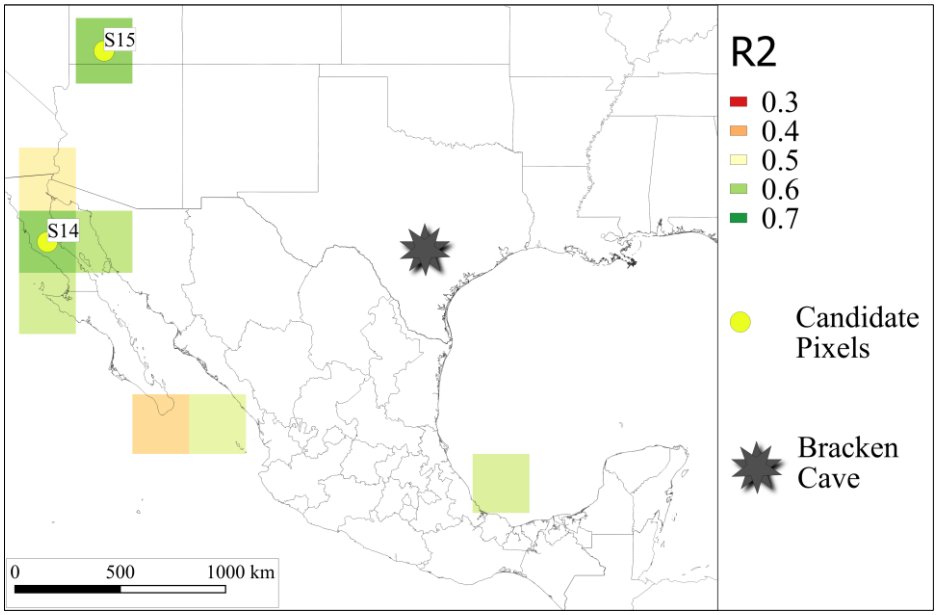
S15
S14
R2
0.3
0.4
0.5
0.6
0.7
Candidate Pixels
Bracken Cave
0
500
1000 km

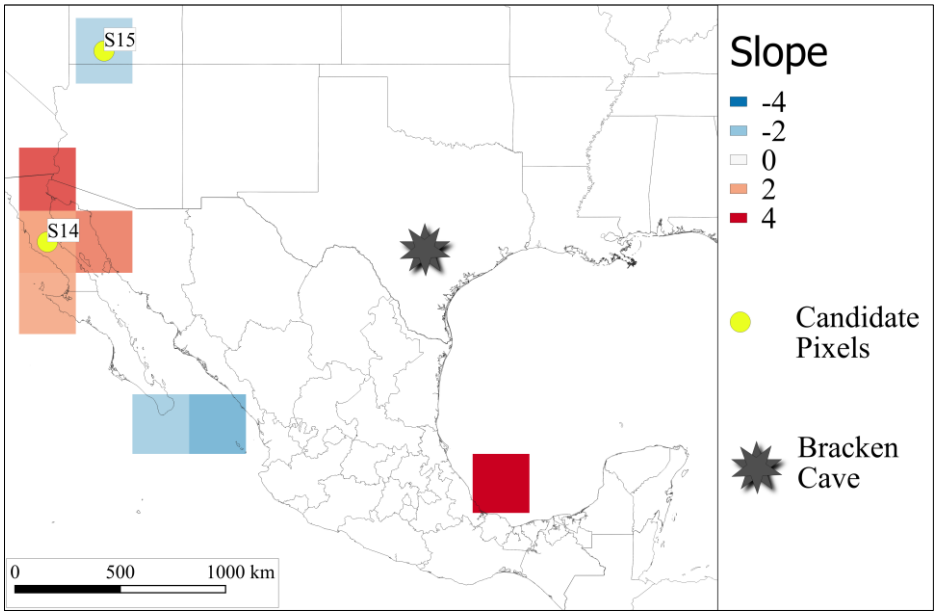
S15
S14
Slope
-4
-2
0
2
4
Candidate Pixels
Bracken Cave
0
500
1000 km

Figure S6 Per species ΔAICc, adjusted R^2, and regression coefficient maps of the identified best time windows for the influence on spring migration phenology of the number of days with winds at the 850-hPa pressure level going in the direction of Bracken Cave. The ΔAICc values are the difference of the AICc value of the model with the selected best time window for each grid cell with the AICc value of the baseline model (arrival/passage = $\alpha + \beta$*year). ΔAICc values are only shown for grid cells that had a probability Pc value < 0.3, i.e., grid cells for which the relation between the identified time window and arrival/passage dates had a ΔAICc that is less likely to obtain due to chance. The adjusted R^2 values are for the models that have as independent variables both the best identified time window for number of days with wind going in the direction of Bracken Cave and the „year" term to account for trends. The regression coefficient maps show the regression coefficient (days/day) of the best identified time window for the number of days with wind going in the direction of Bracken Cave when „year" terms to account for trends are also included in the model. Yellow dots with annotated numbers indicate the candidate grid cells selected as potentially influencing spring migration phenology at Bracken Cave. The ID values are used consistently throughout all supplementary figures and tables for ease of reference.

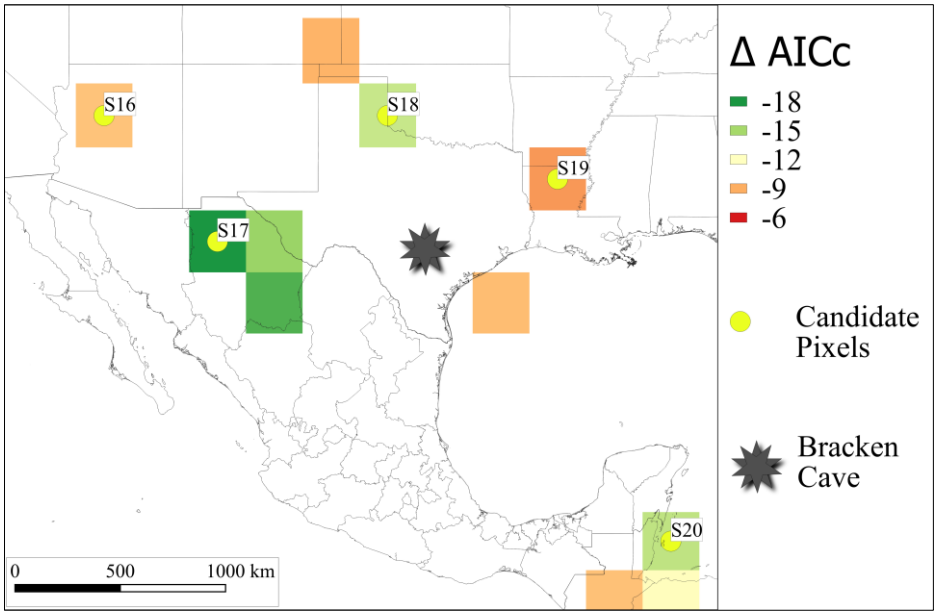
S16
S18
S19
S17
S20
0
500
1000 km
Δ AICc
-18
-15
-12
-9
-6
Candidate Pixels
Bracken Cave

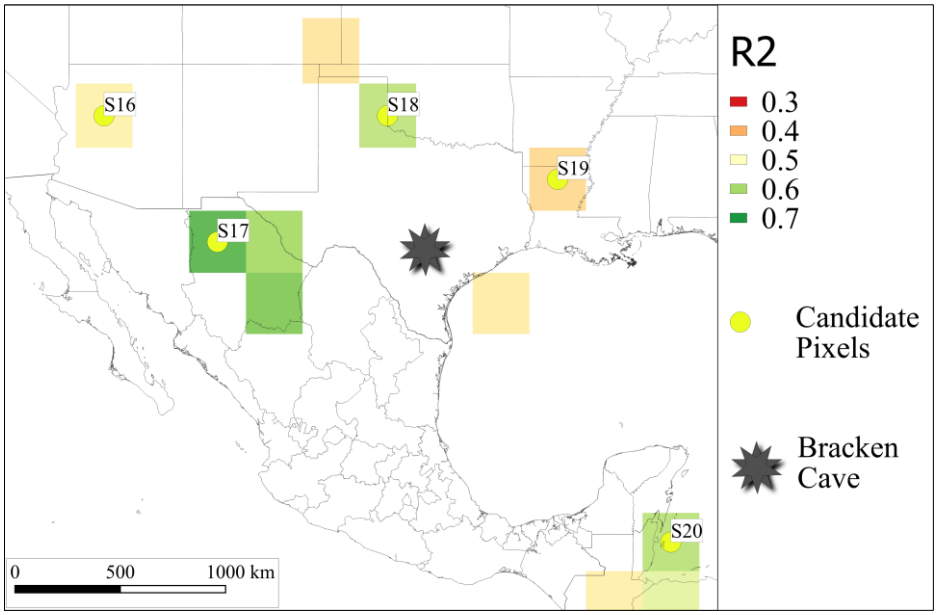
S16
S18
S19
S17
S20
0
500
1000 km
R2
0.3
0.4
0.5
0.6
0.7
Candidate Pixels
Bracken Cave

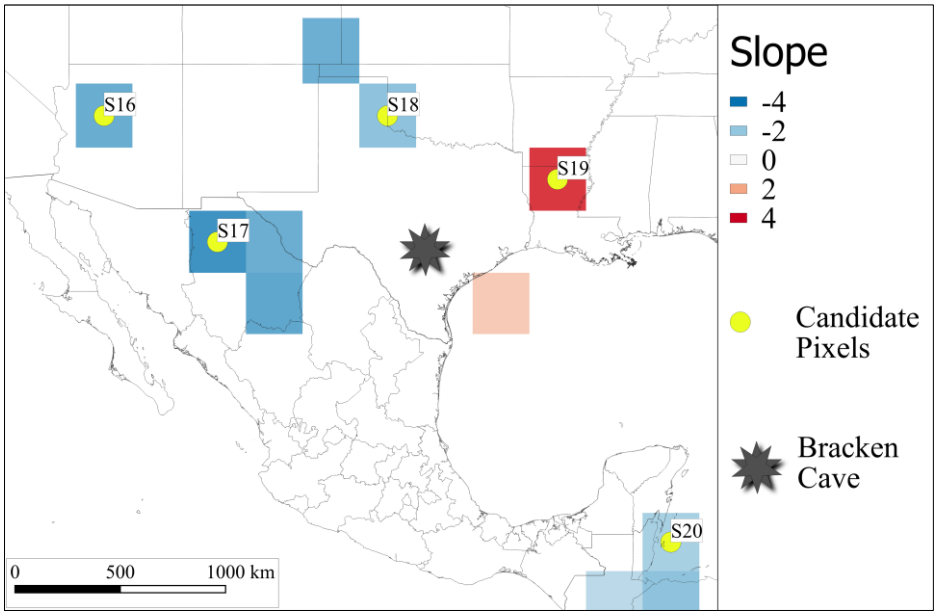
S16
S18
S19
S17
S20
0
500
1000 km
Slope
-4
-2
0
2
4
Candidate Pixels
Bracken Cave

Figure S7 Per species ΔAICc, adjusted R^2, and regression coefficient maps of the identified best time windows for the influence on spring migration phenology of the number of days with winds at the 700-hPa pressure level coming from the direction of Bracken Cave. The ΔAICc values are the difference of the AICc value of the model with the selected best time window for each grid cell with the AICc value of the baseline model (arrival/passage = $\alpha + \beta$*year). ΔAICc values are only shown for grid cells that had a probability Pc value < 0.3, i.e., grid cells for which the relation between the identified time window and arrival/passage dates had a ΔAICc that is less likely to obtain due to chance. The adjusted R^2 values are for the models that have as independent variables both the best identified time window for number of days with wind coming from Bracken Cave and the „year" term to account for trends. The regression coefficient maps show the regression coefficient (days/day) of the best identified time window for the number of days with wind coming from Bracken Cave when „year" terms to account for trends are also included in the model. Yellow dots with annotated numbers indicate the candidate grid cells selected as potentially influencing spring migration phenology at Bracken Cave. The ID values are used consistently throughout all supplementary figures and tables for ease of reference.

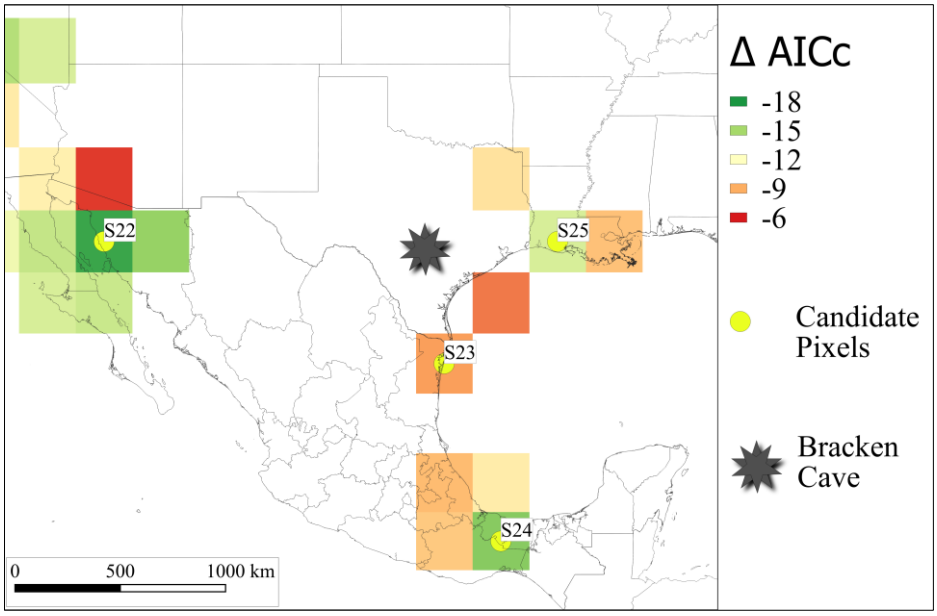
Δ AICc
-18
-15
-12
-9
-6
Candidate Pixels
Bracken Cave
S22
S25
S23
S24
0
500
1000 km

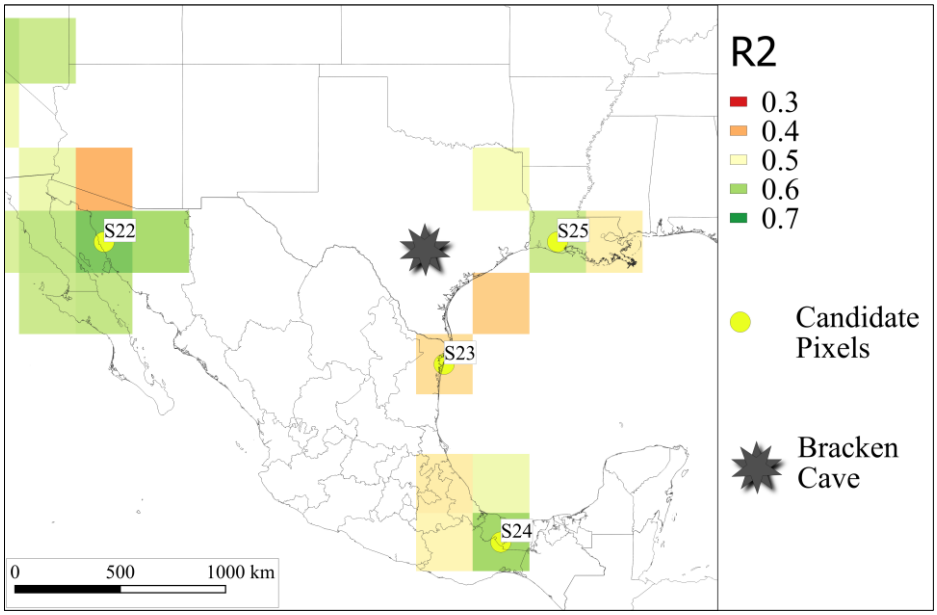
R2
0.3
0.4
0.5
0.6
0.7
Candidate Pixels
Bracken Cave
S22
S25
S23
S24
0
500
1000 km

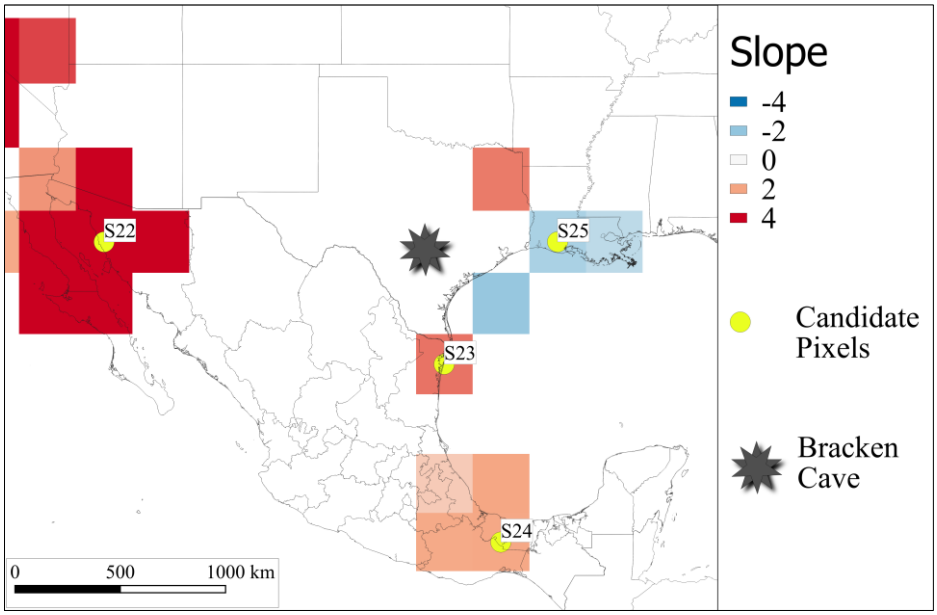
Slope
-4
-2
0
2
4
Candidate Pixels
Bracken Cave
S22
S25
S23
S24
0
500
1000 km

Figure S8 Per species ΔAICc, adjusted R^2, and regression coefficient maps of the identified best time windows for the influence on spring migration phenology of the number of days with winds at the 700-hPa pressure level going in the direction of Bracken Cave. The ΔAICc values are the difference of the AICc value of the model with the selected best time window for each grid cell with the AICc value of the baseline model (arrival/passage = $\alpha + \beta$*year). ΔAICc values are only shown for grid cells that had a probability Pc value < 0.3, i.e., grid cells for which the relation between the identified time window and arrival/passage dates had a ΔAICc that is less likely to obtain due to chance. The adjusted R^2 values are for the models that have as independent variables both the best identified time window for number of days with wind going in the direction of Bracken Cave and the „year" term to account for trends. The regression coefficient maps show the regression coefficient (days/day) of the best identified time window for the number of days with wind going in the direction of Bracken Cave when „year" terms to account for trends are also included in the model. Yellow dots with annotated numbers indicate the candidate grid cells selected as potentially influencing spring migration phenology at Bracken Cave. The ID values are used consistently throughout all supplementary figures and tables for ease of reference.

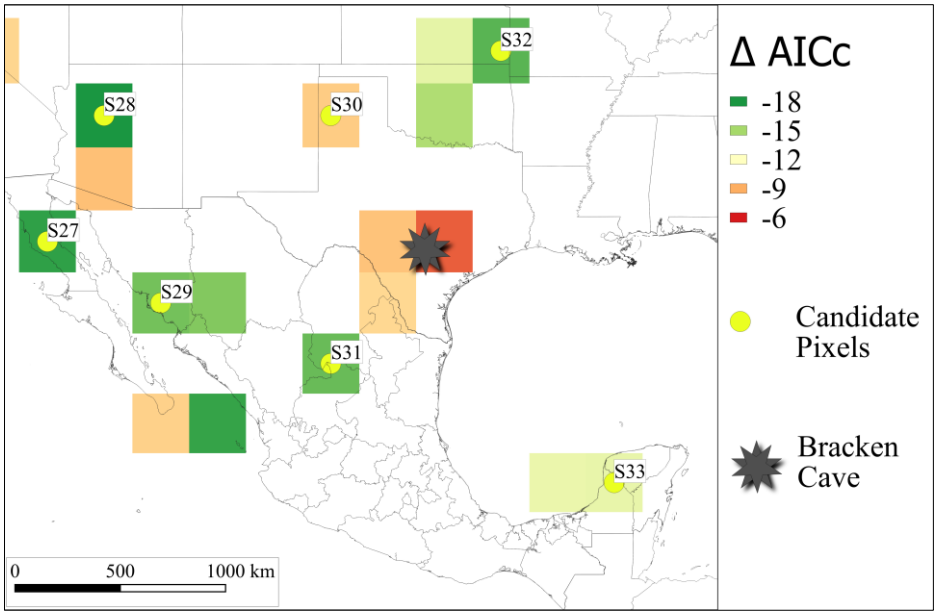
S28
S30
S32
S27
S29
S31
S33
0
500
1000 km
Δ AICc
-18
-15
-12
-9
-6
Candidate Pixels
Bracken Cave

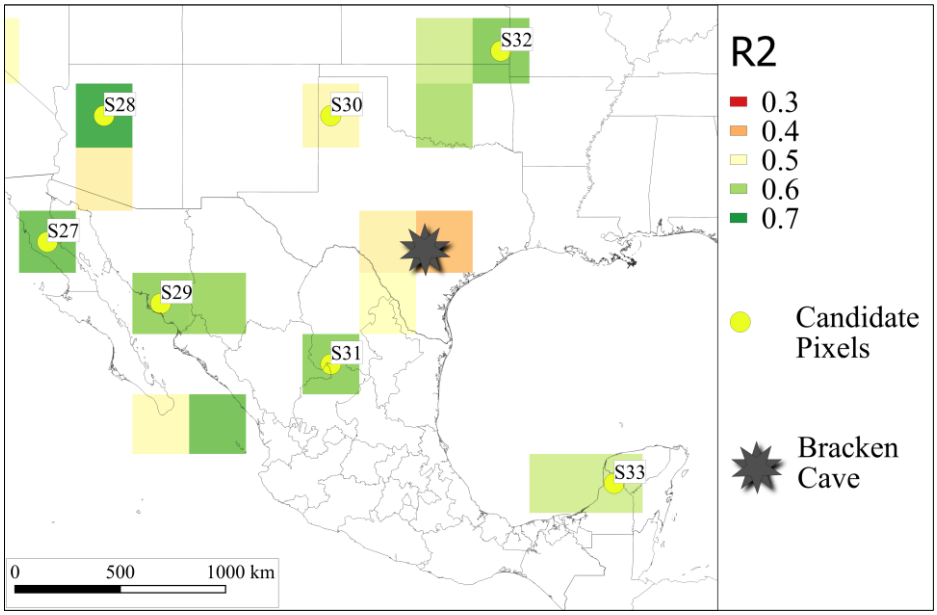
S28
S30
S32
S27
S29
S31
S33
0
500
1000 km
R2
0.3
0.4
0.5
0.6
0.7
Candidate Pixels
Bracken Cave

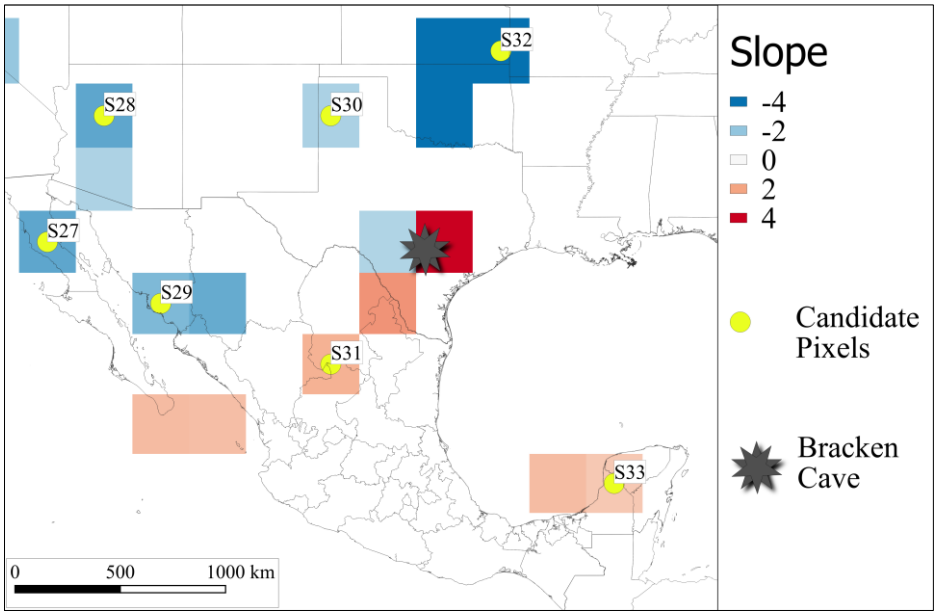
S28
S30
S32
S27
S29
S31
S33
0
500
1000 km
Slope
-4
-2
0
2
4
Candidate Pixels
Bracken Cave

Figure S9 Per species ΔAICc, adjusted R^2, and regression coefficient maps of the identified best time windows for the influence of wind assistance at the 925-hPa pressure level on spring migration phenology. The ΔAICc values are the difference of the AICc value of the model with the selected best time window for each grid cell with the AICc value of the baseline model (arrival/passage = α + β*year). ΔAICc values are only shown for grid cells that had a probability Pc value < 0.3, i.e., grid cells for which the relation between the identified time window and arrival/passage dates had a ΔAICc that is less likely to obtain due to chance. The adjusted R^2 values are for the models that have as independent variables both the best identified time window for wind assistance and the „year" term to account for trends. The regression coefficient maps show the regression coefficient (days/m*s^{-1}) of the best identified time window for the wind assistance when „year" terms to account for trends are also included in the model. Yellow dots with annotated numbers indicate the candidate grid cells selected as potentially influencing spring migration phenology at Bracken Cave. The ID values are used consistently throughout all supplementary figures and tables for ease of reference.

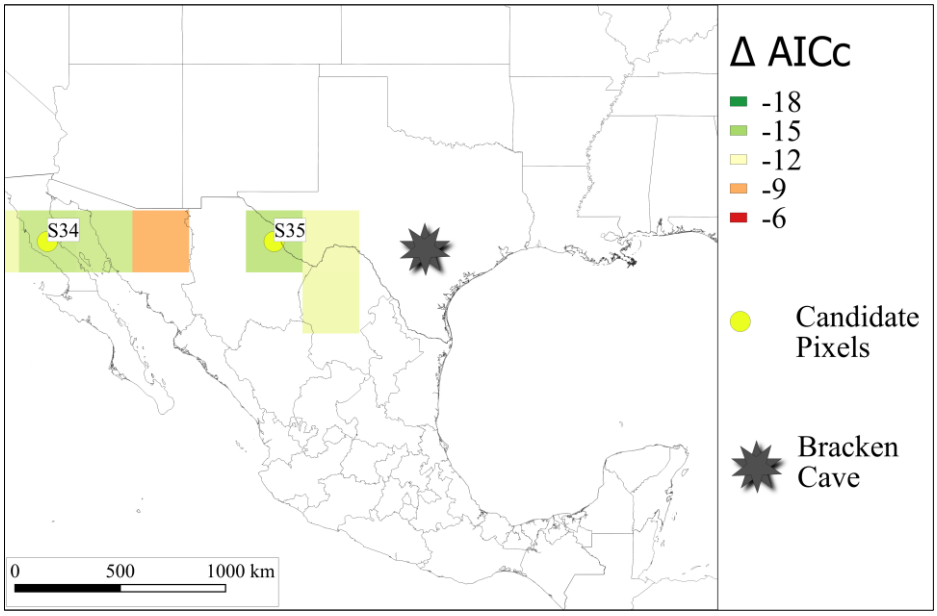
Δ AICc
-18
-15
-12
-9
-6
S34
S35
Candidate Pixels
Bracken Cave
0
500
1000 km

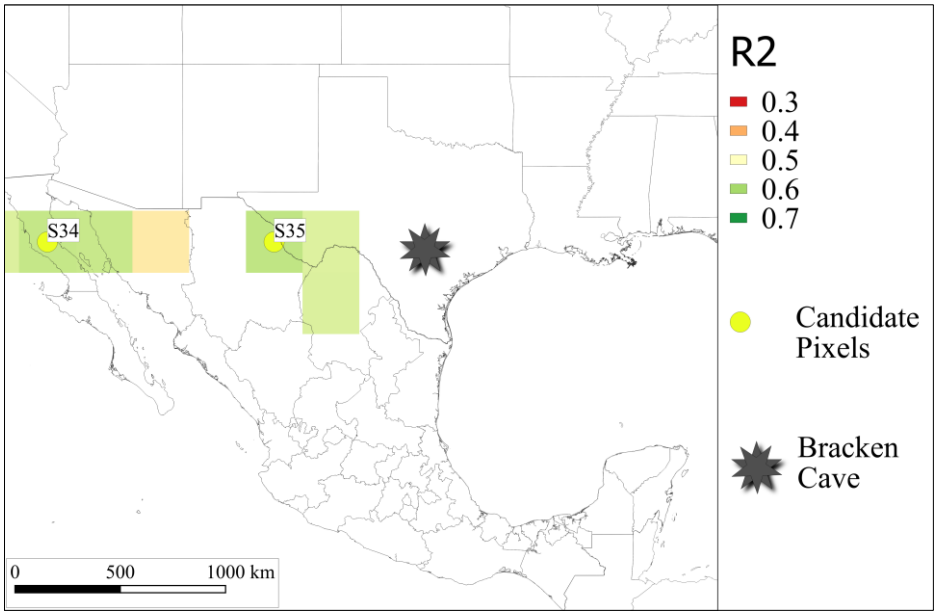
R2
0.3
0.4
0.5
0.6
0.7
S34
S35
Candidate Pixels
Bracken Cave
0
500
1000 km

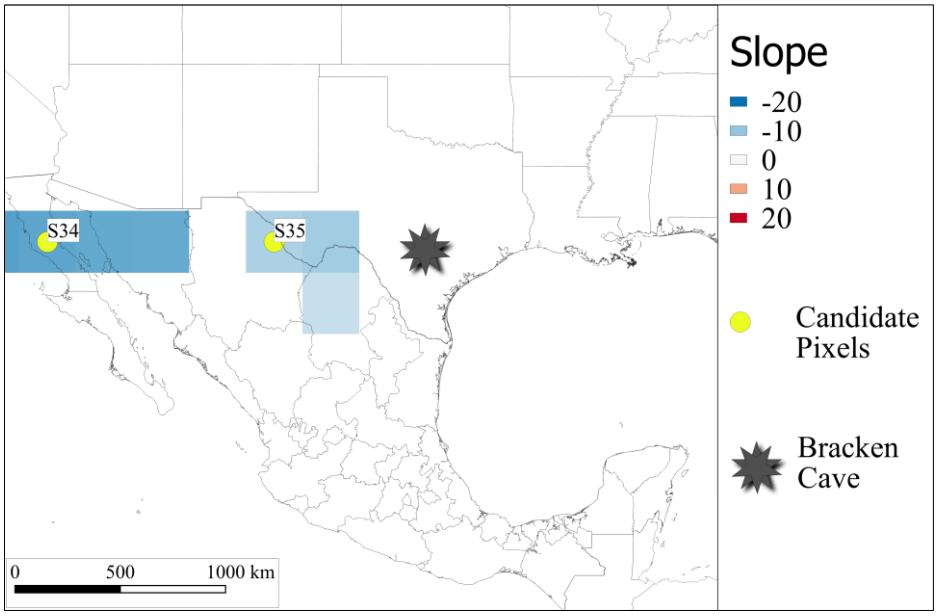
Slope
-20
-10
0
10
20
S34
S35
Candidate Pixels
Bracken Cave
0
500
1000 km

Figure S10 Per species ΔAICc, adjusted R^2, and regression coefficient maps of the identified best time windows for the influence of wind assistance at the 850-hPa pressure level on spring migration phenology. The ΔAICc values are the difference of the AICc value of the model with the selected best time window for each grid cell with the AICc value of the baseline model (arrival/passage = α + β*year). ΔAICc values are only shown for grid cells that had a probability Pc value < 0.3, i.e., grid cells for which the relation between the identified time window and arrival/passage dates had a ΔAICc that is less likely to obtain due to chance. The adjusted R^2 values are for the models that have as independent variables both the best identified time window for wind assistance and the „year" term to account for trends. The regression coefficient maps show the regression coefficient (days/m*s^{-1}) of the best identified time window for the wind assistance when „year" terms to account for trends are also included in the model. Yellow dots with annotated numbers indicate the candidate grid cells selected as potentially influencing spring migration phenology at Bracken Cave. The ID values are used consistently throughout all supplementary figures and tables for ease of reference.

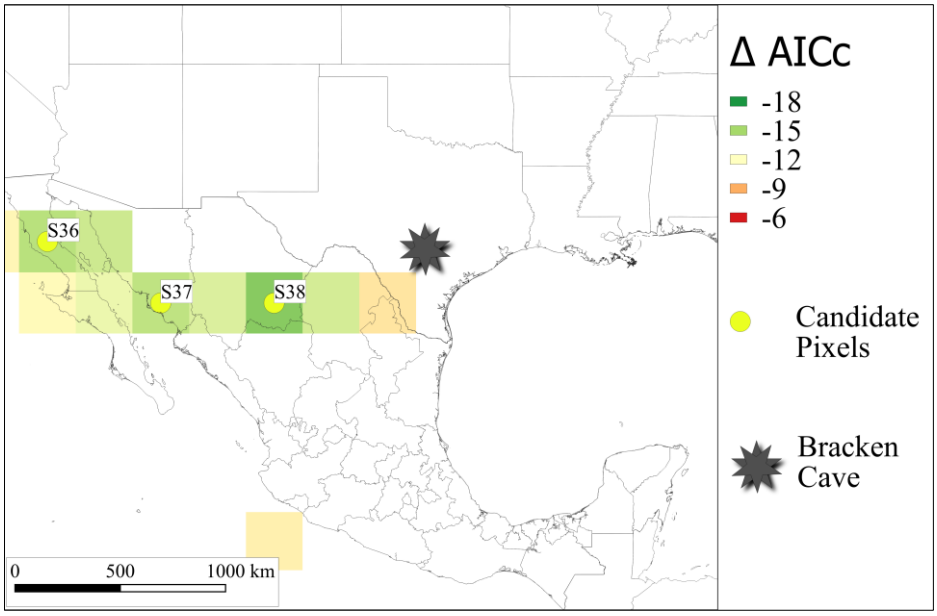
Δ AICc
-18
-15
-12
-9
-6
Candidate Pixels
Bracken Cave
S36
S37
S38
0
500
1000 km

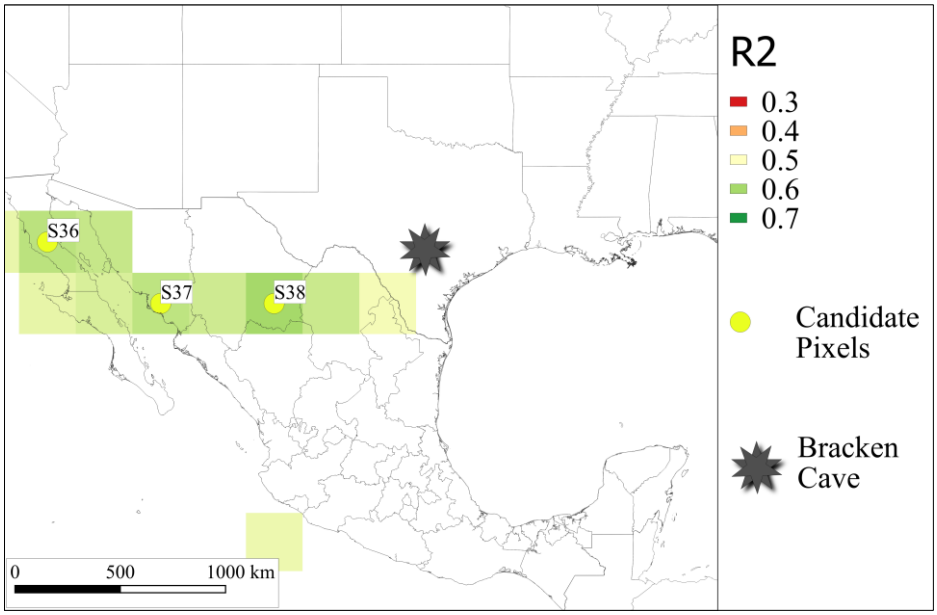
R2
0.3
0.4
0.5
0.6
0.7
Candidate Pixels
Bracken Cave
S36
S37
S38
0
500
1000 km

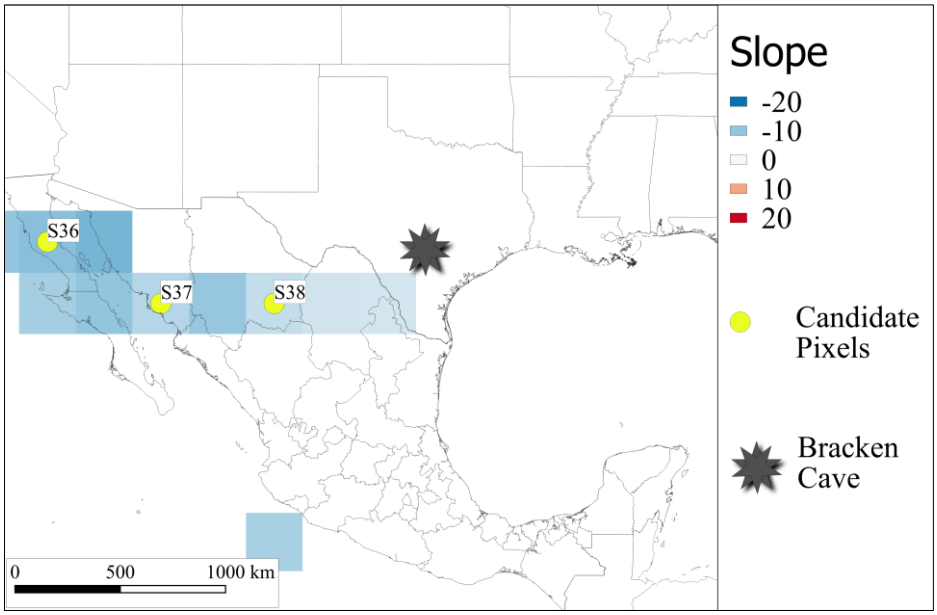
Slope
-20
-10
0
10
20
Candidate Pixels
Bracken Cave
S36
S37
S38
0
500
1000 km

Figure S11 Per species ΔAICc, adjusted R^2, and regression coefficient maps of the identified best time windows for the influence of wind assistance at the 700-hPa pressure level on spring migration phenology. The ΔAICc values are the difference of the AICc value of the model with the selected best time window for each grid cell with the AICc value of the baseline model (arrival/passage = α + β*year). ΔAICc values are only shown for grid cells that had a probability Pc value < 0.3, i.e., grid cells for which the relation between the identified time window and arrival/passage dates had a ΔAICc that is less likely to obtain due to chance. The adjusted R^2 values are for the models that have as independent variables both the best identified time window for wind assistance and the „year" term to account for trends. The regression coefficient maps show the regression coefficient (days/m*s^{-1}) of the best identified time window for the wind assistance when „year" terms to account for trends are also included in the model. Yellow dots with annotated numbers indicate the candidate grid cells selected as potentially influencing spring migration phenology at Bracken Cave. The ID values are used consistently throughout all supplementary figures and tables for ease of reference.

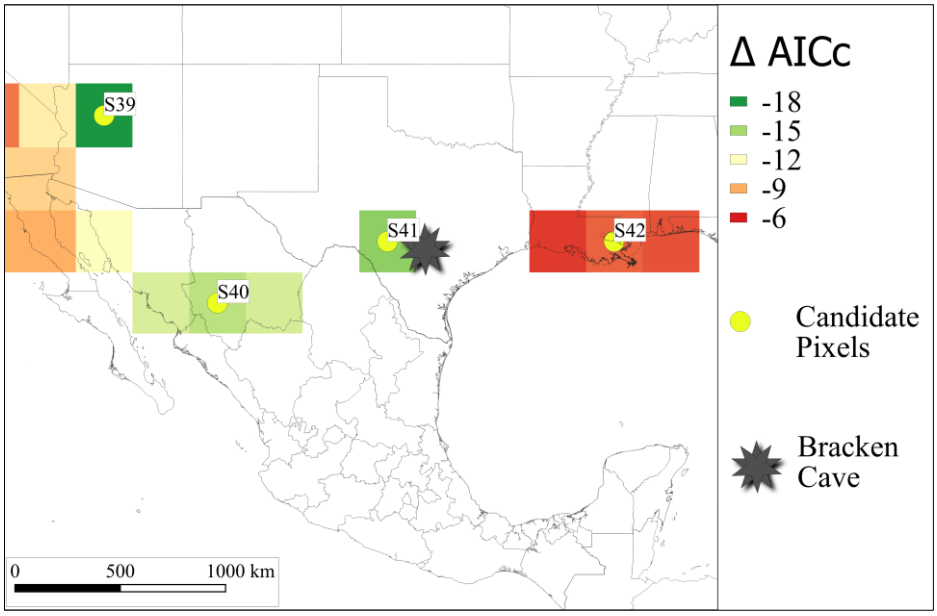
S39
S41
S42
S40
0
500
1000 km
Δ AICc
-18
-15
-12
-9
-6
Candidate Pixels
Bracken Cave

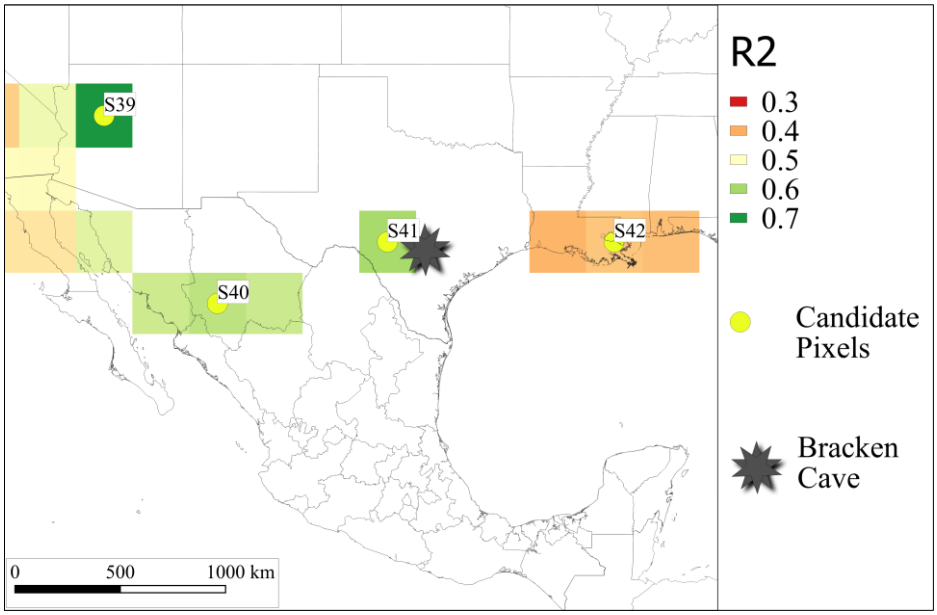
S39
S41
S42
S40
0
500
1000 km
R2
0.3
0.4
0.5
0.6
0.7
Candidate Pixels
Bracken Cave

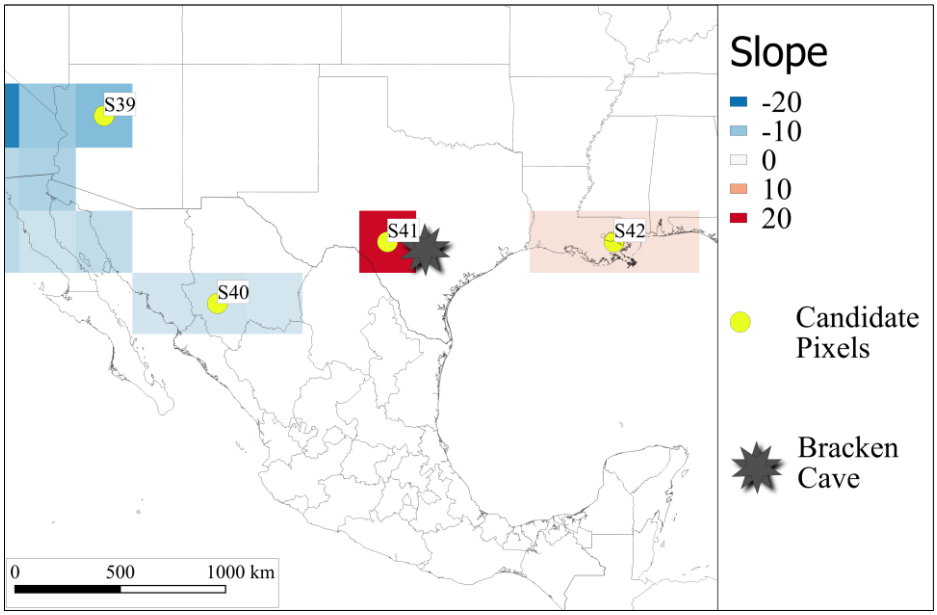
S39
S41
S42
S40
0
500
1000 km
Slope
-20
-10
0
10
20
Candidate Pixels
Bracken Cave

Figure S12 Per species ΔAICc, adjusted R^2, and regression coefficient maps of the identified best time windows for temperature influence on autumn migration phenology. The ΔAICc values are the difference of the AICc value of the model with the selected best time window for each grid cell with the AICc value of the baseline model (arrival/passage = α + β*year). ΔAICc values are only shown for grid cells that had a probability Pc value < 0.3, i.e., grid cells for which the relation between the identified time window and arrival/passage dates had a ΔAICc that is less likely to obtain due to chance. The adjusted R^2 values are for the models that have as independent variables both the best identified time window for temperature and the „year" term to account for trends. The regression coefficient maps show the regression coefficient (days/°C) of the best identified time window for temperature when „year" terms to account for trends are also included in the model. Yellow dots with annotated numbers indicate the candidate grid cells selected as potentially influencing autumn migration phenology at Bracken Cave. The ID values are used consistently throughout all supplementary figures and tables for ease of reference.

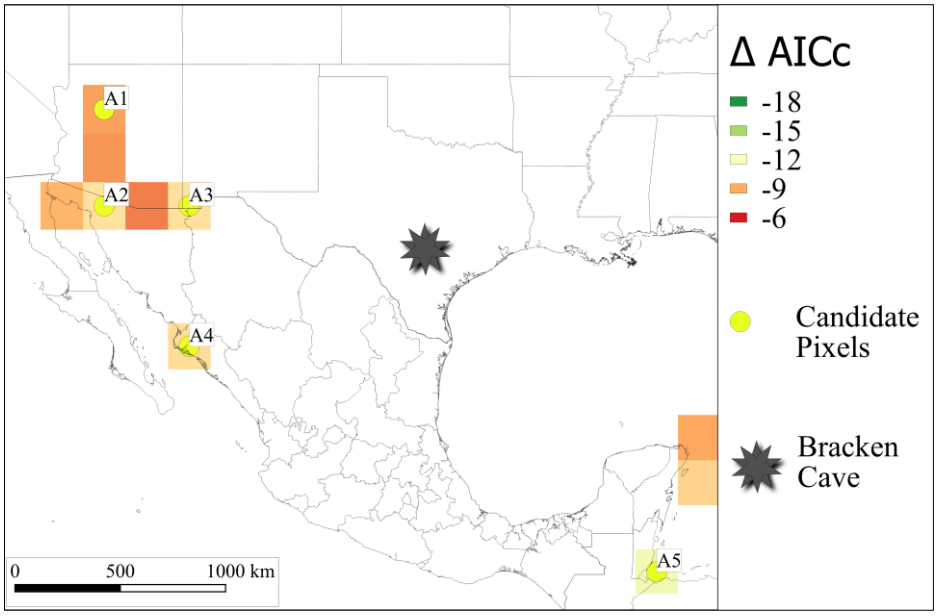
Δ AICc
-18
-15
-12
-9
-6
Candidate Pixels
Bracken Cave
A1
A2
A3
A4
A5
0
500
1000 km

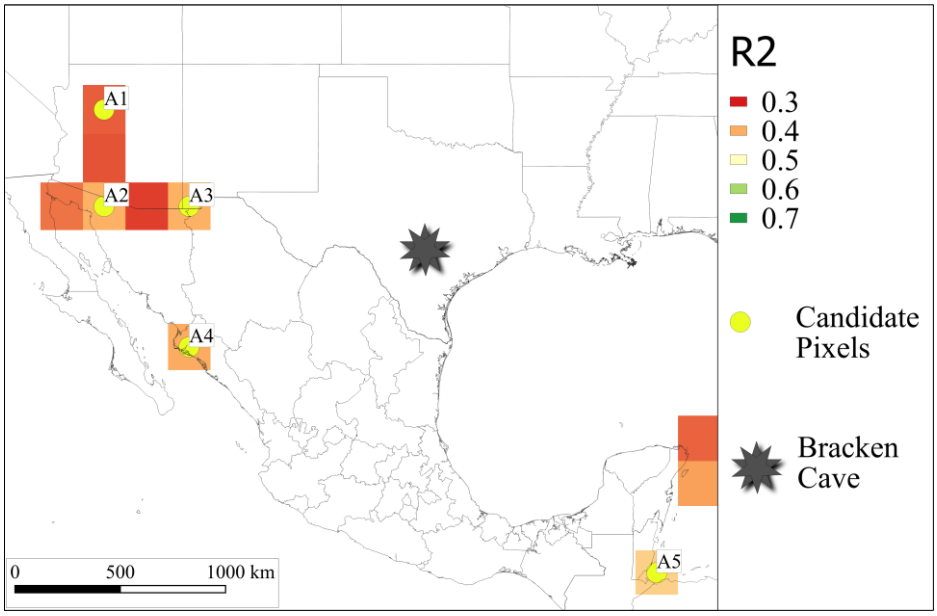
R2
0.3
0.4
0.5
0.6
0.7
Candidate Pixels
Bracken Cave
A1
A2
A3
A4
A5
0
500
1000 km

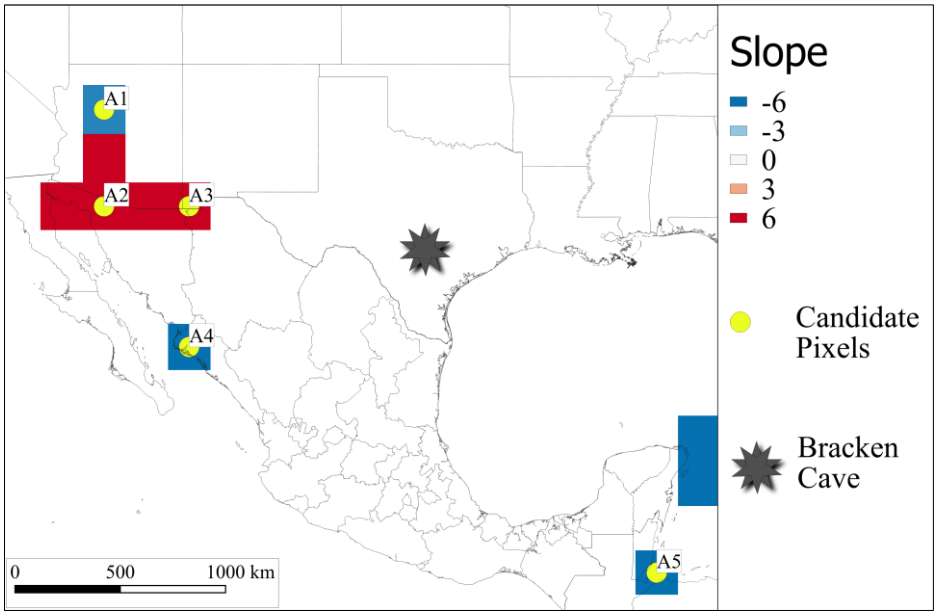
Slope
-6
-3
0
3
6
Candidate Pixels
Bracken Cave
A1
A2
A3
A4
A5
0
500
1000 km

Figure S13 Per species ΔAICc, adjusted R^2, and regression coefficient maps of the identified best time windows for precipitation influence on autumn migration phenology. The ΔAICc values are the difference of the AICc value of the model with the selected best time window for each grid cell with the AICc value of the baseline model (arrival/passage = α + β*year). ΔAICc values are only shown for grid cells that had a probability Pc value < 0.3, i.e., grid cells for which the relation between the identified time window and arrival/passage dates had a ΔAICc that is less likely to obtain due to chance. The adjusted R^2 values are for the models that have as independent variables both the best identified time window for precipitation and the „year" term to account for trends. The regression coefficient maps show the regression coefficient (days/mm) of the best identified time window for precipitation when „year" terms to account for trends are also included in the model. Yellow dots with annotated numbers indicate the candidate grid cells selected as potentially influencing autumn migration phenology at Bracken Cave. The ID values are used consistently throughout all supplementary figures and tables for ease of reference.

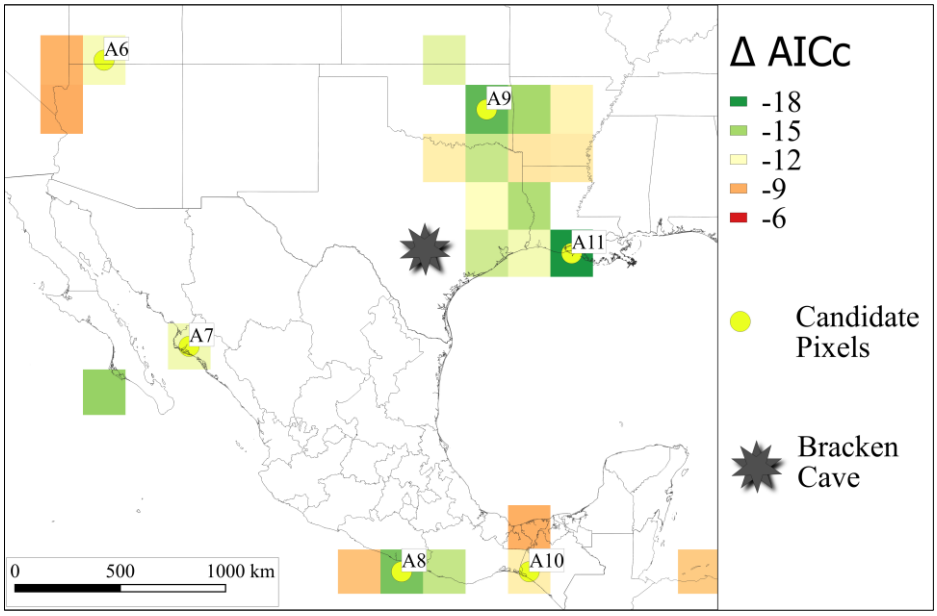
A6
A9
A11
A7
A8
A10
0
500
1000 km
Δ AICc
-18
-15
-12
-9
-6
Candidate Pixels
Bracken Cave

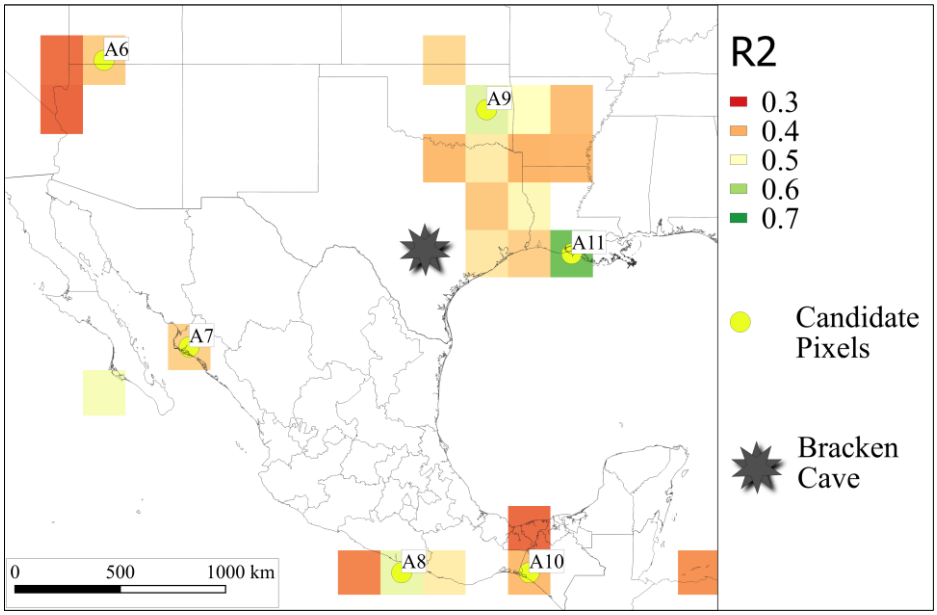
A6
A9
A11
A7
A8
A10
0
500
1000 km
R2
0.3
0.4
0.5
0.6
0.7
Candidate Pixels
Bracken Cave

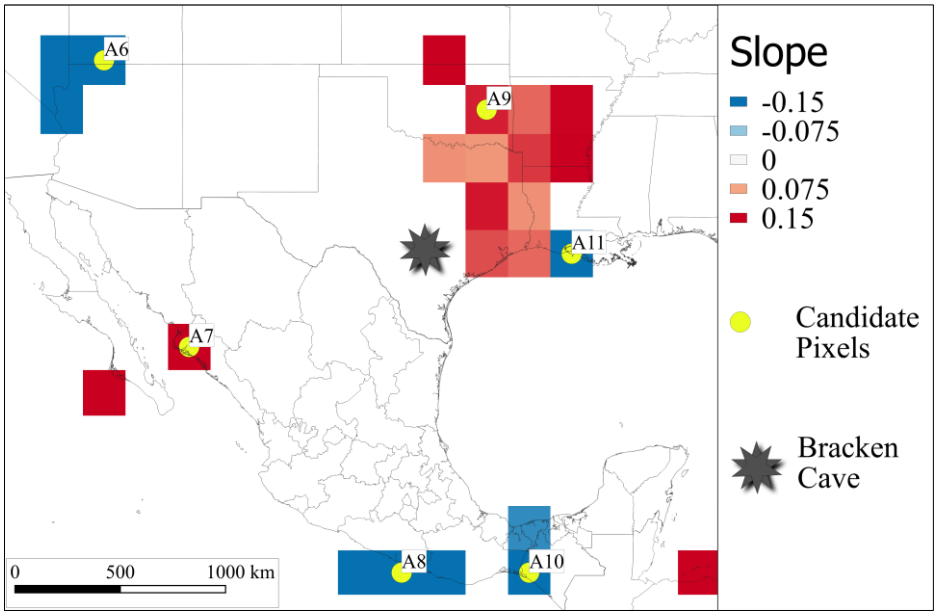
A6
A9
A11
A7
A8
A10
0
500
1000 km
Slope
-0.15
-0.075
0
0.075
0.15
Candidate Pixels
Bracken Cave

Figure S14 Per species ΔAICc, adjusted R^2, and regression coefficient maps of the identified best time windows for the influence on autumn migration phenology of the number of days with winds at the 925-hPa pressure level coming from the direction of Bracken Cave. The ΔAICc values are the difference of the AICc value of the model with the selected best time window for each grid cell with the AICc value of the baseline model (arrival/passage = $\alpha + \beta$*year). ΔAICc values are only shown for grid cells that had a probability Pc value < 0.3, i.e., grid cells for which the relation between the identified time window and arrival/passage dates had a ΔAICc that is less likely to obtain due to chance. The adjusted R^2 values are for the models that have as independent variables both the best identified time window for number of days with wind coming from Bracken Cave and the „year" term to account for trends. The regression coefficient maps show the regression coefficient (days/day) of the best identified time window for the number of days with wind coming from Bracken Cave when „year" terms to account for trends are also included in the model. Yellow dots with annotated numbers indicate the candidate grid cells selected as potentially influencing autumn migration phenology at Bracken Cave. The ID values are used consistently throughout all supplementary figures and tables for ease of reference.

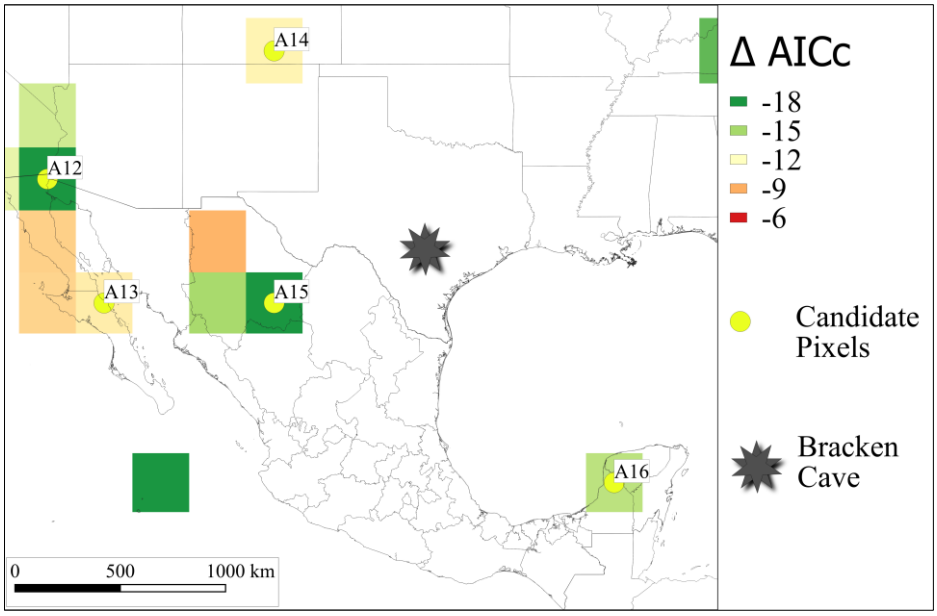
A14
A12
A13
A15
A16
0
500
1000 km
Δ AICc
-18
-15
-12
-9
-6
Candidate Pixels
Bracken Cave

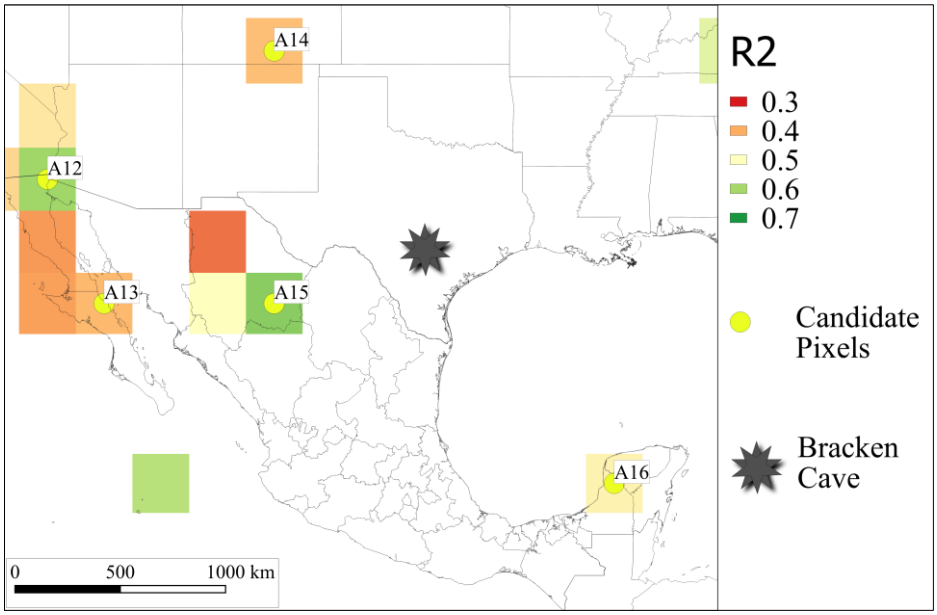
A14
A12
A13
A15
A16
0
500
1000 km
R2
0.3
0.4
0.5
0.6
0.7
Candidate Pixels
Bracken Cave

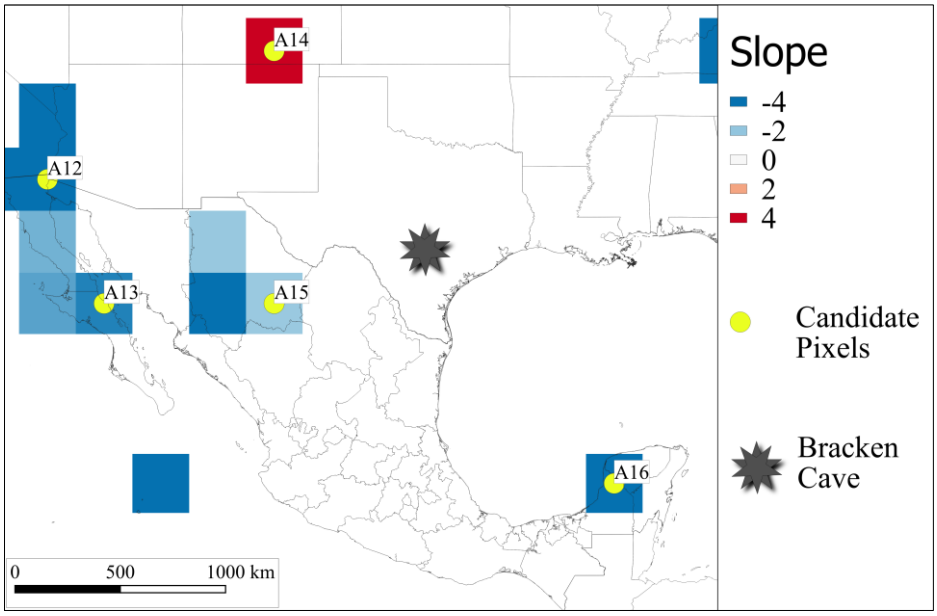
A14
A12
A13
A15
A16
0
500
1000 km
Slope
-4
-2
0
2
4
Candidate Pixels
Bracken Cave

Figure S15 Per species ΔAICc, adjusted R^2, and regression coefficient maps of the identified best time windows for the influence on autumn migration phenology of the number of days with winds at the 925-hPa pressure level going in the direction of Bracken Cave. The ΔAICc values are the difference of the AICc value of the model with the selected best time window for each grid cell with the AICc value of the baseline model (arrival/passage = $\alpha + \beta$*year). ΔAICc values are only shown for grid cells that had a probability Pc value < 0.3, i.e., grid cells for which the relation between the identified time window and arrival/passage dates had a ΔAICc that is less likely to obtain due to chance. The adjusted R^2 values are for the models that have as independent variables both the best identified time window for number of days with wind going in the direction of Bracken Cave and the „year" term to account for trends. The regression coefficient maps show the regression coefficient (days/day) of the best identified time window for the number of days with wind going in the direction of Bracken Cave when „year" terms to account for trends are also included in the model. Yellow dots with annotated numbers indicate the candidate grid cells selected as potentially influencing autumn migration phenology at Bracken Cave. The ID values are used consistently throughout all supplementary figures and tables for ease of reference.

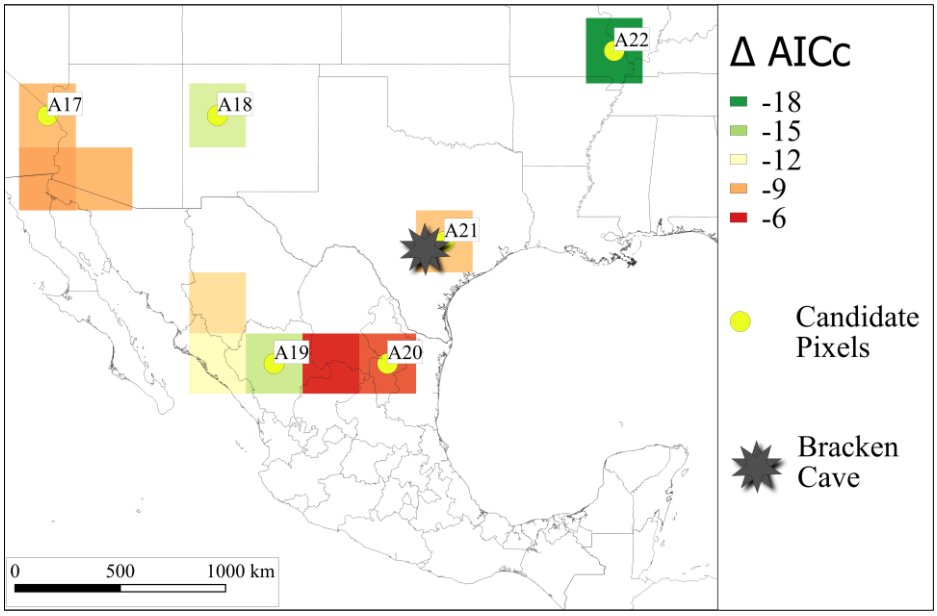
A17
A18
A22
A21
A19
A20
0
500
1000 km
Δ AICc
-18
-15
-12
-9
-6
Candidate Pixels
Bracken Cave

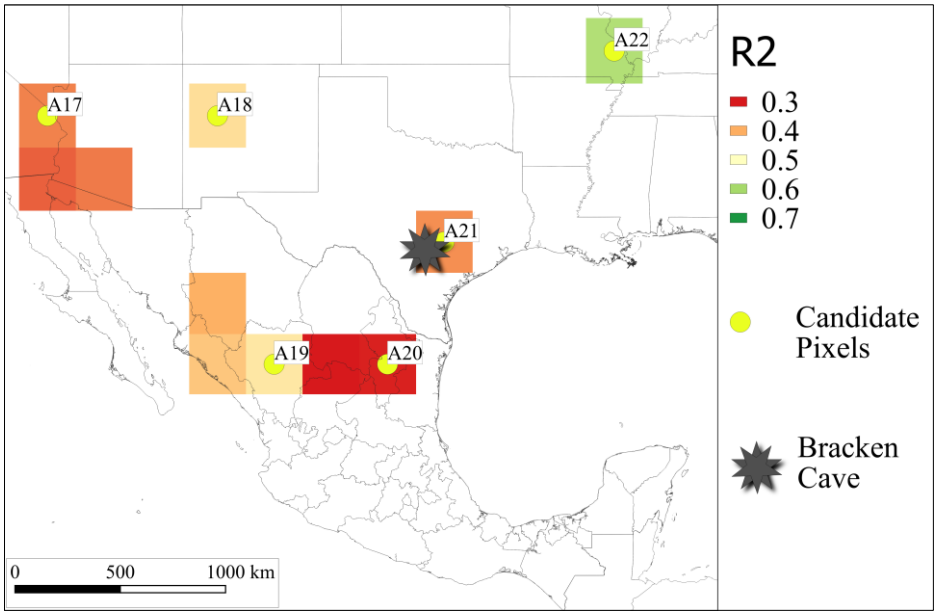
A17
A18
A22
A21
A19
A20
0
500
1000 km
R2
0.3
0.4
0.5
0.6
0.7
Candidate Pixels
Bracken Cave

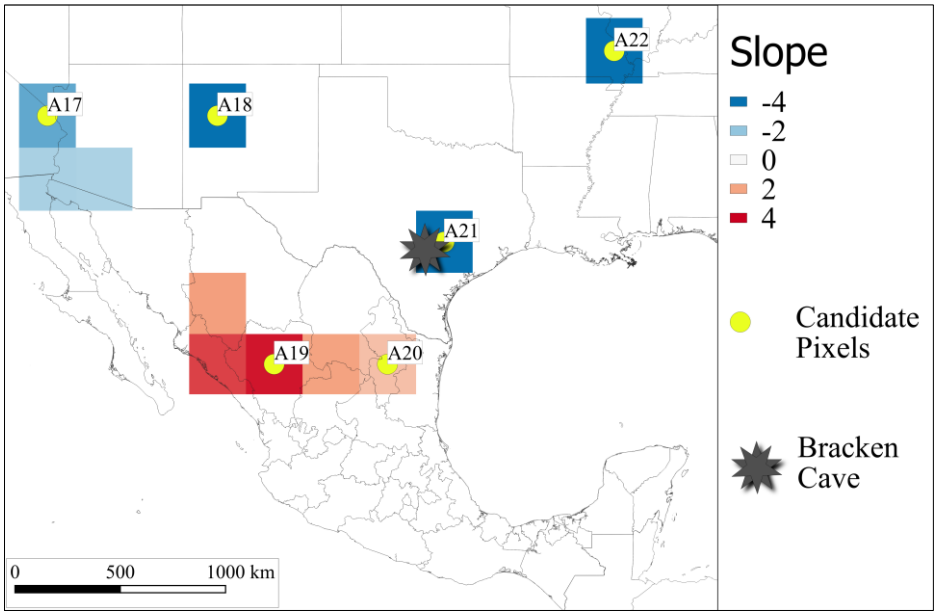
A17
A18
A22
A21
A19
A20
0
500
1000 km
Slope
-4
-2
0
2
4
Candidate Pixels
Bracken Cave

Figure S16 Per species ΔAICc, adjusted R^2, and regression coefficient maps of the identified best time windows for the influence on autumn migration phenology of the number of days with winds at the 850-hPa pressure level coming from the direction of Bracken Cave. The ΔAICc values are the difference of the AICc value of the model with the selected best time window for each grid cell with the AICc value of the baseline model (arrival/passage = $\alpha + \beta$*year). ΔAICc values are only shown for grid cells that had a probability Pc value < 0.3, i.e., grid cells for which the relation between the identified time window and arrival/passage dates had a ΔAICc that is less likely to obtain due to chance. The adjusted R^2 values are for the models that have as independent variables both the best identified time window for number of days with wind coming from Bracken Cave and the „year" term to account for trends. The regression coefficient maps show the regression coefficient (days/day) of the best identified time window for the number of days with wind coming from Bracken Cave when „year" terms to account for trends are also included in the model. Yellow dots with annotated numbers indicate the candidate grid cells selected as potentially influencing autumn migration phenology at Bracken Cave. The ID values are used consistently throughout all supplementary figures and tables for ease of reference.

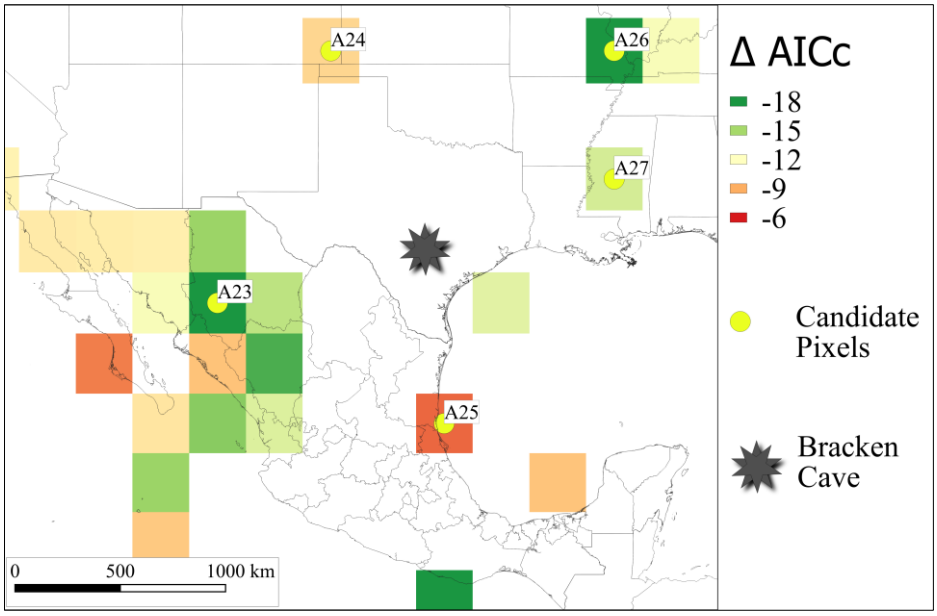
A24
A26
A27
A23
A25
0
500
1000 km
Δ AICc
-18
-15
-12
-9
-6
Candidate Pixels
Bracken Cave

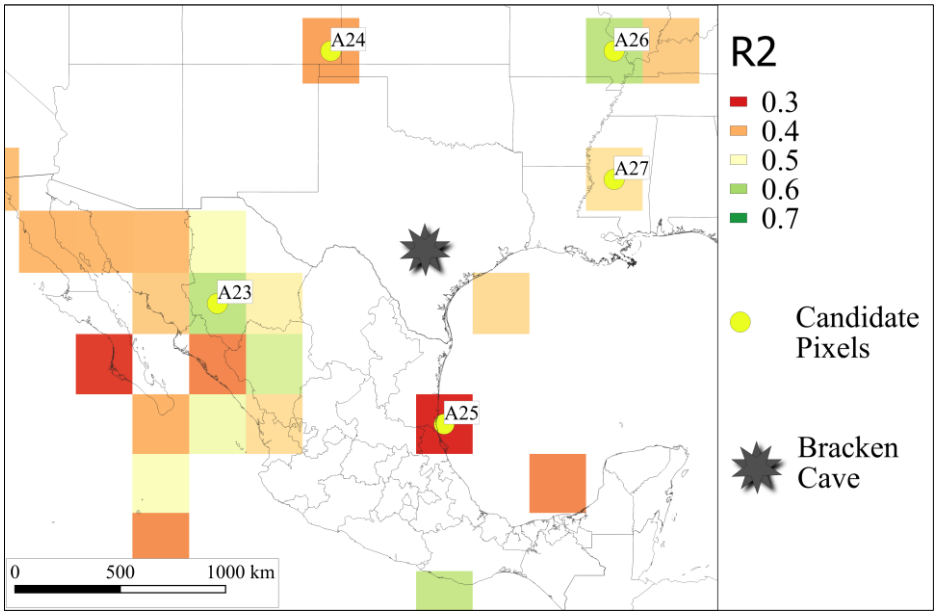
A24
A26
A27
A23
A25
0
500
1000 km
R2
0.3
0.4
0.5
0.6
0.7
Candidate Pixels
Bracken Cave

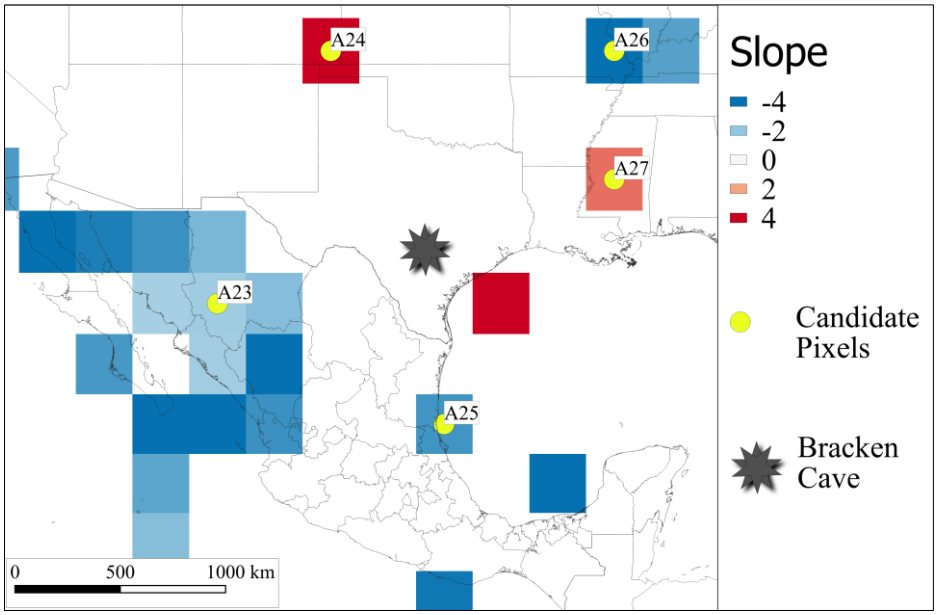
A24
A26
A27
A23
A25
0
500
1000 km
Slope
-4
-2
0
2
4
Candidate Pixels
Bracken Cave

Figure S17 Per species ΔAICc, adjusted R^2, and regression coefficient maps of the identified best time windows for the influence on autumn migration phenology of the number of days with winds at the 850-hPa pressure level going in the direction of Bracken Cave. The ΔAICc values are the difference of the AICc value of the model with the selected best time window for each grid cell with the AICc value of the baseline model (arrival/passage = $\alpha + \beta$*year). ΔAICc values are only shown for grid cells that had a probability Pc value < 0.3, i.e., grid cells for which the relation between the identified time window and arrival/passage dates had a ΔAICc that is less likely to obtain due to chance. The adjusted R^2 values are for the models that have as independent variables both the best identified time window for number of days with wind going in the direction of Bracken Cave and the „year" term to account for trends. The regression coefficient maps show the regression coefficient (days/day) of the best identified time window for the number of days with wind going in the direction of Bracken Cave when „year" terms to account for trends are also included in the model. Yellow dots with annotated numbers indicate the candidate grid cells selected as potentially influencing autumn migration phenology at Bracken Cave. The ID values are used consistently throughout all supplementary figures and tables for ease of reference.

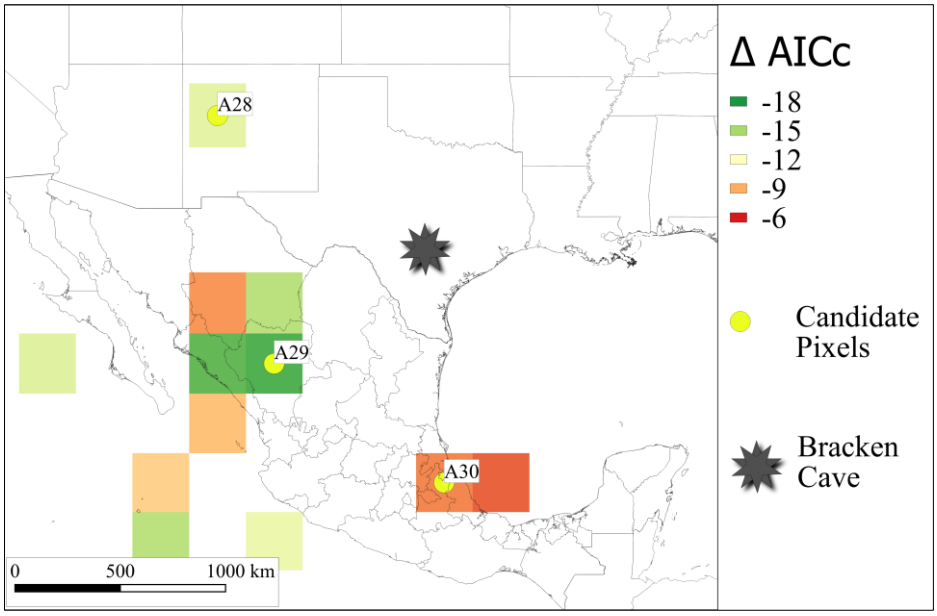
A28
A29
A30
0
500
1000 km
Δ AICc
-18
-15
-12
-9
-6
Candidate Pixels
Bracken Cave

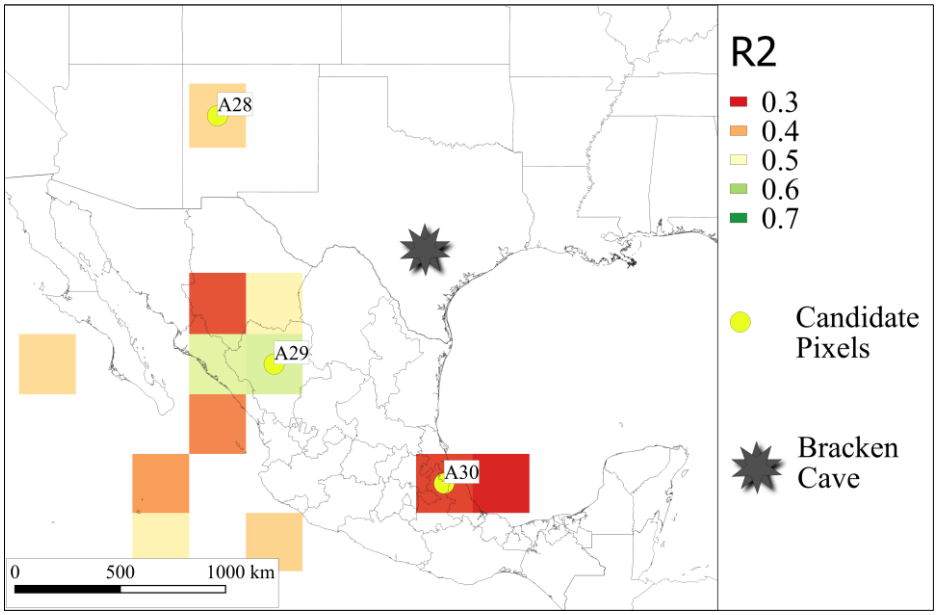
A28
A29
A30
0
500
1000 km
R2
0.3
0.4
0.5
0.6
0.7
Candidate Pixels
Bracken Cave

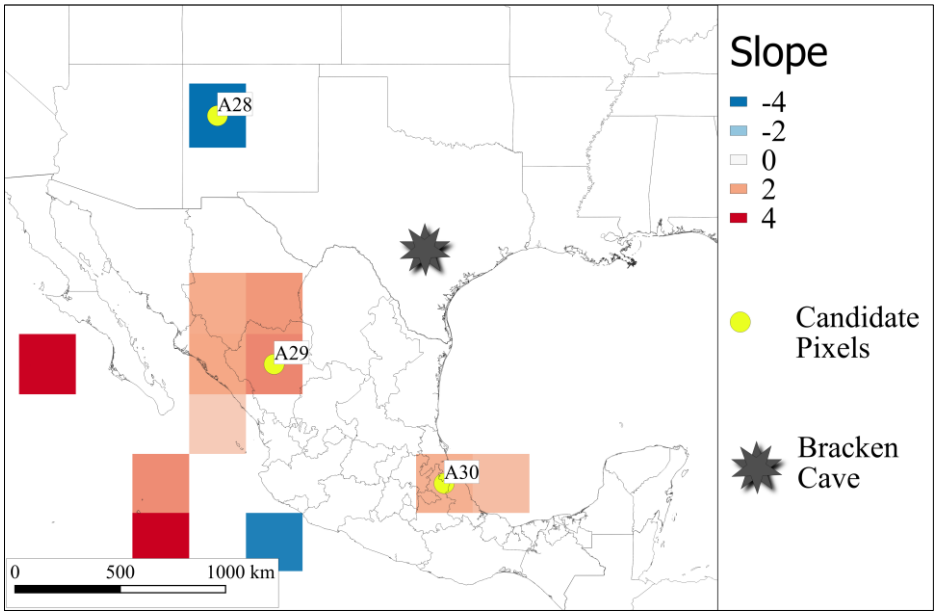
A28
A29
A30
0
500
1000 km
Slope
-4
-2
0
2
4
Candidate Pixels
Bracken Cave

Figure S18 Per species ΔAICc, adjusted R^2, and regression coefficient maps of the identified best time windows for the influence on autumn migration phenology of the number of days with winds at the 700-hPa pressure level coming from the direction of Bracken Cave. The ΔAICc values are the difference of the AICc value of the model with the selected best time window for each grid cell with the AICc value of the baseline model (arrival/passage = $\alpha + \beta$*year). ΔAICc values are only shown for grid cells that had a probability Pc value < 0.3, i.e., grid cells for which the relation between the identified time window and arrival/passage dates had a ΔAICc that is less likely to obtain due to chance. The adjusted R^2 values are for the models that have as independent variables both the best identified time window for number of days with wind coming from Bracken Cave and the „year" term to account for trends. The regression coefficient maps show the regression coefficient (days/day) of the best identified time window for the number of days with wind coming from Bracken Cave when „year" terms to account for trends are also included in the model. Yellow dots with annotated numbers indicate the candidate grid cells selected as potentially influencing autumn migration phenology at Bracken Cave. The ID values are used consistently throughout all supplementary figures and tables for ease of reference.

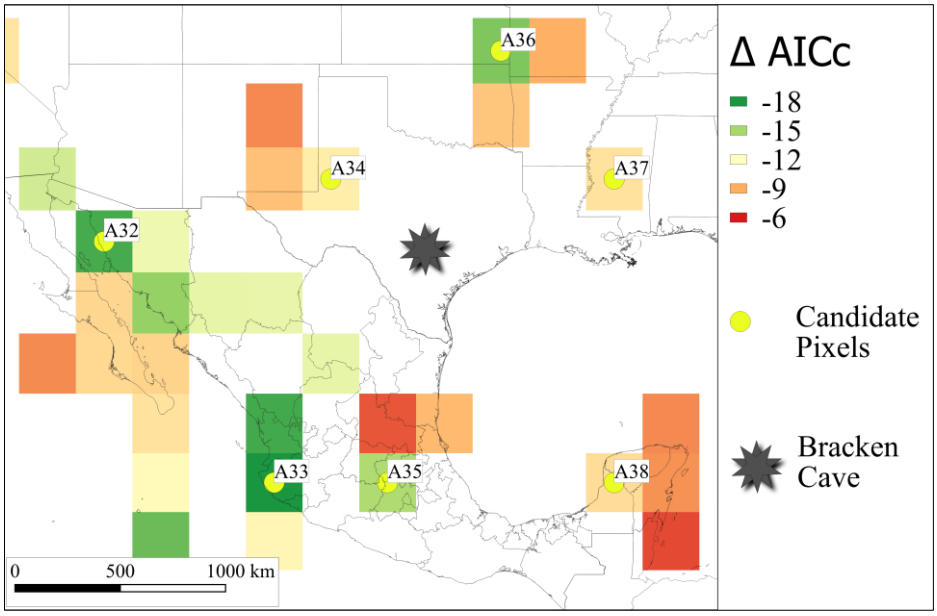
A36
A34
A37
A32
A33
A35
A38
0
500
1000 km
Δ AICc
-18
-15
-12
-9
-6
Candidate Pixels
Bracken Cave

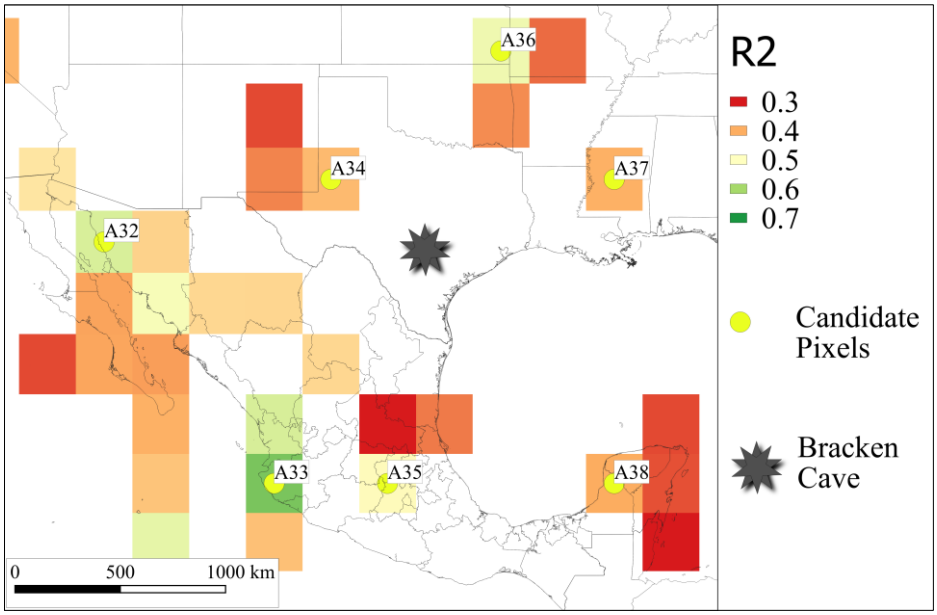
A36
A34
A37
A32
A33
A35
A38
0
500
1000 km
R2
0.3
0.4
0.5
0.6
0.7
Candidate Pixels
Bracken Cave

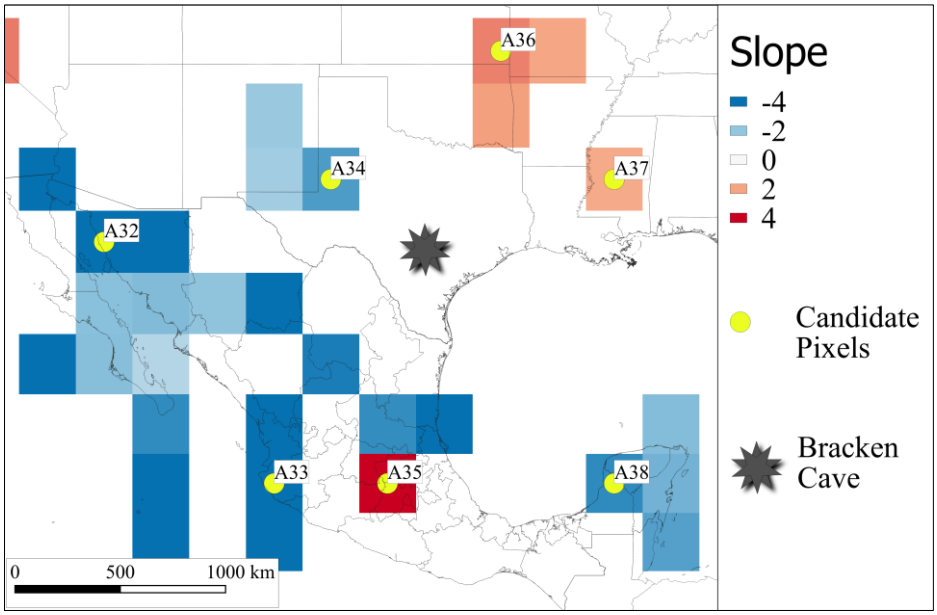
A36
A34
A37
A32
A33
A35
A38
0
500
1000 km
Slope
-4
-2
0
2
4
Candidate Pixels
Bracken Cave

Figure S19 Per species ΔAICc, adjusted R^2, and regression coefficient maps of the identified best time windows for the influence on autumn migration phenology of the number of days with winds at the 700-hPa pressure level going in the direction of Bracken Cave. The ΔAICc values are the difference of the AICc value of the model with the selected best time window for each grid cell with the AICc value of the baseline model (arrival/passage = $\alpha + \beta$*year). ΔAICc values are only shown for grid cells that had a probability Pc value < 0.3, i.e., grid cells for which the relation between the identified time window and arrival/passage dates had a ΔAICc that is less likely to obtain due to chance. The adjusted R^2 values are for the models that have as independent variables both the best identified time window for number of days with wind going in the direction of Bracken Cave and the „year" term to account for trends. The regression coefficient maps show the regression coefficient (days/day) of the best identified time window for the number of days with wind going in the direction of Bracken Cave when „year" terms to account for trends are also included in the model. Yellow dots with annotated numbers indicate the candidate grid cells selected as potentially influencing autumn migration phenology at Bracken Cave. The ID values are used consistently throughout all supplementary figures and tables for ease of reference.

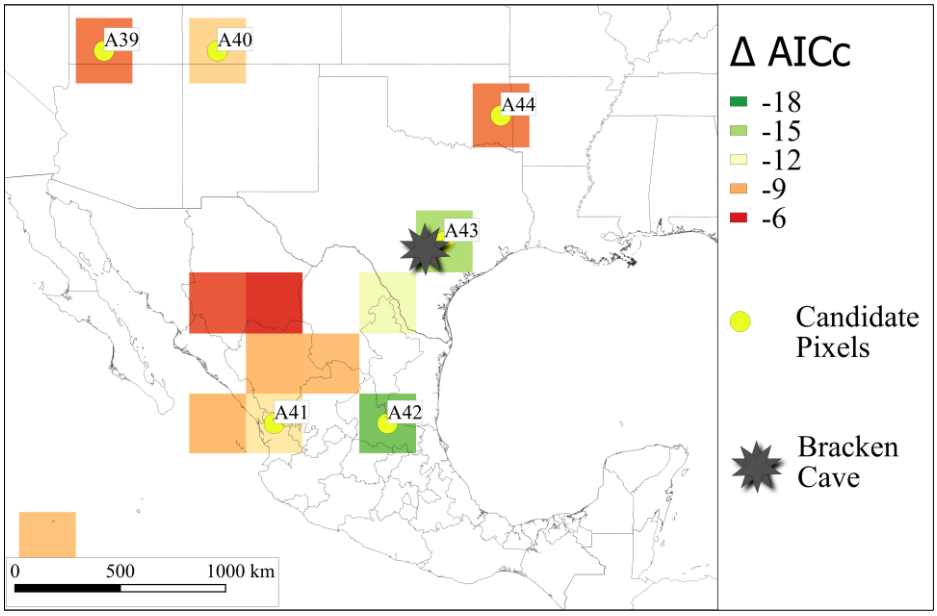
A39
A40
A44
A43
A41
A42
0
500
1000 km
Δ AICc
-18
-15
-12
-9
-6
Candidate Pixels
Bracken Cave

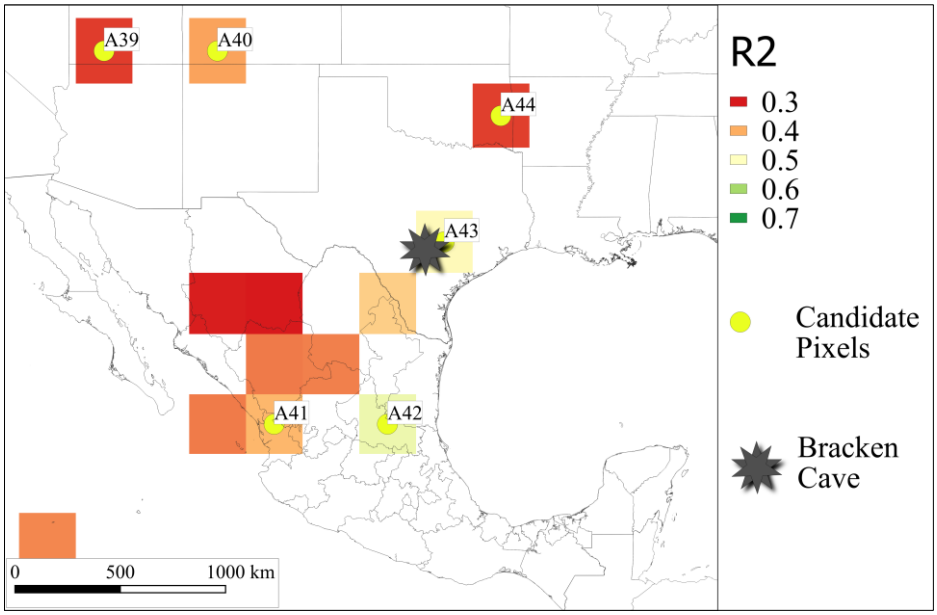
A39
A40
A44
A43
A41
A42
0
500
1000 km
R2
0.3
0.4
0.5
0.6
0.7
Candidate Pixels
Bracken Cave

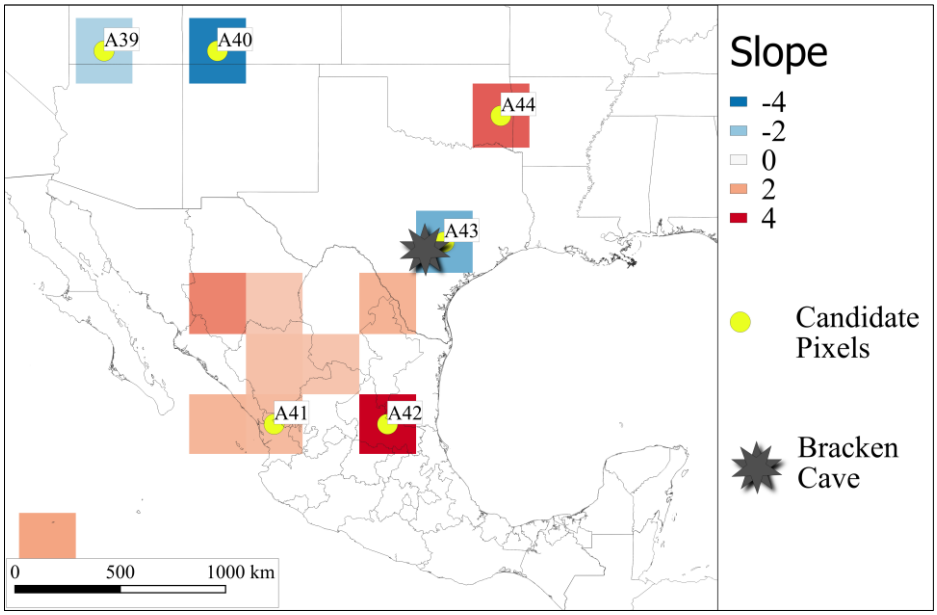
A39
A40
A44
A43
A41
A42
0
500
1000 km
Slope
-4
-2
0
2
4
Candidate Pixels
Bracken Cave

Figure S20 Per species ΔAICc, adjusted R^2, and regression coefficient maps of the identified best time windows for the influence of wind assistance at the 925-hPa pressure level on autumn migration phenology. The ΔAICc values are the difference of the AICc value of the model with the selected best time window for each grid cell with the AICc value of the baseline model (arrival/passage = α + β*year). ΔAICc values are only shown for grid cells that had a probability Pc value < 0.3, i.e., grid cells for which the relation between the identified time window and arrival/passage dates had a ΔAICc that is less likely to obtain due to chance. The adjusted R^2 values are for the models that have as independent variables both the best identified time window for wind assistance and the „year" term to account for trends. The regression coefficient maps show the regression coefficient (days/m*s^{-1}) of the best identified time window for the wind assistance when „year" terms to account for trends are also included in the model. Yellow dots with annotated numbers indicate the candidate grid cells selected as potentially influencing autumn migration phenology at Bracken Cave. The ID values are used consistently throughout all supplementary figures and tables for ease of reference.

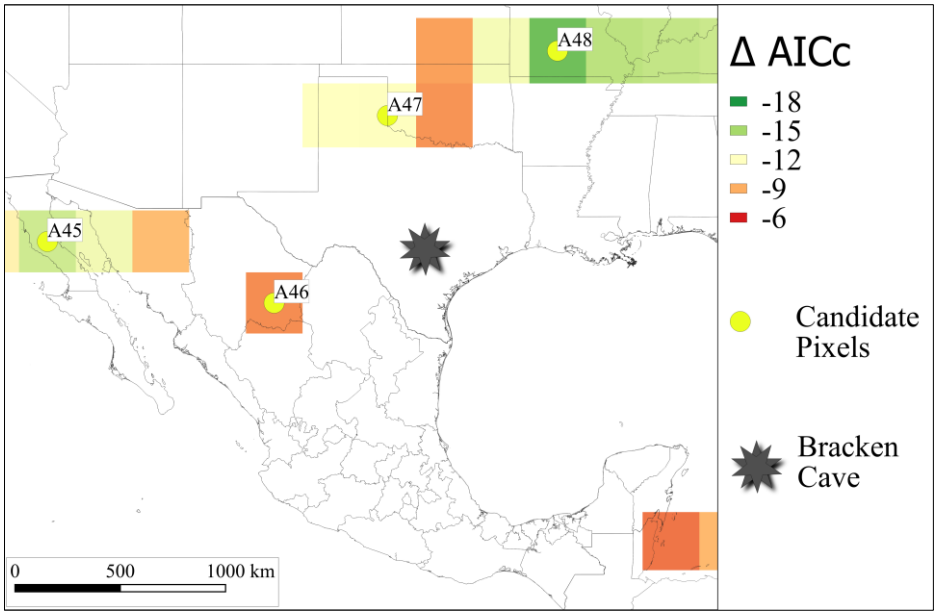
A48
A47
A45
A46
0
500
1000 km
Δ AICc
-18
-15
-12
-9
-6
Candidate Pixels
Bracken Cave

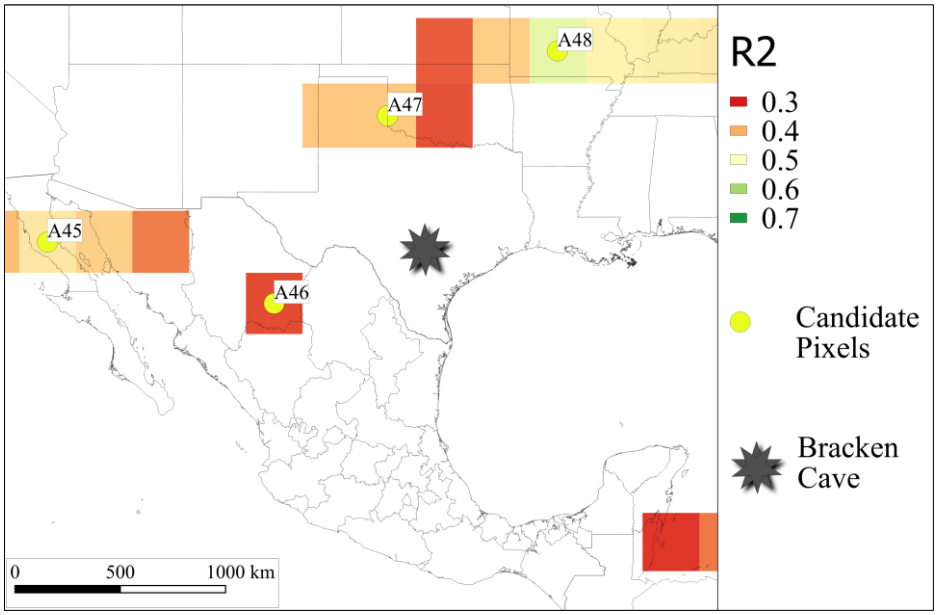
A48
A47
A45
A46
0
500
1000 km
R2
0.3
0.4
0.5
0.6
0.7
Candidate Pixels
Bracken Cave

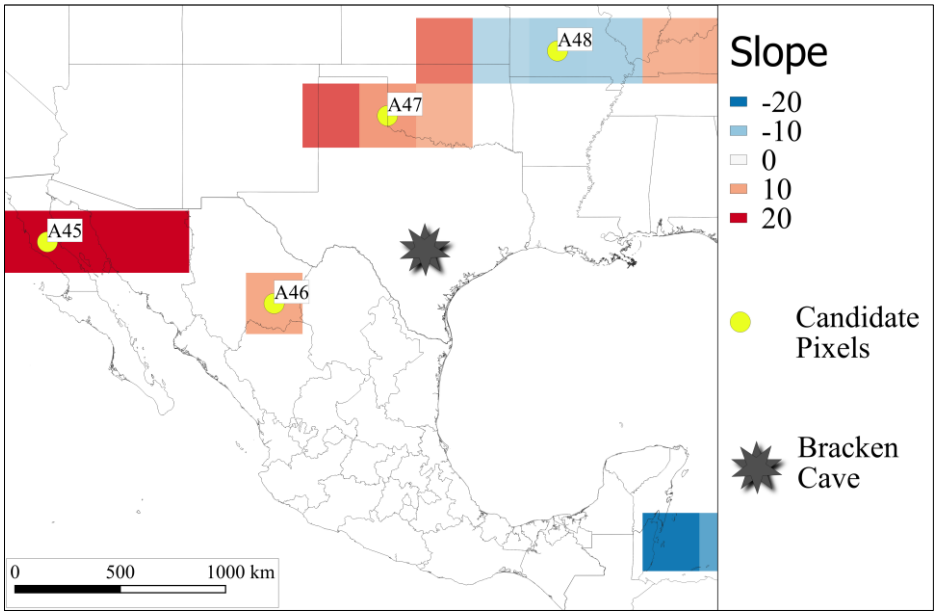
A48
A47
A45
A46
0
500
1000 km
Slope
-20
-10
0
10
20
Candidate Pixels
Bracken Cave

Figure S21 Per species ΔAICc, adjusted R^2, and regression coefficient maps of the identified best time windows for the influence of wind assistance at the 850-hPa pressure level on autumn migration phenology. The ΔAICc values are the difference of the AICc value of the model with the selected best time window for each grid cell with the AICc value of the baseline model (arrival/passage = α + β*year). ΔAICc values are only shown for grid cells that had a probability Pc value < 0.3, i.e., grid cells for which the relation between the identified time window and arrival/passage dates had a ΔAICc that is less likely to obtain due to chance. The adjusted R^2 values are for the models that have as independent variables both the best identified time window for wind assistance and the „year" term to account for trends. The regression coefficient maps show the regression coefficient (days/m*s^{-1}) of the best identified time window for the wind assistance when „year" terms to account for trends are also included in the model. Yellow dots with annotated numbers indicate the candidate grid cells selected as potentially influencing autumn migration phenology at Bracken Cave. The ID values are used consistently throughout all supplementary figures and tables for ease of reference.

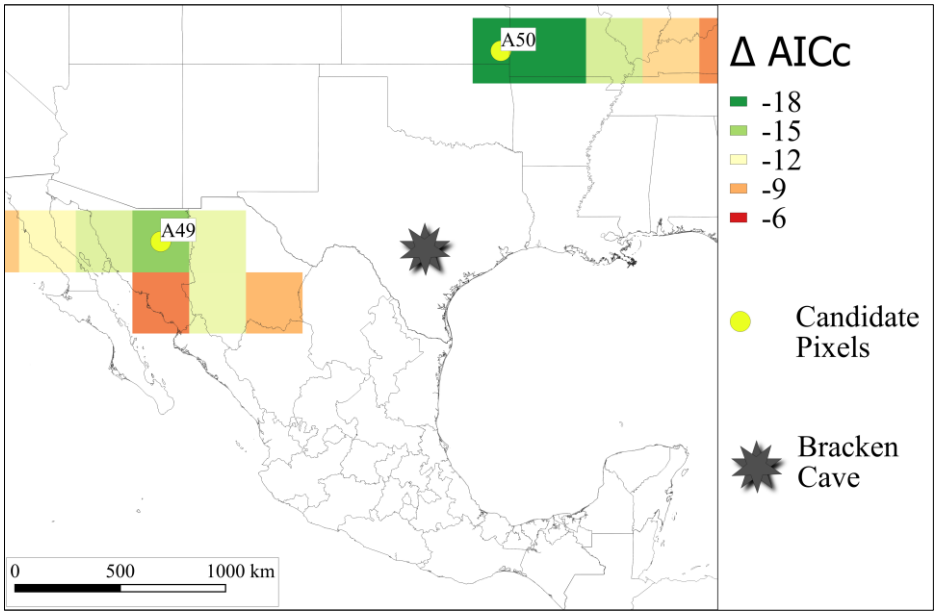
A50
A49
Δ AICc
-18
-15
-12
-9
-6
Candidate Pixels
Bracken Cave
0
500
1000 km

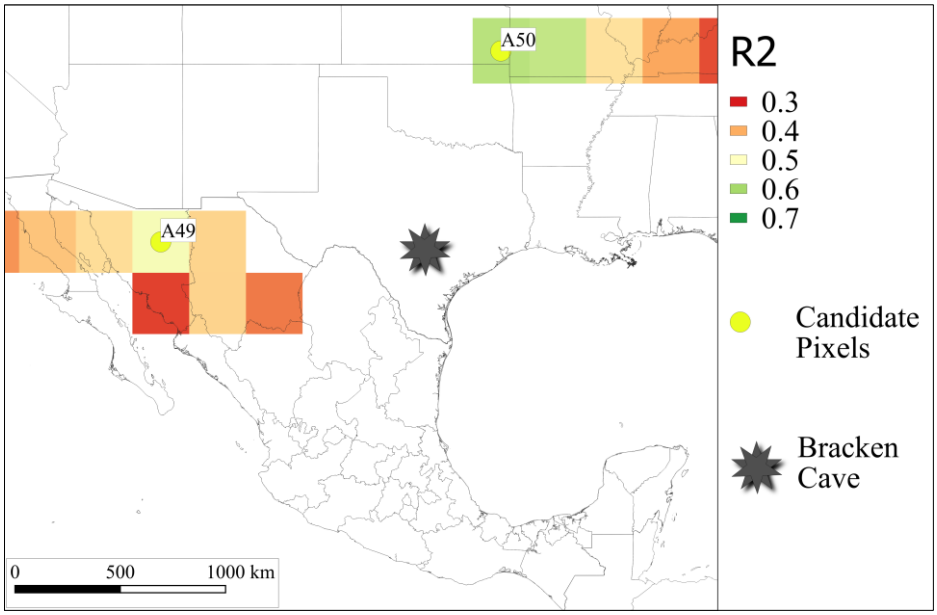
A50
A49
R2
0.3
0.4
0.5
0.6
0.7
Candidate Pixels
Bracken Cave
0
500
1000 km

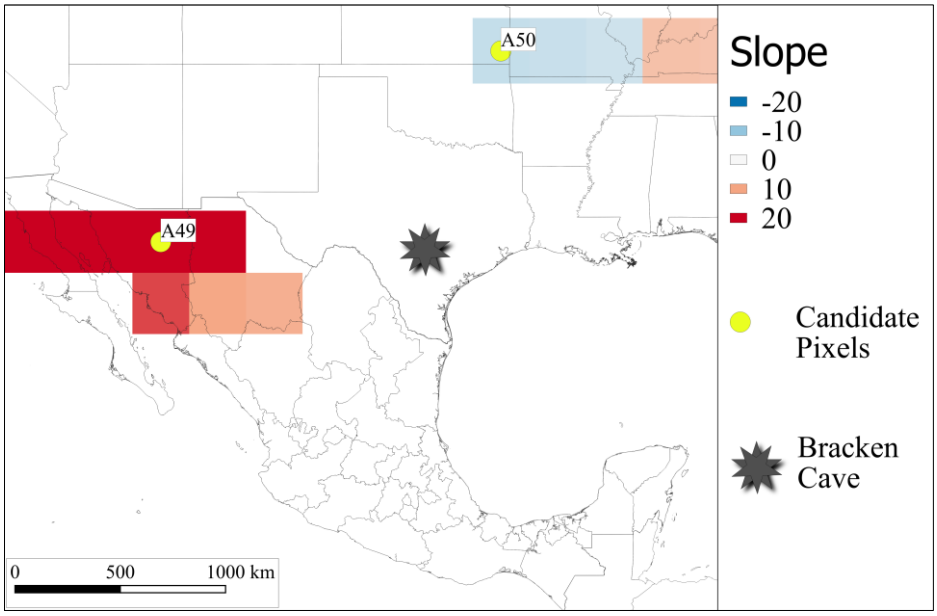
A50
A49
Slope
-20
-10
0
10
20
Candidate Pixels
Bracken Cave
0
500
1000 km

Figure S22 Per species ΔAICc, adjusted R^2, and regression coefficient maps of the identified best time windows for the influence of wind assistance at the 700-hPa pressure level on autumn migration phenology. The ΔAICc values are the difference of the AICc value of the model with the selected best time window for each grid cell with the AICc value of the baseline model (arrival/passage = α + β*year). ΔAICc values are only shown for grid cells that had a probability Pc value < 0.3, i.e., grid cells for which the relation between the identified time window and arrival/passage dates had a ΔAICc that is less likely to obtain due to chance. The adjusted R^2 values are for the models that have as independent variables both the best identified time window for wind assistance and the „year" term to account for trends. The regression coefficient maps show the regression coefficient (days/m*s^{-1}) of the best identified time window for the wind assistance when „year" terms to account for trends are also included in the model. Yellow dots with annotated numbers indicate the candidate grid cells selected as potentially influencing autumn migration phenology at Bracken Cave. The ID values are used consistently throughout all supplementary figures and tables for ease of reference.

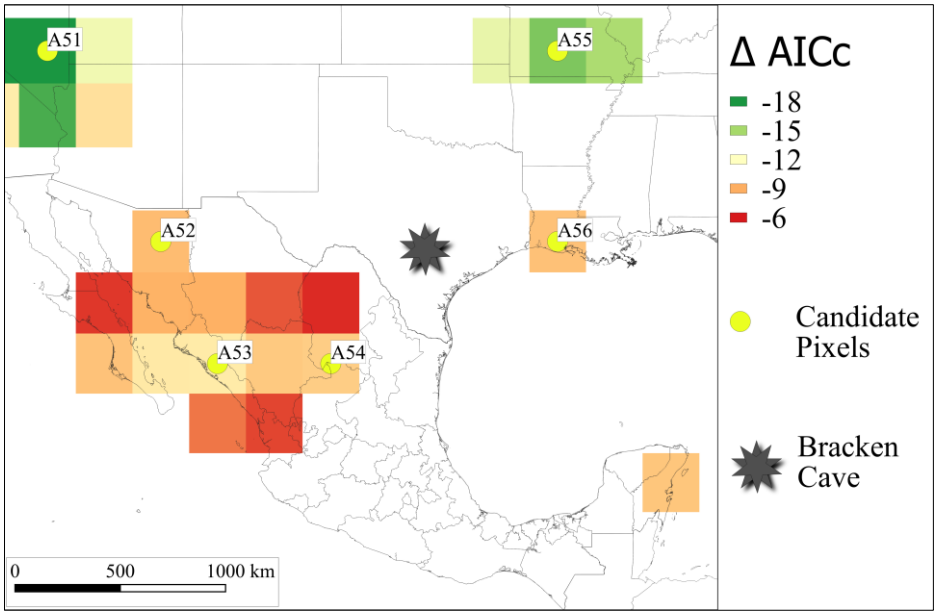
A51
A55
A52
A56
A53
A54
0
500
1000 km
Δ AICc
-18
-15
-12
-9
-6
Candidate Pixels
Bracken Cave

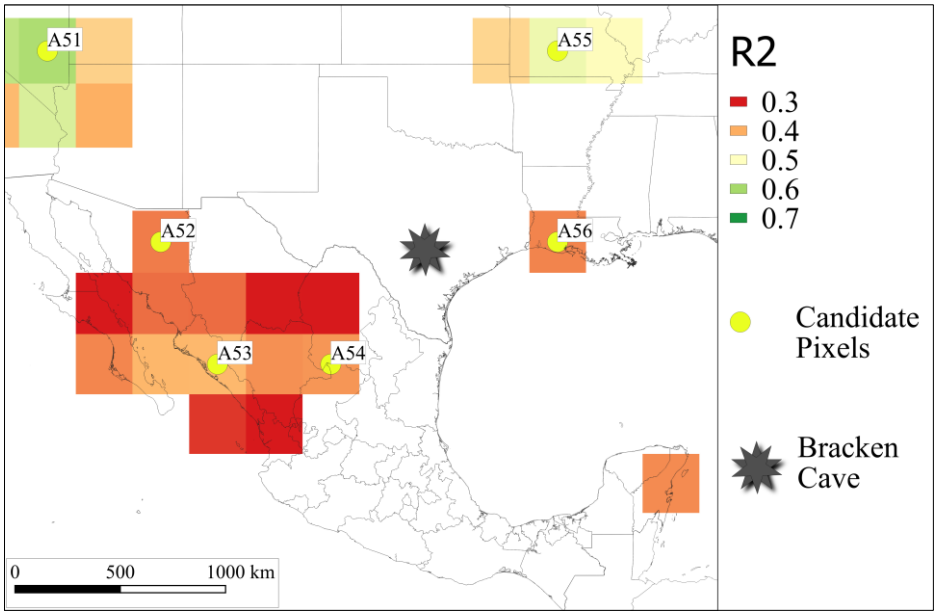
A51
A55
A52
A56
A53
A54
0
500
1000 km
R2
0.3
0.4
0.5
0.6
0.7
Candidate Pixels
Bracken Cave

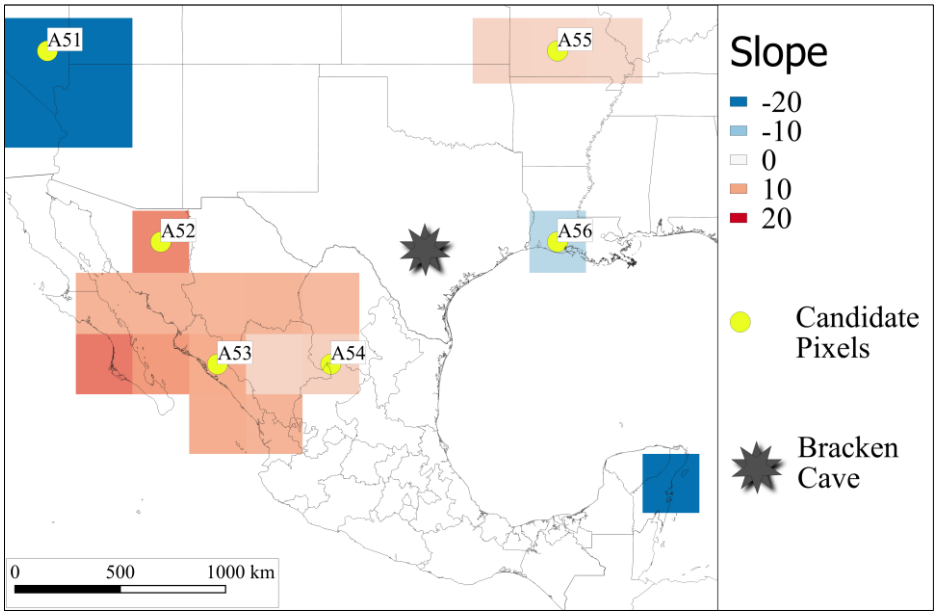
A51
A55
A52
A56
A53
A54
0
500
1000 km
Slope
-20
-10
0
10
20
Candidate Pixels
Bracken Cave

Figure S23 Elevation map of the study area. Data source: Jarvis *et al.* (2008)

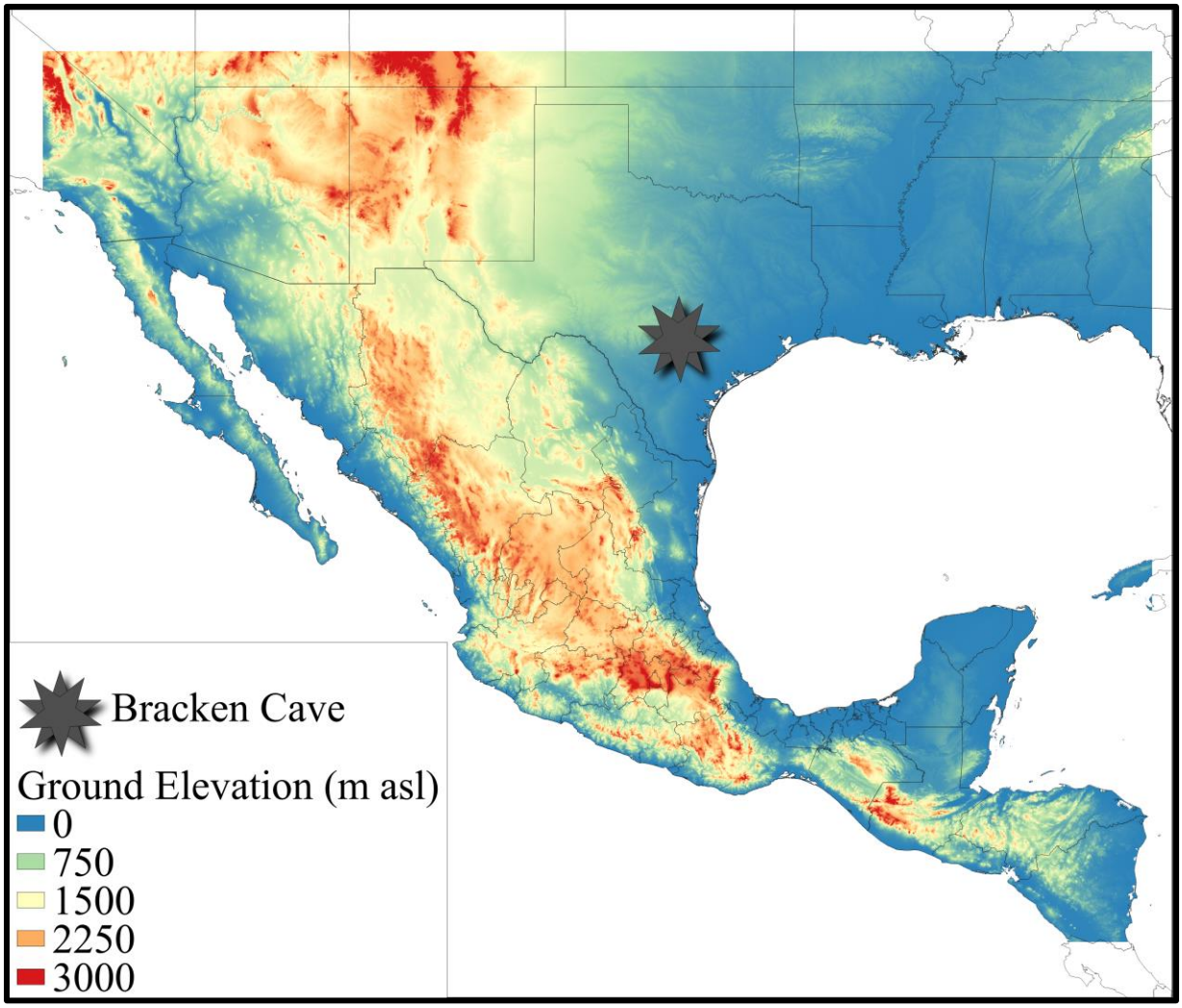

Table S1 General settings for the time window analyses

Reference day of the year:	
- Spring:	1 June
- Autumn:	31 December
Minimum time window length:	14
P_c* limit:	< 0.3

* Bailey & van de Pol (2016); van de Pol et al. (2016); Haest et al. (2018)

Table S2 Settings for the time window analysis, specific to each of the analysed weather variables

Weather variable*	**Operation on each time window**	**Maximum time window length**	**Period of the year analysed (approximate)**	**Number of windows analysed per grid cell**
Temperature	mean	365	Spring: 2 June to 1 June Autumn: 1 January to 31 December	62481
Precipitation	sum			
Wind - 925-hPa pressure level - coming from Bracken Cave	number of days	182	Spring: 1 December to 1 June Autumn: 2 July to 31 December	14706
Wind - 925-hPa pressure level - going to Bracken Cave				
Wind - 850-hPa pressure level - coming from Bracken Cave				
Wind - 850-hPa pressure level - going to Bracken Cave				
Wind - 700-hPa pressure level - coming from Bracken Cave				
Wind - 700-hPa pressure level - going to Bracken Cave				
Wind - 925-hPa pressure level - wind assistance	mean			
Wind - 850-hPa pressure level - wind assistance				
Wind - 700-hPa pressure level - wind assistance				

*For definitions of how the weather variables were calculated, see the "*Materials and Methods – Weather data"* section.

Table S3 Overview of the relative variable importance of the candidate weather signals for spring migration phenology, calculated using three different methods: (a) the sum of the multi-model AICc weights across all the possible models with maximum four independent variables (Burnham & Anderson, 2002); (b) the boruta method (Kursa & Rudnicki, 2010); and (c) the game-theory-based LMG metric for variance decomposition in linear models (Grömping, 2006, 2015). This table includes only the candidate weather signals that were not removed due to high collinearity with another better performing candidate signal, low performance compared to an intercept-only model, or because of relative variable importances using the boruta method that are likely obtained by chance. The ID values are used consistently throughout all supplementary figures and tables for ease of reference. WindGT: Wind going in the direction of Bracken Cave; WindCF: Wind coming from the direction of Bracken Cave.

						Relative Variable Importance				**Ranks of Relative Variable Importance**				
Climate variable	**ID**	**ΔAICc (compared to trend model)**	**ΔAICc (compared to intercept-only model)**	**Window Open Date**	**Window Close Date**	**Model weights**	**LMG**	**Boruta**	**Mean**	**Model weights**	**LMG**	**Boruta**	**Mean Rank**	**Rank of the mean**
WindGT – 925-hPa	**S12**	**-17.29**	**-19.35**	**13 Feb**	**13 Mar**	**0.25**	**0.09**	**0.10**	**0.15**	**14**	**12**	**14**	**13.3**	**14**
WindGT – 850-hPa	**S17**	**-18.51**	**-23.11**	**05 Dec**	**25 Dec**	**0.25**	**0.11**	**0.08**	**0.15**	**13**	**14**	**9**	**12**	**13**
WindGT – 850-hPa	S16	-9.77	-12.33	23 Feb	23 Mar	0.20	0.08	0.07	0.12	12	10	8	10	12
WindGT – 850-hPa	S20	-14.15	-19.02	04 Dec	19 Jan	0.09	0.10	0.10	0.10	11	13	12	12	11
WindGT – 700-hPa	S27	-17.54	-16.75	17 Dec	31 Dec	0.04	0.08	0.10	0.07	9	11	13	11	10
Wind Assistance – 850-hPa	S37	-14.15	-16.01	18 Dec	09 Jan	0.05	0.07	0.07	0.07	10	9	7	8.7	9
WindCF – 700-hPa	S21	-14.48	-15.25	04 Dec	24 Dec	0.03	0.07	0.09	0.06	7	7	11	8.3	8
WindGT – 700-hPa	S32	-16.64	-15.83	17 Feb	07 Mar	0.03	0.07	0.06	0.06	8	8	6	7.3	7
Wind Assistance – 925-hPa	S34	-13.70	-11.36	06 Dec	09 Feb	0.00	0.05	0.09	0.05	2	2	10	4.7	6
Wind Assistance – 700-hPa	S43	-15.60	-14.42	15 Feb	05 Mar	0.01	0.06	0.06	0.04	6	6	5	5.7	5
WindGT– 700-hPa	S28	-19.72	-13.36	04 Mar	25 Mar	0.01	0.06	0.04	0.04	4	5	1	3.3	4
WindGT – 925-hPa	S10	-12.02	-10.89	15 Mar	10 May	0.01	0.06	0.04	0.04	5	4	2	3.7	3
WindCF – 700-hPa	S25	-13.33	-9.25	20 Apr	27 May	0.01	0.05	0.05	0.03	3	1	4	2.7	2
Precipitation	S5	-10.30	-12.89	27 Aug	25 Feb	0.00	0.05	0.05	0.03	1	3	3	2.3	1

Table S4 Overview of the relative variable importance of the candidate weather signals for autumn migration phenology, calculated using three different methods: (a) the sum of the multi-model AICc weights across all the possible models with maximum four independent variables (Burnham & Anderson, 2002); (b) the boruta method (Kursa & Rudnicki, 2010); and (c) the game-theory-based LMG metric for variance decomposition in linear models (Grömping, 2006, 2015). This table includes only the candidate weather signals that were not removed due to high collinearity with another better performing candidate signal, low performance compared to an intercept-only model, or because of relative variable importances using the boruta method that are likely obtained by chance. The ID values are used consistently throughout all supplementary figures and tables for ease of reference. WindGT: Wind going in the direction of Bracken Cave; WindCF: Wind coming from the direction of Bracken Cave.

						Relative Variable Importance				Ranks of Relative Variable Importance				
Climate variable	**ID**	**ΔAICc (compared to trend model)**	**ΔAICc (compared to intercept-only model)**	**Window Open Date**	**Window Close Date**	**Model weights**	**LMG**	**Boruta**	**Mean**	**Model weights**	**LMG**	**Boruta**	**Mean Rank**	**Rank of the mean**
Precipitation	**A11**	**-22.27**	**-19.41**	**23-Feb**	**14-Mar**	**0.24**	**0.09**	**0.09**	**0.14**	**14**	**12**	**11**	**12.3**	**14**
Precipitation	**A9**	**-16.46**	**-14.50**	**03-Aug**	**26-Dec**	**0.22**	**0.08**	**0.09**	**0.13**	**13**	**10**	**12**	**11.7**	**13**
WindCF – 700-hPa	**A32**	**-17.05**	**-17.49**	**03-Nov**	**28-Nov**	**0.16**	**0.09**	**0.11**	**0.12**	**12**	**13**	**14**	**13**	**12**
Wind Assistance – 925-hPa	A47	-12.03	-11.79	09-Nov	01-Dec	0.05	0.07	0.11	0.08	7	8	13	9.3	11
WindCF – 700-hPa	A33	-21.97	-22.51	23-Sep	30-Oct	0.05	0.10	0.07	0.07	10	14	9	11	10
WindCF – 700-hPa	A36	-15.81	-14.40	10-Sep	01-Dec	0.07	0.07	0.06	0.07	11	7	6	8	9
Wind Assistance – 700-hPa	A51	-19.57	-15.33	31-Aug	14-Oct	0.05	0.08	0.06	0.06	9	11	3	7.7	8
Precipitation	A7	-12.44	-12.16	01-Oct	18-Dec	0.05	0.08	0.06	0.06	8	9	5	7.3	7
WindGT – 700-hPa	A43	-14.59	-12.14	22-Jul	31-Aug	0.02	0.07	0.07	0.05	5	6	10	7	6
WindGT – 925-hPa	A21	-9.95	-9.63	28-Oct	18-Nov	0.05	0.06	0.05	0.05	6	5	1	4	5
WindGT – 700-hPa	A42	-15.92	-14.60	22-Jul	08-Aug	0.00	0.06	0.07	0.04	1	4	8	4.3	4
Wind Assistance – 700-hPa	A52	-9.48	-10.02	10-Oct	29-Nov	0.02	0.05	0.06	0.04	4	2	4	3.3	3
WindGT – 700-hPa	A44	-8.04	-8.59	29-Aug	28-Sep	0.01	0.05	0.06	0.04	3	1	7	3.7	2
Wind Assistance – 925-hPa	A46	-8.33	-8.82	04-Sep	23-Sep	0.00	0.06	0.06	0.04	2	3	2	2.3	1

Table S5 Contribution of the effect of each weather variable on mean passage date (MPD) in spring and autumn to the overall trend in MPD over the period 1995-2017. Negative values are in italics. IDs are identical to those in Table S3 and S4, and Figure S1 to S22. Coef.: coefficient; SE: standard error. The ID values are used consistently throughout all supplementary figures and tables for ease of reference.

			$\frac{\partial MPD}{\partial Climate}$		$\frac{dClimate}{dTime}$		$\frac{\partial MPD}{\partial Climate} \times \frac{dClimate}{dTime}$		**Total change over 23 years**
Season	**Climate variable**	**ID**	**Coef.**	**SE**	**Coef.**	**SE**	**Coef.**	**SE**	**(days)**
Spring	tailwind 925-hPa	S12	-2.20	0.45	0.09	0.07	-0.21	0.16	-4.81
	tailwind 850-hPa	S17	-2.06	0.36	0.24	0.07	-0.50	0.17	-11.54
Autumn	precipitation	A9	0.06	0.01	-5.77	2.70	-0.34	0.18	-7.88
	precipitation	A11	-0.41	0.07	-0.43	0.60	0.18	0.25	4.08
	headwind 700-hPa	A32	-2.46	0.75	0.06	0.06	-0.14	0.16	-3.24

SI References

Bailey, L. D., & van de Pol, M. (2016). climwin: An R Toolbox for Climate Window Analysis. *PLoS ONE*, *11*(12), e0167980. https://doi.org/10.1371/journal.pone.0167980

Burnham, K. P., & Anderson, D. R. (2002). *Model Selection and Multimodel Inference: A Practical Information-Theoretic Approach - 2nd edition*. Springer Science+Business Media LLC

Grömping, U. (2006). R package relaimpo: relative importance for linear regression. *Journal Of Statistical Software*, *17*(1), 139–147. https://doi.org/10.1016/j.foreco.2006.08.245

Grömping, U. (2015). Variable importance in regression models. *Wiley Interdisciplinary Reviews: Computational Statistics*, *7*(2), 137–152. https://doi.org/10.1002/wics.1346

Haest, B., Hüppop, O., & Bairlein, F. (2018a). Challenging a 15-year-old claim: The North Atlantic Oscillation index as a predictor of spring migration phenology of birds. *Global Change Biology*, *24*(4), 1523–1537. https://doi.org/10.1111/gcb.14023

Jarvis, A., Reuter, H. I., Nelson, A., & Guevara, E. (2008). *Hole-filled SRTM for the globe Version 4, available from the CGIAR-CSI SRTM 90m Database (http://srtm.csi.cgiar.org)*.

Kemp, M. U., van Loon, E., Shamoun-Baranes, J., & Bouten, W. (2012a). RNCEP: Global weather and climate data at your fingertips. *Methods in Ecology and Evolution*, *3*(1), 65–70. https://doi.org/10.1111/j.2041-210X.2011.00138.x

Kemp, M. U., Shamoun-Baranes, J., van Loon, E., McLaren, J. D., Dokter, A. M., & Bouten, W. (2012b). Quantifying flow-assistance and implications for movement research. *Journal of Theoretical Biology*, *308*(June), 56–67. https://doi.org/10.1016/j.jtbi.2012.05.026

Kursa, M. B., & Rudnicki, W. R. (2010). Feature Selection with the Boruta Package. *Journal Of Statistical Software*, *36*(11), 1–13

McCracken, G. F., Safi, K., Kunz, T. H., Dechmann, D. K. N., Swartz, S. M., & Wikelski, M. (2016). Airplane tracking documents the fastest flight speeds recorded for bats. *Royal Society Open Science*, *3*(11). https://doi.org/10.1098/rsos.160398

van de Pol, M., Bailey, L. D., McLean, N., Rijsdijk, L., Lawson, C. R., & Brouwer, L. (2016). Identifying the best climatic predictors in ecology and evolution. *Methods in Ecology and Evolution*, *7*(10), 1246–1257. https://doi.org/10.1111/2041-210X.12590